

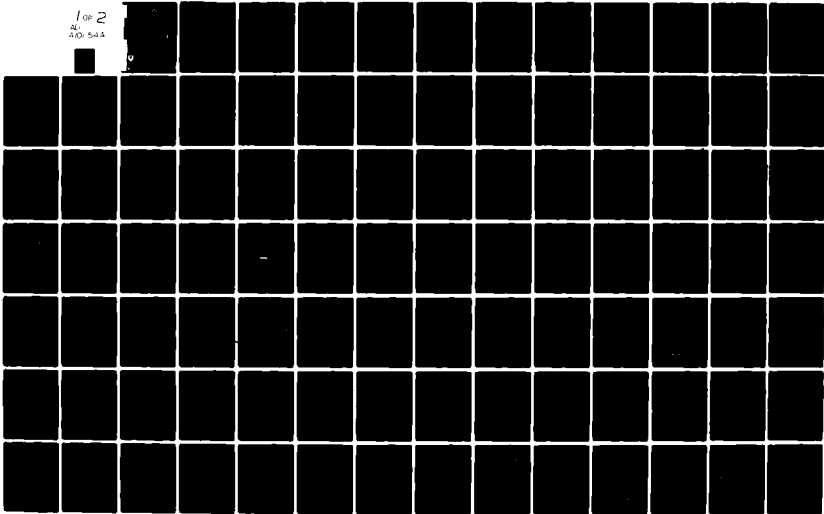
AD-A101 544

UNITED TECHNOLOGIES RESEARCH CENTER EAST HARTFORD CT F/G 17/5
DESIGN APPROACH FOR A LASER WIRE AND WIRE LIKE OBJECT DETECTION--ETC(U)
MAY 81 B B SILVERMAN; H HEYNAU; R J MONGEON DAAK80-79-C-0278

UNCLASSIFIED

USAAVRADCOM-TR-79-0278-F NL

1 of 2
AL
DD-544



AVRADCOM

LEVEL



Technical Report-TR-79-0278-F

DESIGN APPROACH FOR A LASER WIRE AND WIRE-LIKE OBJECT DETECTION SYSTEM (WWLODS)

B.B. Silverman
H. Heynau
R.J. Mongeon

Prepared Under Contract
DAAK80-79-C-0278 *-new*

May 1981

DTIC
ELECTE
JUL 17 1981
S D
C

DISTRIBUTION STATEMENT A
Approved for public release;
Distribution Unlimited



Research and Development Technical Report
Aviation Research and Development Command

81 7 15 013

AD A101544

DTIC FILE NO.

NOTICES

Disclaimers

The citation of trade names and names of manufacturers in this report is not to be construed as official Government indorsement or approval of commercial products or services referenced herein.

Disposition

Destroy this report when it is no longer needed. Do not return it to the originator.

HISA-FM-633-78

UNCLASSIFIED

SECURITY CLASSIFICATION OF THIS PAGE (When Data Entered)

REPORT DOCUMENTATION PAGE		READ INSTRUCTIONS BEFORE COMPLETING FORM
1. REPORT NUMBER US A AVRADCOM TR-79-0278-F	2. GOVT ACCESSION NO. AD-A301544	3. RECIPIENT'S CATALOG NUMBER
4. TITLE (and Subtitle) Design Approach for a Laser Wire and Wire Like Object Detection System (WWLODS).	5. TYPE OF REPORT & PERIOD COVERED Final Technical Report Aug 79 - Nov 80 - Fr 84	6. PERFORMING ORG. REPORT NUMBER
7. AUTHOR(s) B. B. Silverman H. Heynau R. J. Mongeon	8. CONTRACT OR GRANT NUMBER(s) DAAK80-79-C-0278	
9. PERFORMING ORGANIZATION NAME AND ADDRESS United Technologies Research Center 400 Main Street East Hartford, CT 06108	10. PROGRAM ELEMENT, PROJECT, TASK AREA & WORK UNIT NUMBERS 63207A 1L263207DB97-17-001	
11. CONTROLLING OFFICE NAME AND ADDRESS US Army Avionics R&D Activity ATTN: DAVAA-E Fort Monmouth, NJ 07703	12. REPORT DATE May 81	
14. MONITORING AGENCY NAME & ADDRESS (if different from Controlling Office)	13. NUMBER OF PAGES 137	
	15. SECURITY CLASS. (of this report) Unclassified	
	15a. DECLASSIFICATION/DOWNGRADING SCHEDULE	
16. DISTRIBUTION STATEMENT (of this Report) Approved for public release; distribution unlimited.		
17. DISTRIBUTION STATEMENT (of the abstract entered in Block 20, if different from Report)		
18. SUPPLEMENTARY NOTES		
19. KEY WORDS (Continue on reverse side if necessary and identify by block number) Carbon dioxide laser, heterodyned laser, wire detection, airborne laser.		
20. ABSTRACT (Continue on reverse side if necessary and identify by block number) A conceptual design and tradeoff study has been performed for a Wire and Wire-Like Object Detection System (WWLODS). The objective of the study was to recommend three alternative design approaches for a pod-mounted system to be carried on Army helicopters, to be capable of detecting 1/8 inch Army field wire, and to meet a weight goal of 50 pounds, a size goal of 1 cubic foot, and a cost goal of \$50,000 per unit averaged over a production run of 4,000 units. The study established WWLODS performance requirements on range, field-of-view, frame		

DD FORM 1 JAN 73 1473

EDITION OF 1 NOV 65 IS OBSOLETE
S/N 0102-LF-014-6601

UNCLASSIFIED
SECURITY CLASSIFICATION OF THIS PAGE (When Data Entered)

409252

UNCLASSIFIED

SECURITY CLASSIFICATION OF THIS PAGE (When Data Entered)

time, and scan pattern based on helicopter flight performance limitations and helicopter pilot practices. It was found that a WWLODS based on active Infrared Coherent Optical Radar (ICOR) technology could be designed to meet the weight, volume, and cost goals, but that its range performance would be short enough to require a significant limitation on helicopter flight speed. Relaxing the weight limit to 70 pounds and the volume limit to 1.3 cubic feet would allow the design of a longer-range system with a much higher speed capability, but still within the production cost goal.

S/N 0102- LF-014-6601

UNCLASSIFIED

11

SECURITY CLASSIFICATION OF THIS PAGE(When Data Entered)

FOREWORD

This work was performed during the period from August 1979 to June 1980 under Contract DAAK80-79-C-0278. The project officers were Dr. Robert L. DelBoca and Mr. Michael Wilken, DAVAA-E, Ft. Monmouth, N.J. 07703. During the period of this study, experiments to determine the performance of RF-excited waveguide lasers and to compare them with DC-excited waveguide lasers were under way but not completed. Therefore, the DC-excited laser was selected as the baseline in this study. Since that time, RF-excited waveguide lasers have been shown to be equal to or better than DC-excited waveguide lasers in performance. In addition, RF excitation has advantages in simplicity, controllability, reliability, and resistance to air breakdown in low pressure environments. Therefore, in future work RF excitation would be selected as the baseline. In the present study, the selection of RF excitation would have no significant effect on the weight, volume, or cost of the recommended design approaches.

Accession For	<input checked="" type="checkbox"/>
NTIS GRA&I	
DTIC TAB	
Unannounced	
Justification	
By	
Distribution	
Availability Codes	
Dist. Statement	
A	

Design Approach for a Laser Wire and Wire-Like Object
Detection System (WWLODS)

TABLE OF CONTENTS

	<u>Page</u>
1.0 SUMMARY	1
2.0 INTRODUCTION	2
3.0 OBJECTIVE, GOALS, AND SCOPE OF PROGRAM	7
4.0 STUDY APPROACH	9
5.0 AIRCRAFT CONSTRAINTS AND PILOT INPUTS.	12
6.0 SENSOR PERFORMANCE REQUIREMENTS.	22
7.0 LASER TECHNOLOGY BASE.	41
8.0 SCANNER DESIGN STUDY	46
8.1 Scanner Candidates.	46
8.2 Dither Mechanism Candidates	55
8.3 Scanner Candidate Tradeoffs	56
8.4 Baseline Scanner Selection and Parameters	69
9.0 SELECTION OF RECOMMENDED DESIGN APPROACHES	78
9.1 Selection Procedure	78
9.2 Tradeoff Evaluation	87
9.3 Recommended Design Approaches	102
9.4 Preliminary Design Concepts	110
10.0 PROGRAM PLANS, RISKS AND COST ESTIMATES	115
10.1 6.3B Program	115
10.2 6.4 Program	123
10.3 Program Risks	127
10.4 Program Cost	129
11.0 REFERENCES	133

LIST OF FIGURES

<u>Figure No.</u>		<u>Page</u>
2.1	Angular Dependence of Wire Detection.	4
2.2	CO ₂ Sensor Terrain Returns.	5
4.1	WWLODS Study Program.	10
5.1	Pilot Survey Data	17
5.2	Pilot Survey Data	18
5.3	Pilot Survey Data	19
5.4	Pilot Survey Data	21
6.1	NOE VFOV Requirements	23
6.2	Sensor Range Required for Stopping Maneuver	25
6.3	Enroute Popup Maneuver.	26
6.4	Range and VFOV Requirements for Enroute Popup Maneuver.	28
6.5	Sensor Range Requirement for Popup Maneuver	29
6.6	Sensor Vertical FOV Limits for Popup Maneuver	30
6.7	Enroute Turn Maneuver	32
6.8	WWLODS FOV and Range Requirements for Enroute Turn Maneuver.	33
6.9	WWLODS FOV and Range Requirements for Enroute Turn Maneuver.	34
6.10	False Warning Criterion for Pulse Length.	36
6.11	False Warning Limits on Range and Pulse Length.	37
6.12	False Warning Limits on Range and Pulse Length.	38
6.13	Clearance Height.	40
7.1	Basic Laser Configurations.	42
7.2	Laser Weight Considerations	45
8.1	1-Pair Dual Wedge Scanner	48
8.2	2-Pair Dual Wedge Scanner	50
8.3	Dual Wedge/Turret Scanner	51
8.4	Ball Joint Scanner.	52
8.5	Variable Wedge Scanner.	54
8.6	Tilting Wedge Dither Mechanization.	57
8.7	Pre-Expander Galvanometer Mirror Dither Mechanization	58
8.8	Scan Patterns	61
8.9	Scanner Weight vs Clear Aperture.	63
8.10	Scanner Optical Train Losses.	67

LIST OF FIGURES (Cont'd)

<u>Figure No.</u>		<u>Page</u>
8.11	2-in. Ball Joint Scanner Mechanization.	71
8.12	Ball Joint Scan Pattern	73
8.13	2 in. Ball Joint Scan Parameters.	74
8.14	2 in. Ball Joint Scanner Implementation	75
9.1	Tradeoff/Evaluation Process	80
9.2	Transceiver Subsystem Weight.	82
9.3	CW to Pulsed Laser Power Conversion	83
9.4	Scanner and POD Subsystem Weight.	84
9.5	NOE Speed/Range Performance	88
9.6	NOE Speed/Range Performance	89
9.7	NOE Speed/Range Performance	90
9.8	NOE Speed/Range Performance	91
9.9	NOE Speed/Range Performance	92
9.10	NOE Speed/Range Performance	93
9.11	NOE Speed/Range Performance	94
9.12	NOE Speed/Range Performance	95
9.13	NOE Speed/Range Performance	96
9.14	NOE Speed/Range Performance	97
9.15	NOE Speed/Range Performance	98
9.16	NOE Speed/Weight Tradeoff	99
9.17	NOE Sppeed/Weight Tradeoff	100
9.18	NOE Speed/Weight Tradeoff	101
9.19	False Warning Limits on Range and Pulse Length.	106
9.20	False Warning Limits on Range and Pulse Length.	107
9.21	Crosswind Capabilities.	109
9.22	Preliminary Design Concepts for 2-in. Dual Wedge Scanner WWLODS	111
9.23	WWLODS Installation	112
9.24	POD Design Summary	113
10.1	Hypothetical Scene.	118
10.2	Minimum Display Option.	120
10.3	Preferred Display	121
10.4	Display Presentation of a Typical Flight Profile.	122
10.5	6.3B Program Structure.	124
10.6	6.4 Program Schedule.	126
10.7	Lower Risk Program.	128
10.8	Higher Risk Program	130
10.9	Estimated Cost of WWLODS.	131

LIST OF TABLES

<u>Table No.</u>		<u>Page</u>
5.1	Helicopter Inventory.	13
7.1	Summary of Laser Technology Considerations.	44
8.1	Scanner Requirements.	47
8.2	Candidate Scanner Tradeoffs	59
8.3	Scanner Relative Weight vs Frame Time	64
8.4	Scanner Relative Weight vs FOV/FOR.	66
8.5	Scanner Window Considerations	68
8.6	Scanner Power Requirements.	70
8.7	2-in. Ball Joint Scanner Weight Estimate.	77
9.1	System Design Options	79
9.2	Range Analysis.	85
9.3	SNR Requirements.	86
9.4	Recommended Design Approaches and Performance Capabilities	104
9.5	Special Performance Capabilities.	105
10.1	Major Elements of 6.3B Program.	116
10.2	6.4 Program	125

1.0 SUMMARY

A conceptual design and tradeoff study has been performed for a Wire and Wire-Like Object Detection System (WWLODS). The objective of the study was to recommend three alternative design approaches for a pod-mounted system to be carried on Army helicopters, to be capable of detecting 1/8 inch Army field wire, and to meet a weight goal of 50 pounds, a size goal of 1 cubic foot, and a cost goal of \$50,000 per unit averaged over a production run of 4,000 units. The study established WWLODS performance requirements on range, field-of-view, frame time, and scan pattern based on helicopter flight performance limitations and helicopter pilot practices. It was found that a WWLODS based on active Infrared Coherent Optical Radar (ICOR) technology could be designed to meet the weight, volume, and cost goals, but that its range performance would be short enough to require a significant limitation on helicopter flight speed. Relaxing the weight limit to 70 pounds and the volume limit to 1.3 cubic feet would allow the design of a longer-range system with a much higher speed capability, but still within the production cost goal.

2.0 INTRODUCTION

As set forth in Ref. 1, in future tactical warfare US Army Aviation Units will have to operate in an environment of very high threat density. This environment will include intensive electronic warfare (both active and passive) and numerous small- and large-caliber Anti-Aircraft Artillery (AAA), Surface-to-Air Missile (SAM), and Air-to-Air Missile (AAM) threats. Night vision devices used by Egyptian and Syrian forces in the 1973 Middle East war indicate that future battles will be fought on an around-the-clock basis. The accepted assessment of this threat environment is that any target that can be seen or detected by the enemy can be engaged and destroyed. Therefore, aircraft must fly close to the ground and must use both terrain and vegetation for masking to the greatest degree possible, and must also move continually in order to avoid detection.

Within about 5 km of the Forward Edge of the Battle Area (FEBA), the threat includes large numbers of small arms, small AAA, and small man-portable missiles, all capable of line-of-sight operation. In this region Nap-of-the-Earth (NOE) flight, nominally at zero altitude and speeds of 0 to 40 kts, is required. In the holding area, which is farther from the FEBA (5 to 10 km), nominal speeds may range up to 100 kts and altitudes may range from 0 to 50 feet, but the flight patterns are similar to those in NOE operations except that there is more emphasis on range made good over the ground. Farther back, in the Forward Area Refueling and Rearming Point (FARRP) which is 10 to 20 km from the FEBA, Contour Flight at altitudes of around 50 feet above the ground and speeds of 80 to 100 kts will be used for point-to-point travel. In the rear area, Low Level flight at an altitude of 400 feet above the highest anticipated obstacle and at the speed for maximum range (from about 120 to 160 kts) will be used. In no case will the aircraft altitude exceed roughly 1000 feet above the ground. It is customary for pilots operating in NOE and Contour conditions to concentrate their full attention on the terrain outside the cockpit, and to look at instruments only when their attention is demanded by an annunciator to respond to an abnormal condition. Instrument flight which requires constant monitoring of a headsdown display is not practical in these circumstances, although it can be used in Low Level flight.

Current Army aviation operations are conducted primarily under Visual Flight Rules (VFR) conditions in good weather. Only very limited exercises are conducted at night and in adverse weather. Nevertheless, even in these normally good conditions, NOE and Contour flight exercises have shown repeatedly that wires and wire-like objects are very hard to see and sometimes, even if seen, are hard to avoid because of the lack of the perspective in looking at a long, thin object. Current Army experience with operations of these kinds result in the approximately two wire strikes per month by Army helicopters. It is normal practice for pilots to fly slowly in NOE and Contour conditions in order to have the best possible chance of seeing and avoiding wires and wire-like objects because the visual detection range

is short. Those pilots who have the most experience with low altitude operations, especially pilots who have flown in Korea and in the Federal Republic of Germany (FRG), tend to fly at the lowest speeds and to express the most worry about encountering wires.

In this study, a range of WWLODS designs based on ICOR technology was investigated. It has been demonstrated that such systems can see wires and wire-like objects at much longer ranges than the human eye. This is true both in good weather and in night/adverse weather conditions. This capability to see wires at long range allows flights to be conducted safely at higher speeds than is possible with visual detection only. This study evaluated the potential for a WWLODS to enhance the speed and safety of NOE and Contour flight within the given weight, volume, and cost goals of 50 lb, 1 cubic ft, and \$50,000. The evaluation is conservative in that demonstrated ICOR technology and performance are used in the analysis and no extreme avoidance maneuvers are required to meet the performance estimated herein. A number of Army pilots were interviewed to establish reasonable bounds on the appropriate helicopter maneuvers and pilot response times and on the flight conditions and sensor parameters that pilots would find useful.

The ICOR technology base is available as a consequence of the exploratory development programs that have been extending the state of the art in 10 micron radars over the past 11 years. In particular, the Army/UTRC Multifunction Laser Obstacle Terrain Avoidance Warning System (LOTAWS) program (Contract number DAAB07-76-C-0920, Refs. 2 and 3), has demonstrated the viability of airborne heterodyning 10 micron radar with respect to the detection of 1/8 in. field wire. In the LOTAWS program, a high PRF short pulse laser was utilized as the transmitter for an optically heterodyned helicopter borne CO₂ laser radar which successfully demonstrated the essential characteristics of a Terrain Following/Terrain Avoidance (TF/TA) and Obstacle Avoidance (OA) system. The most demanding obstacle requiring detection for the LOTAWS application was 0.32 cm (1/8 in.) Army field wire. The detection of that small cross section target was demonstrated in flight at ranges in excess of 1200 m.

The ability to successfully detect these small diameter target wires in flight was a major achievement of the initial flight test program. Comparison of flight test data with static test results obtained with the aircraft on the ground conclusively demonstrated that the LOTAWS system performance did not deteriorate in the airborne environment. A plot of both static and flight wire return data as a function of angle of incidence for 0.32 cm (1/8 in.) field wire at 400 m is shown in Fig. 2.1. In addition to the agreement between the ground and flight data, it is important to note the finite off-axis detectability of this relatively smooth man-made target. This typical 10.6 μ m target cross section characteristic results from the combination of the specular scattering return which decreases very rapidly with increasing angle of incidence and the diffuse scattering return which is responsible for the finite off-axis signal. Additional testing supported the multifunction potential of 10 micron radar. Ground returns substantiating the utility of CO₂ optical radar for terrain following are shown in Fig. 2.2. The Multifunction LOTAWS tests

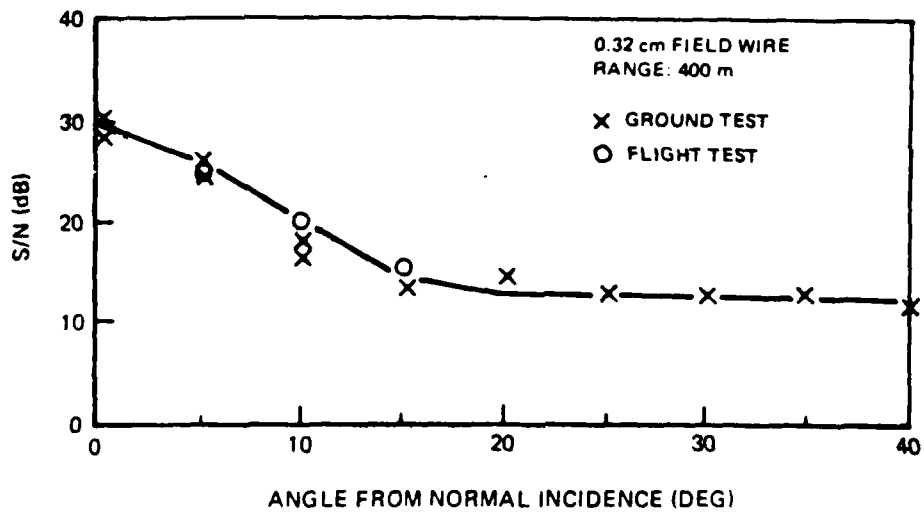


FIGURE 2.1 ANGULAR DEPENDENCE OF WIRE DETECTION

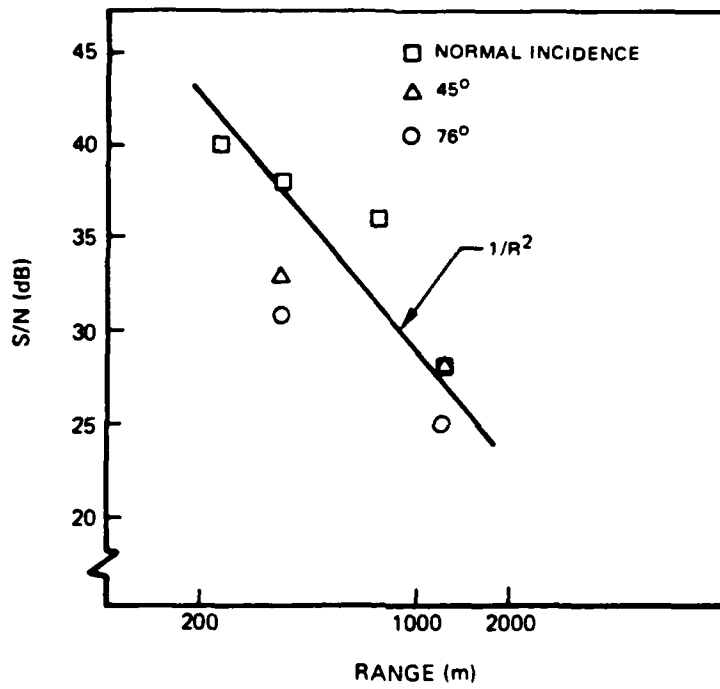


FIGURE 2.2 CO₂ SENSOR TERRAIN RETURNS

demonstrated the operational feasibility of precise laser Doppler navigation, precision hover, and the laser's intrinsic capability for use as a possible target discriminator/identifier.

From a component viewpoint, an active 10 micron ICOR-based WWLODS will introduce only one new component to existing operational systems. Current FLIR systems have established the optics, scanners, and cryogenically cooled detectors as viable components while the multitude of airborne microwave radars has developed the electronics to support the signal processing, displays, and power supplies to a high degree of sophistication. The new component is the CO₂ laser which intrinsically offers high efficiency and extreme versatility with respect to the transmitter output format. It is currently the focus of industry-wide efforts to provide the laser in rugged, air cooled, high lifetime packages that would be compatible with field operation. In particular, the recent advances in ceramic waveguide CO₂ lasers provide the foundation from which one can confidently extrapolate the first generation of compact flyable 10 micron transmitters compatible with the requirements of WWLODS.

In the remainder of this report, Section 3.0 summarizes the contract objectives and the scope of the analysis and design studies conducted. Section 4.0 is a detailed description of the approach taken in the analysis. Section 5.0 summarizes the aircraft constraints on and the pilot inputs to the sensor performance. Section 6.0 contains a detailed discussion of the way in which the specific sensor performance requirements on range, field of view, frame time, etc., were established. Section 7.0 is a description of the laser design approaches and the technology base available, and Section 8.0 describes the scanner design studies. Section 9.0 describes the selection of the recommended design approaches and summarizes their important characteristics. Section 10.0 contains descriptions of alternative program plans: a lower risk option which has an Initial Operational Capability (IOC) date late in Fiscal Year (FY) 1988, and a higher risk option which has an IOC in mid-FY 1985 (assuming a program start at the beginning of FY 1981), and also summarizes a set of noncritical issues which would be important in subsequent phases of the development of a WWLODS system but do not impact significantly on the study at this time.

3.0 OBJECTIVE, GOALS, AND SCOPE OF PROGRAM

The objective of this program, as given in the Statement of Work (SOW) is to define and scope three design approaches for a 10.6 micrometer WWLODS for use in Low Level, Contour and NOE flight. The three approaches are required to differ in some significant parameter such as weight, performance, reliability, cost, schedule, or risk.

The major goals for the WWLODS are:

weight = 50 pounds

volume = 1 cubic foot

cost = \$50,000 for a production of run of approximately 4,000 units

IOC = FY1985

The system is to be compatible with all future Army helicopters and all Army operational environments including peace time, war time, urban and open country environments.

The SOW identifies a number of significant performance and design requirements:

1. The system must detect 1/8 in. WD-1 Army field wire at all aspect angles and at all orientations relative to the ground.
2. The performance of the system against TOW and DRAGON control wires is to be evaluated.
3. Performance is to be evaluated under the following weather conditions:
day and night
4 mm/hr rain
15 mg/m³ fog (100-400 meters visibility, 10 dB/km transmission loss)
AR 70-38 climatic categories 1-7 (category 5, 110 F/85 percent RH, is critical because of its high water vapor content of 51 grams per cubic meter)
4. Detection probability, $P_D = 0.9$ minimum with 0.999 desired
5. Probability of false warning of a wire, $P_{FW} = 0.05$ with 0.01 desired

6. Warm up and operation of the system is to require minimum attention and there is to be no dedicated operator for the system.
7. The system is to have good "ilities" such as high reliability, good safety, simple maintainability, minimal logistic support requirements, etc.
8. To the maximum extent possible, the system is to be compatible with existing displays or those displays planned for the future Army helicopter inventory.
9. The system is to be compatible with all other systems on board Army helicopters.
10. Considerations of electronic countermeasures, counter-countermeasures, and nuclear survivability are to be adequately addressed in the system design.

Within the scope of effort possible under this contract, design details for a complete system could not be addressed. The major effort was therefore devoted to those system elements that strongly impact the weight, volume, cost, utility, and acceptability to the user of the WWLODS. As a result, the first 5 items in the above list of performance and design requirements received major attention because they drive major design choices such as laser power, scanner diameter, scan field of view and format, detector Signal-to-Noise Ratio (SNR), etc. The remaining performance and design requirements are items which can, in fact, be met only by proper consideration in the detailed design process and are, therefore, considered in this study primarily in a negative sense, i.e., no choices were made which are known to be inherently poor in areas 6-10 above.

Design layouts of complete systems were made for the 3 selected approaches in order to verify the weight and volume estimates (see Section 9.0). In order to allow realistic consideration of installation and interface problems, a pod design intended for installation on the UH-60A helicopter was assumed for these layouts as specified in the SOW.

4.0 STUDY APPROACH

The plan of the study program is illustrated in Fig. 4.1. A review of the Army helicopter inventory as anticipated for the FY 1985 time frame, based on information furnished to UTRC by AVRADA, was made. This review identified the helicopter performance capabilities, the options available for displaying detected information to the pilots and those sensors which would be available to interface with the WWLODS to define the attitude and velocity vector of the helicopter with reference to inertial space. A number of Army helicopter pilots were interviewed to obtain pilot inputs on reasonable values of helicopter airspeed (V), climb angle (θ_C), bank angle (θ_B), ground clearance (Δh), frame time (T_F), response time (T_B), and rotor tilt angle (θ_T), which could be used in performing maneuvers to either avoid obstacles or to stop the helicopter. Based on these inputs, a number of simple flight maneuvers were defined and modeled as combinations of straight line and circular arc trajectory elements. These trajectories along with the pilot inputs on speeds, maneuvers and required clearances were used to define the sensor performance requirements in terms of the range (R), T_F , Field of View (FOV) and scan pattern requirements necessary to allow the trajectories desired by the pilots to be flown.

The laser design and performance was defined on the basis of experimental data which has been generated under this program (see Section 7.0 and Ref. 4) and in previous and currently ongoing experimental programs at UTRC. The analysis included an evaluation of the weight and volume of the laser as a function of average power (P), pulse repetition rate (PRF), and pulse length (τ), in the range of approximately 1 to 30 watts of output power, PRF from CW to 100 kHz, and τ from 100 to 300 ns. The laser power supply requirements and design were also defined in this analysis. The scanner design and performance were analyzed by the Norden Systems (NS) subsidiary of United Technologies. In the scanner analysis, alternative configurations were reviewed and promising configurations selected. For these configurations the influence of aperture diameter, D , FOV and scan pattern on T_F , scanner weight and scanner power requirements were evaluated. Alternative WWLODS configurations incorporating various combinations of laser power, laser output format, scanner configuration and aperture size were considered in conjunction with the R , FOV and scan pattern requirements to establish the variation of SNR with system range, T_F , and weather variations as indicated in Fig. 4.1. The analysis of system configurations also resulted in a parametric variation of system weight, including the weight of the pod required to provide aerodynamic fairing, weather protection, aircraft mounting and the proper geometric relationship among all the system components. At this point in the study, information was available on system performance capabilities, system weights and system performance requirements, and a tradeoff evaluation was conducted to select the three recommended design choices. For these three selected design choices a limited amount of preliminary design effort was conducted to address critical issues in the overall system configuration.

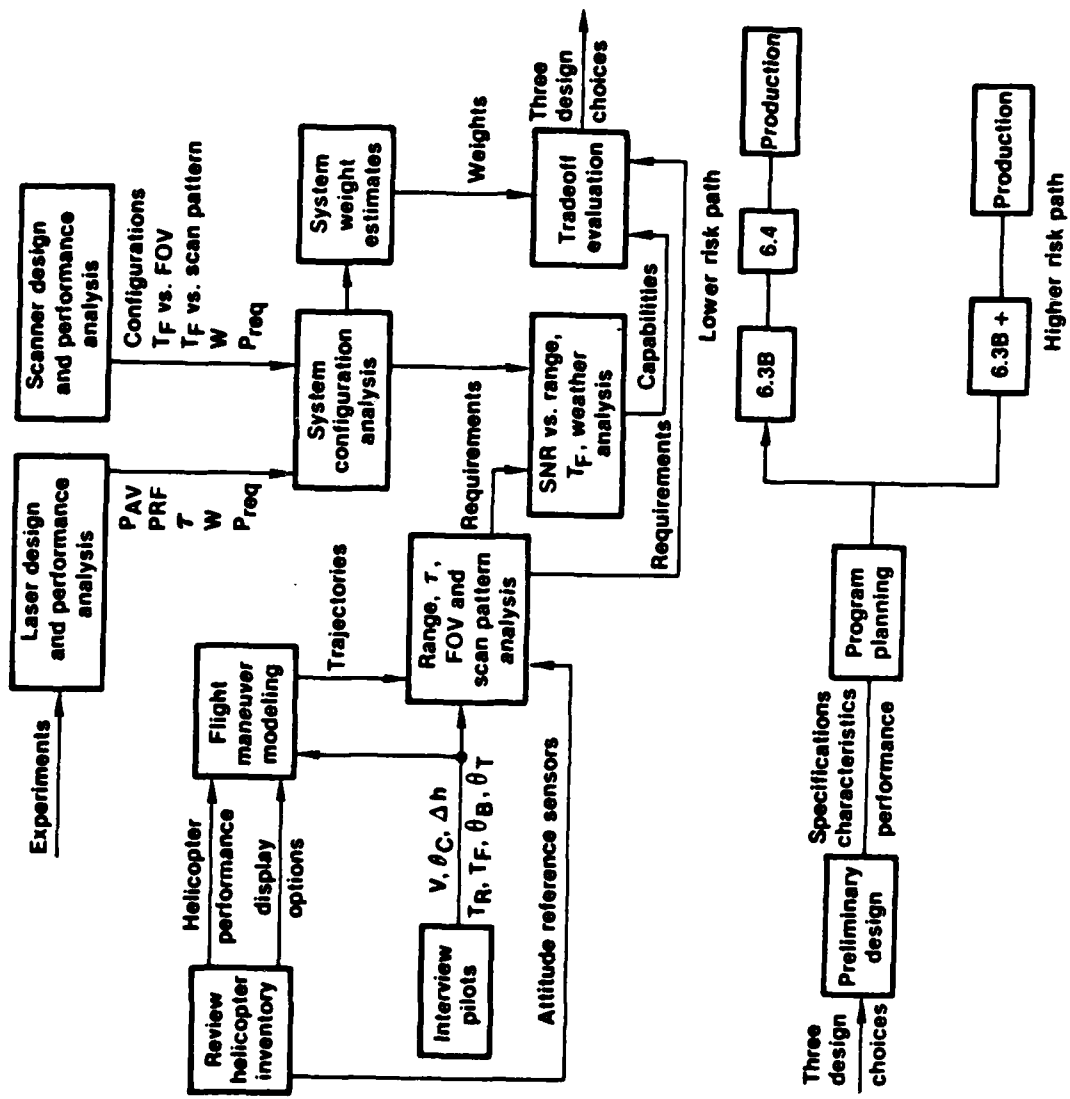


FIGURE 4.1 WWLODS STUDY PROGRAM

At the end of this preliminary design effort the design specifications, overall system characteristics and system performance capabilities had been defined and program planning was conducted. Alternative program plans were generated for each of the three recommended design approaches. The lower risk path involved sequential 6.3B, 6.4 and production programs. The higher risk path was designed to obtain an earlier IOC than could be expected from the lower risk path, and involved shortening and overlapping of the elements of the low risk program; it is labeled 6.3B+ in Fig. 4.1. In all of these programs, risk is assessed not in terms of system performance capability, which was kept constant at the level demanded by the mission requirements, but in terms of the probability of meeting the required schedule, weight and cost goals. The higher risk path has a lower probability of meeting these goals. All programs were assumed to start at the beginning of FY 1981. Cost projections were made in constant 1980 dollars using standard industry cost models for conventional structure and electronics components and pricing analyses of individual components for nonstandard items such as the laser.

5.0 AIRCRAFT CONSTRAINTS AND PILOT INPUTS

The helicopter inventory expected to be available in FY 1985 is shown in Table 5.1. The WWLODS would be used with all of these aircraft. The inventory of instruments available on these aircraft is important to the WWLODS because the scan field of view and scan pattern must be referenced to the local vertical or to the aircraft velocity vector, depending on the mode of flight. Velocity vector information would always be available from the Lightweight Doppler Navigation System (LDNS) which is a component of the instrumentation suite of all of these aircraft. A 3-axis inertial platform known as the Heading Attitude Reference Set (HARS) is programmed for the AAH, AH-1S and ASH aircraft and will be installed in later versions of the UH-60A helicopter, but is not programmed for the CH-47 vehicle. The current inventory of UH-60A and CH-47 aircraft do, however, include a vertical gyro which is part of the Vertical Situation Indicator (VSI) display. Thus, all of the aircraft do have available instrumentation which will provide adequate attitude reference data to the WWLODS for use in directing the ICOR laser beam through the scan pattern.

The situation with respect to available displays is more complex and less satisfactory. The options are an Electromechanical Attitude Director Indicator (EMADI), which is the current standard instrument for instrument flight, and an Electronic Attitude Director Indicator (EADI) which is a future replacement for the EMADI; the APR-39, which is a three-inch-diameter Cathode Ray Tube (CRT) display of radar warning information, and some form of Heads-Up Display (HUD). The HUD displays are the only ones of real interest in connection with the WWLODS system because they are compatible with normal Army pilot practices. The AAH has a helmet mounted CRT known as the IHADSS (Integrated Helmet and Display Sight Subsystem) which is used for night, NOE, and limited adverse weather navigation and for target acquisition and designation. It will display Forward Looking Infrared (FLIR) data and could therefore be adapted to display the data acquired by the WWLODS. The AAH pilot has available an EADI and an APR-39, and the AAH copilot has an EMADI. The AH-1S also has a HUD which is available to the pilot only. It is fed by a CRT and could therefore also display data acquired by the WWLODS. The UH-60A and CH-47 are not scheduled to have a HUD. Displays for the ASH are not completely firm at this time, however consideration will be given to the use of two CRT displays, the EADI and a multi-function display. Either of these could accept data generated by the WWLODS.

Engine power limitations on helicopter flight performance are not a limiting consideration in most Army applications except for the limitations on payload and range imposed by the basic lifting capacity of the helicopter. All of the aircraft in the Table 5.1 inventory have roughly similar flight performance capabilities in terms of such parameters as speed for maximum

Table 5.1
HELICOPTER INVENTORY

Aircraft	Number	Instruments				Displays			
		VG	HARS	LDNS	EMADI	EADI	APR-39	HUD	
AAH	536		✓	✓	✓	✓	✓	✓*	
AH-IS	1000		✓	✓	✓		✓	✓	
UH-60A	1107	✓	(✓)	✓	✓		✓		
ASH	1450		✓	✓		?		?	
CH-47	361	✓		✓			✓		
Total	4454							*IHADSS	

range (120-140 kts), maximum speed (140-160 kts), and maneuvering limits (2.5 to 3.0 g up and -0.50 g down). It would be expected that Low Level flight would be conducted at the speed for maximum range and that no maneuvers would normally be required since the flight altitude is chosen to be above the highest anticipated obstacle. Contour flight would be conducted at the speed for maximum range or less and since it is a low altitude flight condition, maneuvers would be anticipated to avoid obstacles. Power available is not a limiting factor in performing maneuvers in contour flight because the pilot always has available the option of trading speed for maneuverability, i.e., performing a transient maneuver to trade kinetic energy (speed) for potential energy (altitude) or for an abrupt change in direction, and thus is limited primarily by structural or aerodynamic considerations in making avoidance maneuvers. Flight performance is not limiting in NOE flight because it normally does not involve high speed or violent maneuvers; exceptions to these ground rules, such as rapidly crossing an open field from one sheltered area to another, require less power than hovering.

In the course of this study, visits were made to Fort Rucker, Alabama, and Fort Campbell, Kentucky to interview Army pilots, and telephone discussions were held with pilots at AVRADA and at the Sikorsky Aircraft (SA) Division of United Technologies Corporation. The general conclusions that can be drawn from these interviews are as follows:

1. Army pilots always fly as low as possible. In NOE flight they will fly with their skids in the grass or below treetop level if terrain conditions and visibility permit.
2. Pilots will spend an absolute minimum of time monitoring instruments inside the cockpit while performing NOE and Contour Flight. It is essential that they be looking out the window at the real world at all times. A display which required continual or frequent monitoring of a cockpit instrument would not be acceptable and would not be used. If some form of HUD is not available, then an audible warning or possibly a flashing light in the pilot's peripheral vision field would be a minimally acceptable alternative. A HUD or IHADSS is strongly desired by Army helicopter pilots.
3. Pilots who have had experience flying in Korea or in Germany expressed strong concern with the problem of encountering wires. In Korea, for example, wires which span valleys and may have no visible towers were said to have appeared "overnight". One pilot recounted an experience in which he was actually touching a wire and still was unable to see it.

4. There are no hard and fast requirements on the frame time and range requirements for the sensor. In current operations pilots slow down when the information available about obstacles is limited by poor visibility or by confusing background conditions, and they make maneuvers which provide large miss distances when going over or around wires because of the limited perspective information available to them. Thus pilots currently perform a tradeoff between flight speed and maneuver choices, based on the range, frame time (update rate) and FOV of the available sensor information, which is visual information under the usual VFR flight conditions of Army flight operations.
5. Pilots prefer to fly under wires or around obstacles rather than over them.
6. The desire to go under or around rather than over is sufficiently strong that pilots are willing to stop and look around for a period of time before proceeding, in order to avoid increasing altitude and unmasking the helicopter.
7. Data on the distance to a detected obstacle and on whether the obstacle is above or below the current altitude and/or velocity vector would be very useful information to the pilot.
8. Pilots expressed a strong interest in having available an accurate Doppler navigation system for finding, returning to, or designating target location. The possibility that information of this kind could be obtained from a derivative of the WWLODS was very appealing to pilots even though it was not presented to them as an objective of this program.
9. Pilots expressed a great reluctance to see additional weight added to a helicopter. The utility of current helicopters appears to be most strongly limited by lack of adequate payload capacity.

Quantitative data on the way pilots want to operate helicopters and on the information pilots would like to have presented by the WWLODS were obtained in interviews of 25 pilots at Fort Campbell. These pilots included seven scout (OH-58), nine attack (AH-1S), five utility (3 UH-1, 2 UH-60) and four transport (CH-47) pilots. The data gathered were analyzed to determine the mean value, the standard deviation, σ , the median and the mode of each parameter for which pilots gave adequate numbers of answers. The data were analyzed by plotting them in the form of a histogram and the median was established by integrating the histogram data to form a crude cumulative probability curve, and reading the value of the parameter at the fifty percent probability point.

Dimensions of the FOV required for the scanner were arrived at by asking the pilots to define the minimum height and width of a clear window through which they would be willing to fly the helicopter and by asking them to define the minimum range at which they would be able to accept information and use it to choose control inputs. These data are shown in Fig. 5.1 in the form of histograms. As can be seen from Fig. 5.1 there was a large spread in the values presented by the various pilots. The minimum range is important for two reasons, first because it implies a maximum useful pulse length for the transmitter and second because in combination with the window dimensions it determines the maximum angular FOV required of the scanner. Since the allowable pulselength in nanoseconds is on the order of twice the minimum range in feet, the smallest value of pulselength required to meet the minimum range requirement is on the order of 200 nanoseconds. As will be seen in Section 7.0, this is not a restriction on the transmitter. When the mean values of window height, window width and minimum range are combined to determine the angular FOV required for the scanner the resulting dimensions are approximately 15° high by 24° wide. These dimensions represent a lower bound on an angular FOV; as will be seen in Section 6.0, maneuver requirements impose larger demands on the scanner FOV capabilities.

The ground clearances used by pilots in NOE and Contour flight are shown in Fig. 5.2. The mean minimum and maximum altitudes used in NOE flight range from two to four feet, with a number of pilots expressing an interest in flying with their skids in the grass or in the treetops. The one data point at 25 feet was not used in analyzing these data. Mean altitudes in Contour flight range from about 20 to 30 feet. At the altitudes used in NOE flight it is possible for the helicopters to fly under many wire spans; however, these altitudes are low enough so that obstacles such as wire fences, barbed wire barriers, and tree stumps become a hazard. The altitudes used in Contour flight are comparable to the height of many common telephone and power distribution lines and thus the WD-1 Army field wire would be a typical hazard in this kind of flight.

The speeds used in NOE and Contour flight are illustrated in Fig. 5.3. The minimum speed in NOE flight is zero. The mean of the maximum speeds quoted by pilots is 80 kts with a few pilots desiring speeds of 160 to 190 kts for the dash maneuver across an open space. Thus even in NOE flight it is desirable to fly as fast as possible; however, pilots are willing to limit their speed under conditions of limited visibility or restricted maneuverability. The desired speeds in Contour flight range from about 60 to about 120 kts, which encompasses the speeds for maximum rate-of-climb for helicopters. These speeds are dictated by the necessity to maneuver over or around the obstacles encountered at the low ground clearances of 20 to 30 feet used by pilots in Contour flight.

Window Dimensions and Minimum Range

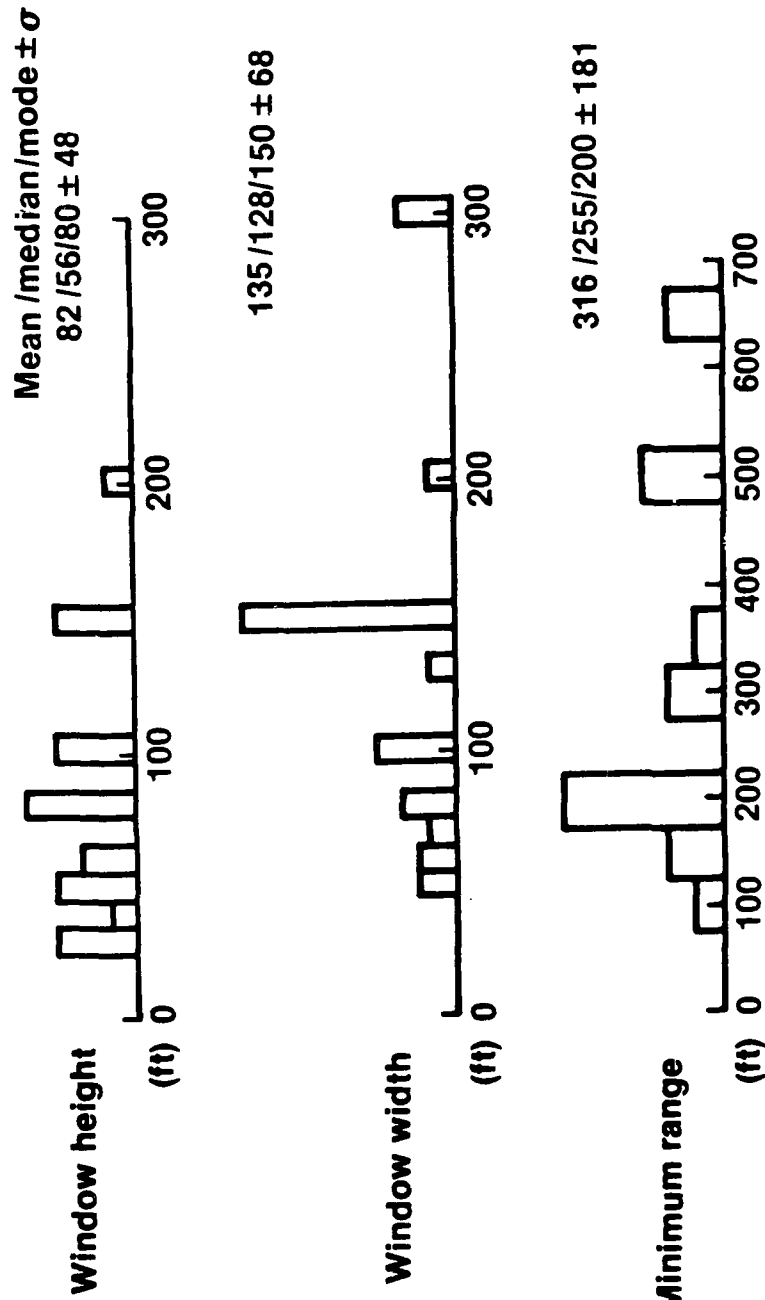


FIGURE 5.1 PILOT SURVEY DATA

Ground Clearance

Mean/median/mode $\pm \sigma$

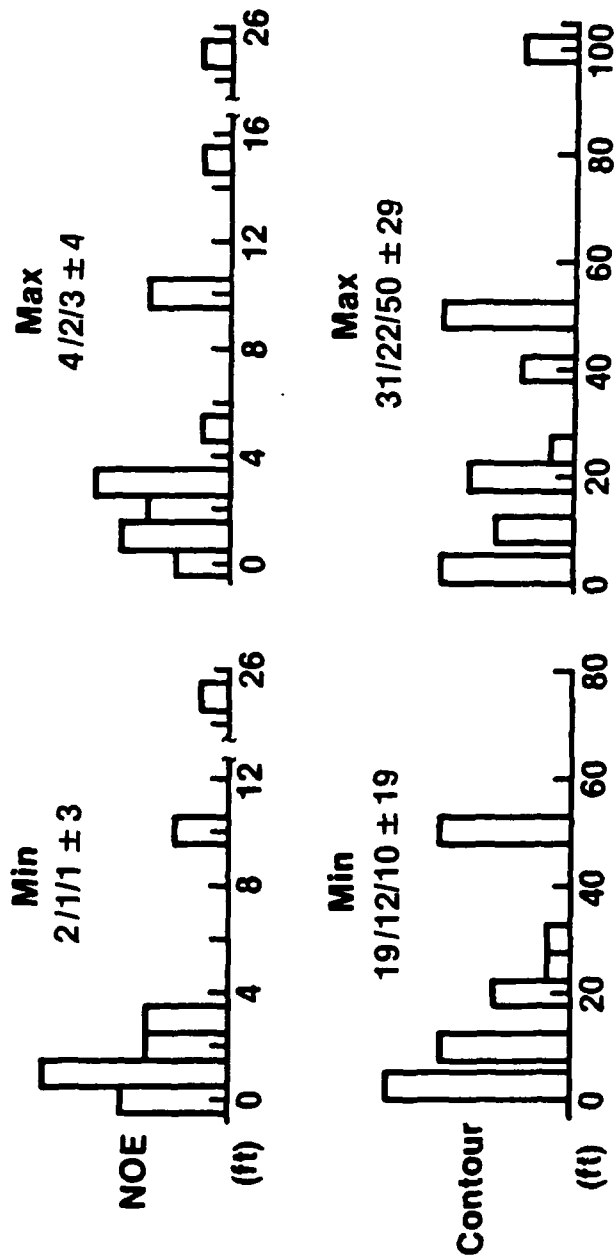


FIGURE 5.2 PILOT SURVEY DATA

Max and Min Speeds

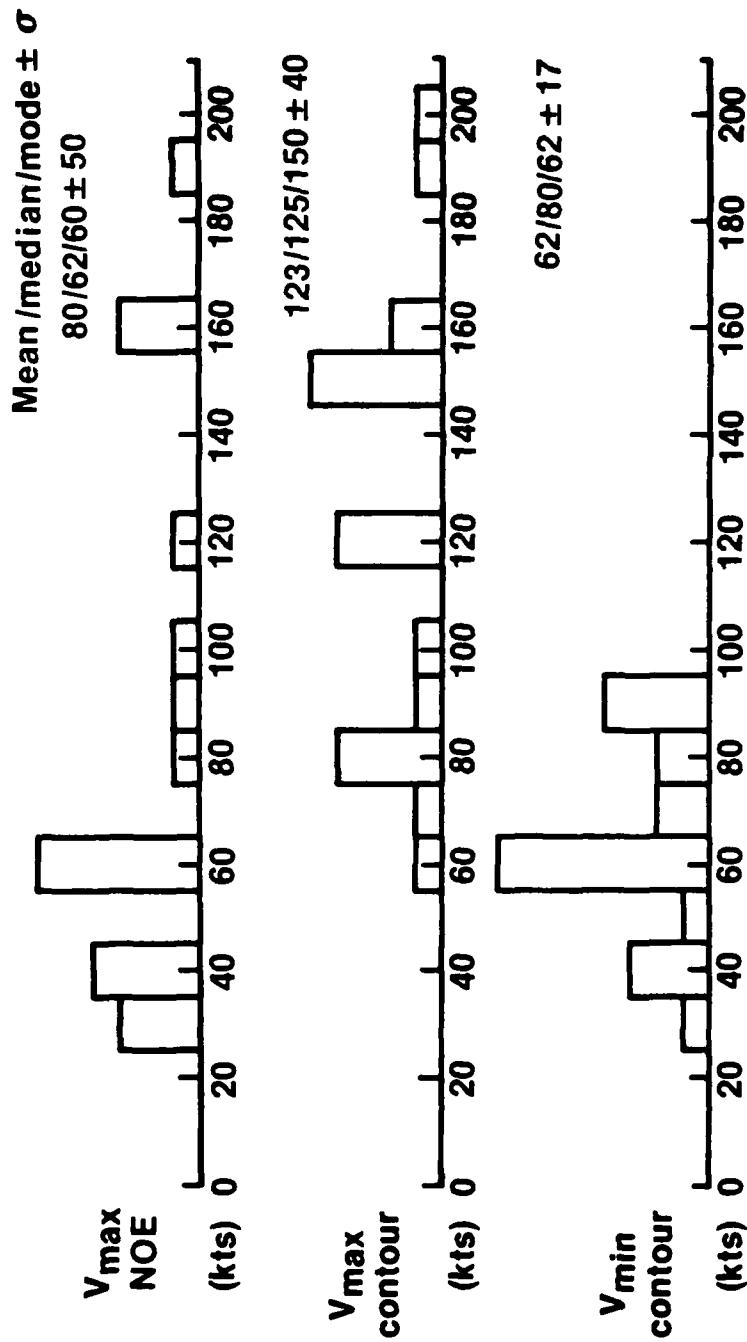


FIGURE 5.3 PILOT SURVEY DATA

Pilot preferences for response time and frame time are illustrated in Fig. 5.4. The difference between minimum and maximum response times are negligible and both are around 2.5 seconds. Pilots expressed a preference for frame times of 2 seconds or less. However, pilots were willing to accept longer frame times provided that information could be obtained from sufficiently long range so that proper action could be taken when required, and presented in a smooth enough manner so that the display would be easy to interpret.

Times

Mean/median/mode $\pm \sigma$

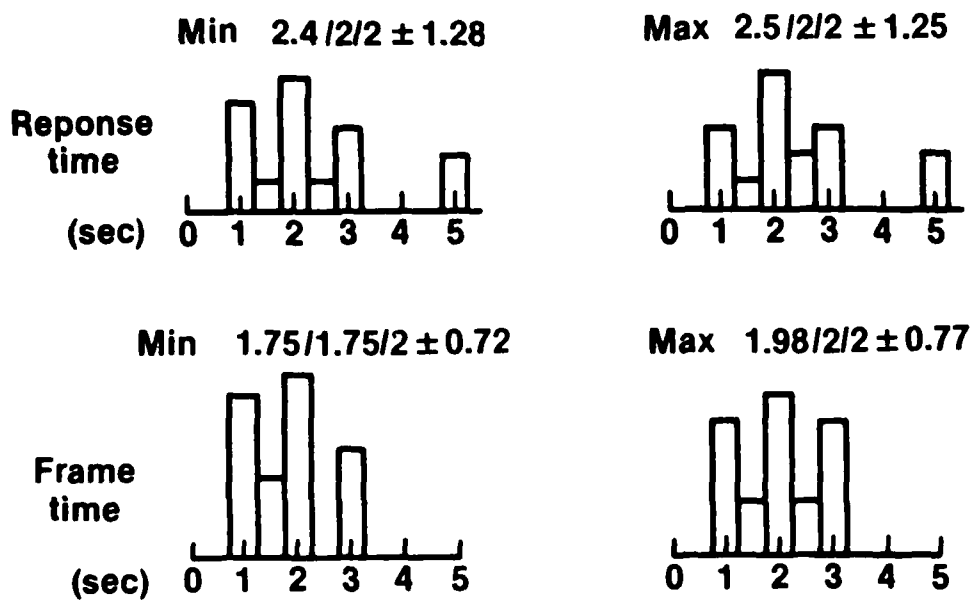


FIGURE 5.4 PILOT SURVEY DATA

6.0 SENSOR PERFORMANCE REQUIREMENTS

The basic mode of operation of Army aviation is VFR in which the pilot looks outside the helicopter at all times and uses visual data to avoid the terrain and large obstacles. The WWLODS must not interfere with this normal mode of operation and therefore it need only present data on wires and wire-like objects which the pilot does not see. The data must be presented in such a way that it does not require the pilot to look inside the cockpit and therefore must either be displayed on some form of HUD or provided by means of an audible or peripheral-vision signal.

The fundamental measures of performance of the WWLODS are R, FOV, and T_F . The requirements on these performance parameters are set by the maneuvers used by the pilot to avoid obstacles. The maneuvers, in turn, are determined by information available to the pilot, by the helicopter performance capabilities, and by pilot preferences. In general, helicopter flight performance is not limiting in these avoidance maneuvers. Pilots frequently do steep banks, steep pullups, and quick stops and are perfectly willing to perform abrupt transient maneuvers to trade speed for maneuverability, i.e., to trade kinetic energy for potential energy or drag energy, within the structural and aerodynamic limits of the helicopter. Army aviation operations do not usually require maximization of helicopter range. Therefore, wide variations in speed are accepted and are normally used.

In the analysis which follows, relatively mild, constant speed maneuvers are assumed. This provides a margin of safety in the sensor performance capabilities as estimated herein because much steeper or quicker transient maneuvers are well within the capabilities of both the pilot and the aircraft. This approach also simplifies the analysis and makes the basis for the design and performance choices made below easier to understand.

The sensor requirements are analyzed in this section for two flight situations, NOE and enroute or Contour flight. In both cases the Lateral Field Of View (LFOV) is symmetrical about the helicopter body axis. The effects of crab angle due to cross winds are discussed in Section 9.0. In the NOE mode of operation the Vertical Field Of View (VFOV) is referenced to the local horizontal and to the height of the helicopter above the ground, Δh , as shown in Fig. 6.1, because the velocity vector may vary rapidly through large angles in this flight regime. Δh is known from the radar altimeter which is available on all the aircraft. The maximum FOV is set by the window dimensions and the minimum range, R_{min} , and as discussed earlier is about 15° high by 24° wide.

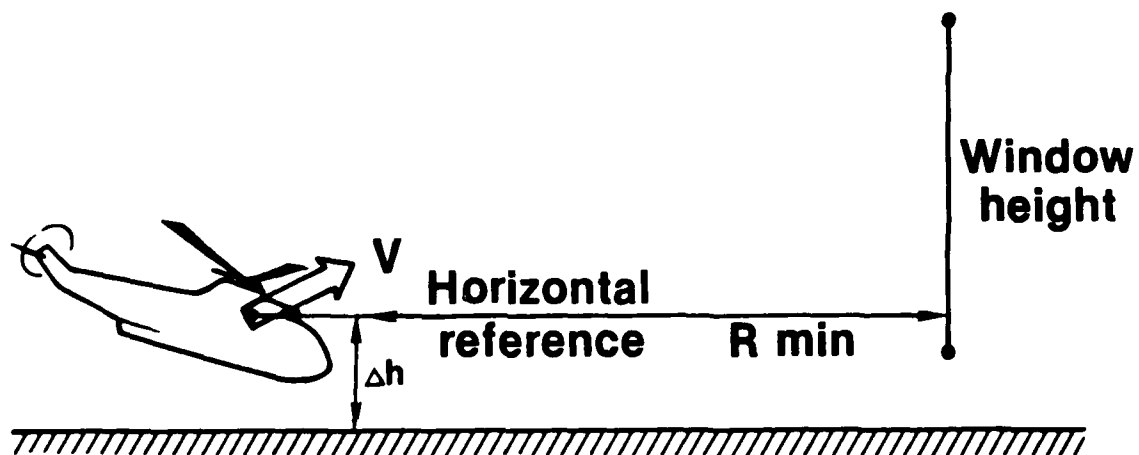


FIGURE 6.1 NOE VFOV REQUIREMENTS

The basic obstacle avoidance maneuver in NOE flight is a straight line stop performed by tilting the rotor back through an angle θ_T . The reason for this choice is twofold; first, the pilot normally does not want to unmask the helicopter and in fact would like to find the obstacle and either go under it or around it, and second, many of the aircraft would not have a HUD and therefore information on the location of the obstacle within the FOV cannot be presented without requiring the pilot to look inside the cockpit. Since this is contrary to the basic VFR mode of operation this choice is not acceptable to pilots. Without a HUD, presence of the obstacle can best be indicated by an audible or possibly by a flashing light signal. This tells the pilot that a clear window does not exist and his only option is then to stop and locate the obstacle visually. Even with a HUD, a pilot in NOE operations may elect to stop to look around for the best path before continuing his flight, in order to prevent unmasking.

The range required for the stopping maneuver is calculated by assuming that the speed remains constant for time equal to the sum of $T_F + T_R$ and that a constant deceleration equal to $g \tan \theta_T$ then takes place until the speed drops to zero. A safety margin of 50 ft (2 rotor radii) is added to the distance covered in this maneuver. The results of calculations of the range required for performing this maneuver with a 40° rotor tilt angle are shown in Fig. 6.2. This calculation is conservative because the deceleration actually starts before the end of the response time and because the obstacle warning could occur anywhere within the scan frame so that the average effective frame time would be $T_F/2$. The rotor tilt angle of 40° is accepted as reasonable by pilots. An increase in the speed can be allowed if steeper rotor tilt angles are used; for example, at a tilt of 60° the 2 sec $T_F + T_R$ curve moves to the right as shown by the dashed line in Fig. 6.2.

In Contour flight the pilot is less concerned with unmasking and more concerned with maintaining reasonably constant speed and therefore could go over or around an obstacle if the display is adequate to present the data to allow him to make the proper choices of maneuvers. In Contour flight the pilot always, of course, has the option to stop if he so desires. In Contour flight the WWLODS will be operated in the enroute mode and the VFOV will be referenced to the velocity vector, which is known from the LDNS and the HARS/VG data. The popup maneuver which would be used to go over the obstacle is shown in Fig. 6.3. The helicopter is initially flying a constant speed at a constant offset Δh parallel to the ground which has a slope of θ_C . The speed remains constant for a time equal to $T_F + T_R$ and the helicopter traverses path 1-3 in this time. At the end of T_R a pullup at constant load factor is made following path 3-4. This, in turn, may be followed by a straight line climb at a constant climb angle, θ_C , for a time T_C along path 4-5. A constant load factor pushover to level flight along path 5-6 finishes this maneuver. In a maximum (transient) pullup, steeper climbs could be used and the straight-line climb segment could be eliminated. Continuation of the pushover to dive angles and return to flight at a constant offset parallel to the ground on the other side of

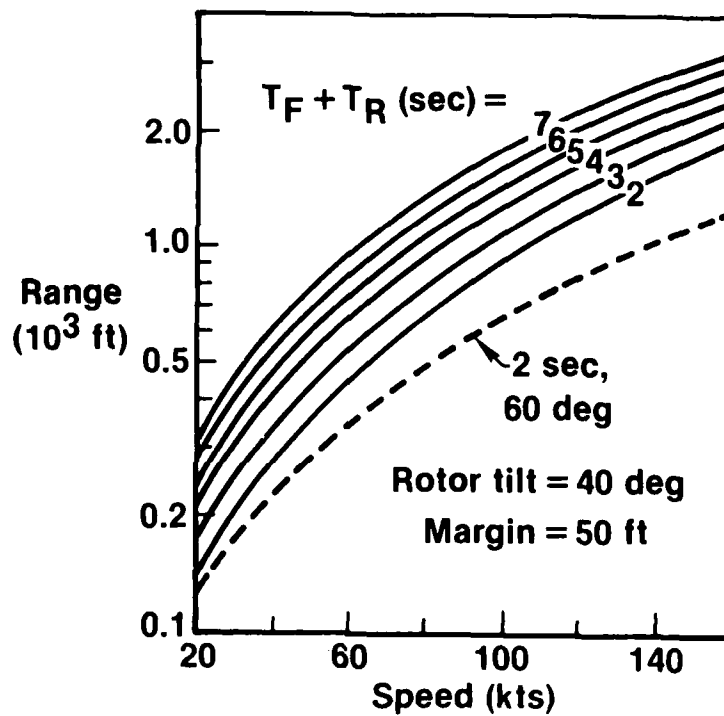


FIGURE 6.2 SENSOR RANGE REQUIRED FOR STOPPING MANEUVER

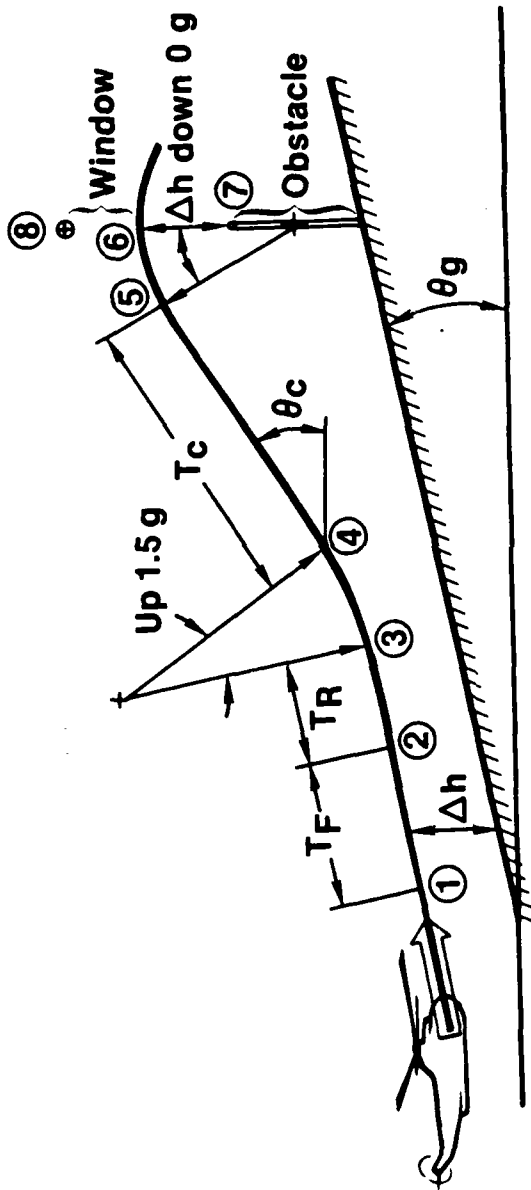


FIGURE 6.3 ENROUTE POPUP MANEUVER

the obstacle is a similar maneuver to the pullup and pushover but is always less demanding than the pullup maneuver. In this analysis a pullup load factor, UPLF, of + 1.5 g and a pushover load factor, DNLF, of 0.0 g, where 1.0 g = straight and level flight, are used. Army helicopters can typically perform flight maneuvers of +2.5 to 3 g and -0.25 to -0.5 g so a considerable margin exists when the pilot chooses to do more vigorous maneuvers.

The definitions of the sensor range, R_{sensr} , and VFOV requirements of the popup maneuver are illustrated in Fig. 6.4. R_{sensr} is measured from the beginning of the scan frame to the location of the obstacle (distance 1-7). The velocity vector is assumed to be parallel to the ground and therefore makes an angle θ_G with the local horizontal. The angle between the velocity vector and top of the clear window, UPFOV, is measured from the end of the frame (2-8). The angle to the bottom of the window, DNFOV, is measured from the point on the climb or pushover at which range is equal to R_{min} , to the top of the obstacle. The VFOV equals the sum of UPFOV and DNFOV and is greater than the angle defined by the window dimensions alone. R_{sensr} , UPFOV and DNFOV, depend on V , θ_G , Δh , UPLF, DNLF, θ_G , T_F , T_R and the height of the obstacle, HOBST. A simple computer program was written to evaluate R_{sensr} , UPFOV, DNFOV, and VFOV over a range of the above parameters and the results of a survey of the parameter space were reviewed to select a consistent set of sensor requirements. Figure 6.5 shows the range requirements for clearing a 100 ft obstacle with $T_F = T_R = 2.5$ sec, $R_{\text{min}} = 200$ ft, UPLF = 1.5, and DNLF = 0.0. These choices are somewhat conservative in that the sensor requirements would be less severe for lower obstacles, larger load factors, shorter T_F , longer R_{min} , etc. The value of 200 ft for R_{min} used in these calculations is less than the mean value of Fig. 5.1 so that the VFOV in these calculations is also conservative. Note that the range requirements are greatest for $\theta_G = + 8$ deg, reflecting the extra burden of flying uphill, and are greater for -8 deg than for 0.0 deg because of the longer pullup/pushover path. The range of θ_G from -8 to +8 deg is typical of rolling terrain such as would be found in the eastern part of West Germany. A tradeoff is possible between VFOV and R_{sensr} ; i.e., VFOV can be decreased if R_{sensr} is increased. Figure 6.5 corresponds to a VFOV of 20 deg. The limit of 20 degrees was chosen for VFOV because it provides some margin over the 15 degree value set by the NOE requirement and because it is a reasonable value from the standpoint of scanner technology.

The upper and lower bounds of the VFOV are shown in Fig. 6.6. At low speeds the maximum UPFOV is around 18 degrees and at high speeds the maximum DNFOV is about -18°. Therefore, the 20° VFOV must be capable of an additional roughly $\pm 10^\circ$ motion in the vertical direction. This requirement impacts on the scanner design as will be discussed in a later section. The LFOV required depends on the width of the window and on the value of R_{min} and is no different from the NOE requirement.

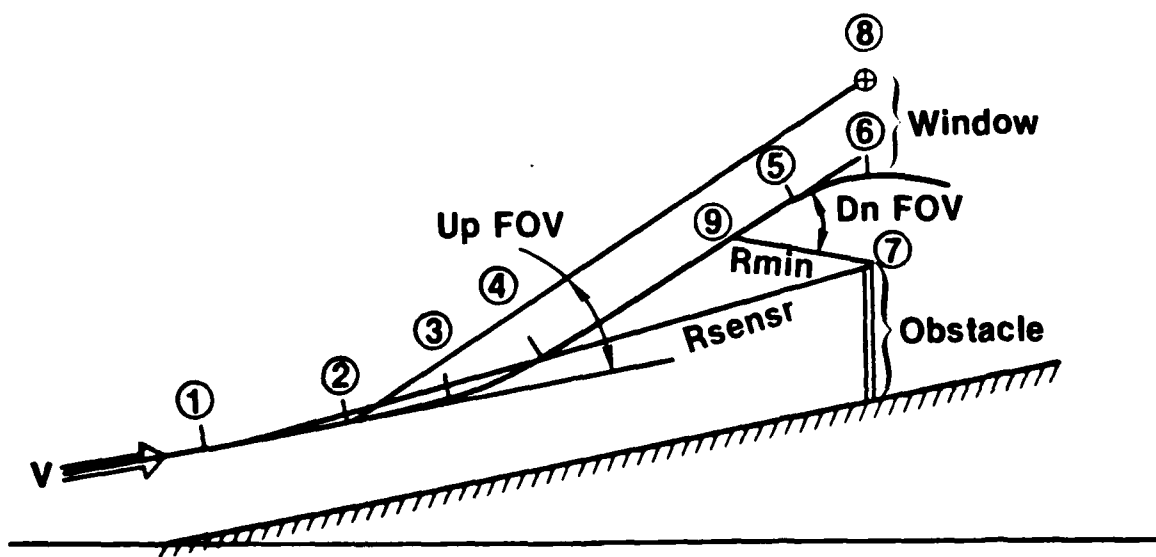


FIGURE 6.4 RANGE AND VFOV REQUIREMENTS FOR ENROUTE POPUP MANEUVER

$T_F = 2.5$ sec
 $T_R = 2.5$ sec

VFOV = 20 deg
HOBST \leq 100 ft

$\theta_C \leq 20$ deg
RMIN = 200 ft

UPLF = 1.5
DNLF = 0

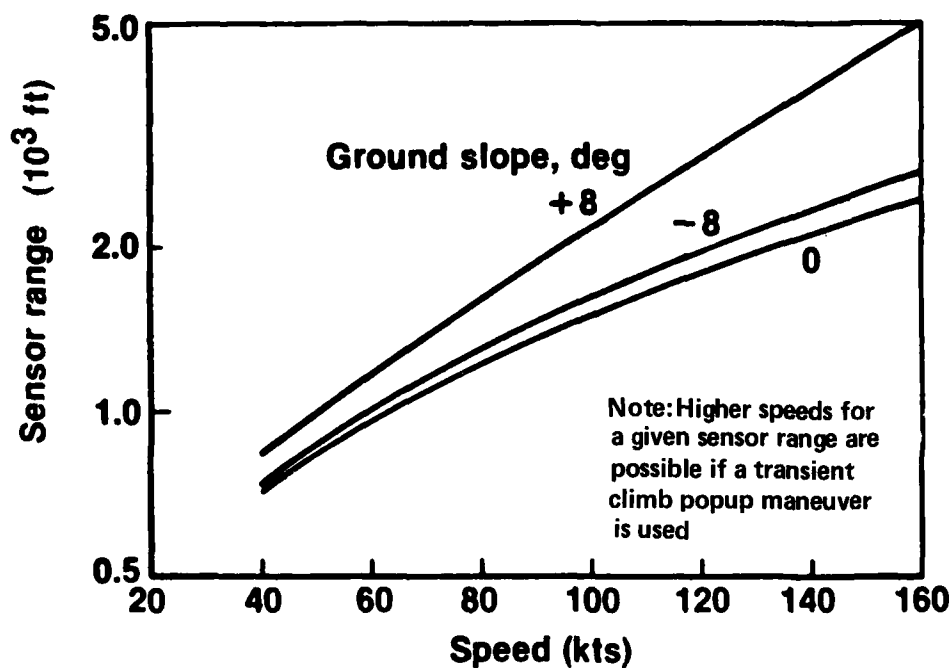


FIGURE 6.5 SENSOR RANGE REQUIREMENT FOR POPUP MANEUVER

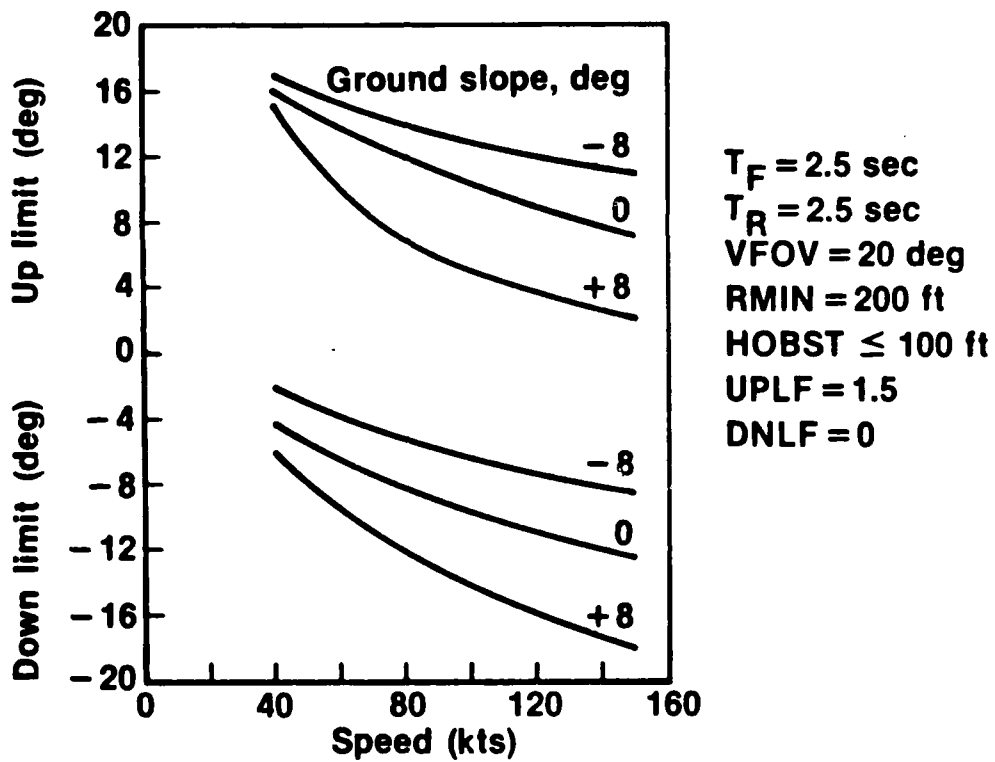


FIGURE 6.6 SENSOR VERTICAL FOV LIMITS FOR POPUP MANEUVER

An alternative to the enroute popup maneuver is the enroute turn maneuver shown in Fig. 6.7. In this maneuver the helicopter flies straight and level at constant speeds for a time equal to $T_F + T_R$, and then initiates a constant bank angle turn. In order to miss an obstacle which was initially directly on the flight path by a distance equal to half of the clear path required it must turn through an angle AB. If the maneuver is being performed simply to change direction then the angle turned through may be larger, as indicated by the angle ABC in Fig. 6.7. At the completion of the turn the helicopter must fly straight and level again for a time equal to $T_F + T_R$ in order to provide information that would permit it to avoid another obstacle if one appears on the new flight path. As indicated in Fig. 6.7, the sensor range required is the distance from the beginning of the frame to the far corner of the clear path and the LFOV is determined by the other two corners of the clear path. The case in which the obstacle is not on the initial heading of the helicopter is less severe than the one shown, therefore sensor requirements are derived based on the geometry shown in Fig. 6.7. In this analysis, it is assumed that this maneuver is performed completely in the horizontal plane. As a result the only parameters influencing the sensor performance requirements are the helicopter speed, the bank angle, θ_B , used in the turn, T_F , T_R , and the width of the clear path.

The resulting sensor performance requirements for $\theta_B = 30^\circ$, $T_F = 1.5$ sec, $T_R = 2.5$ sec, and clear path = 150 feet are shown in Fig. 6.8. It can be seen in Fig. 6.8 that for a constant turn angle the required sensor LFOV decreases and the required sensor range increases as the helicopter speed increases. It can also be seen that a sensor with longer range would permit flight at higher speeds and would require a smaller LFOV than would a sensor with lesser range. The angle AB also decreases with increasing sensor range or with increasing helicopter speed. As shown in Fig. 6.9, increasing the frame time to 2.5 sec shifts the whole performance map down and to the right, which requires increases in sensor range but permits small decreases in LFOV. A sensor LFOV of 30 deg provides a minimally useful turn capability if a range of 1.5×10^3 ft or more is available. A LFOV at 55 to 60 deg makes a much wider range of turn maneuvers possible and also allows the use of shorter ranges and slower flight speeds, which are useful in poor weather. The choice of a bank angle of 30° is conservative in terms of setting sensor requirements. A steeper bank angle would require less sensor range but would also require slightly larger values of LFOV.

Other avoidance maneuvers than that shown in Fig. 6.7 could be chosen by the pilot. For example, in the situation illustrated in Fig. 6.7 the obstacle would be detected at a range significantly greater than that at which the maneuver shown in Fig. 6.7 is initiated. Thus the pilot could have chosen to perform an avoidance maneuver such as an S-turn to displace his flight path to one side or the other by an amount equal to the required

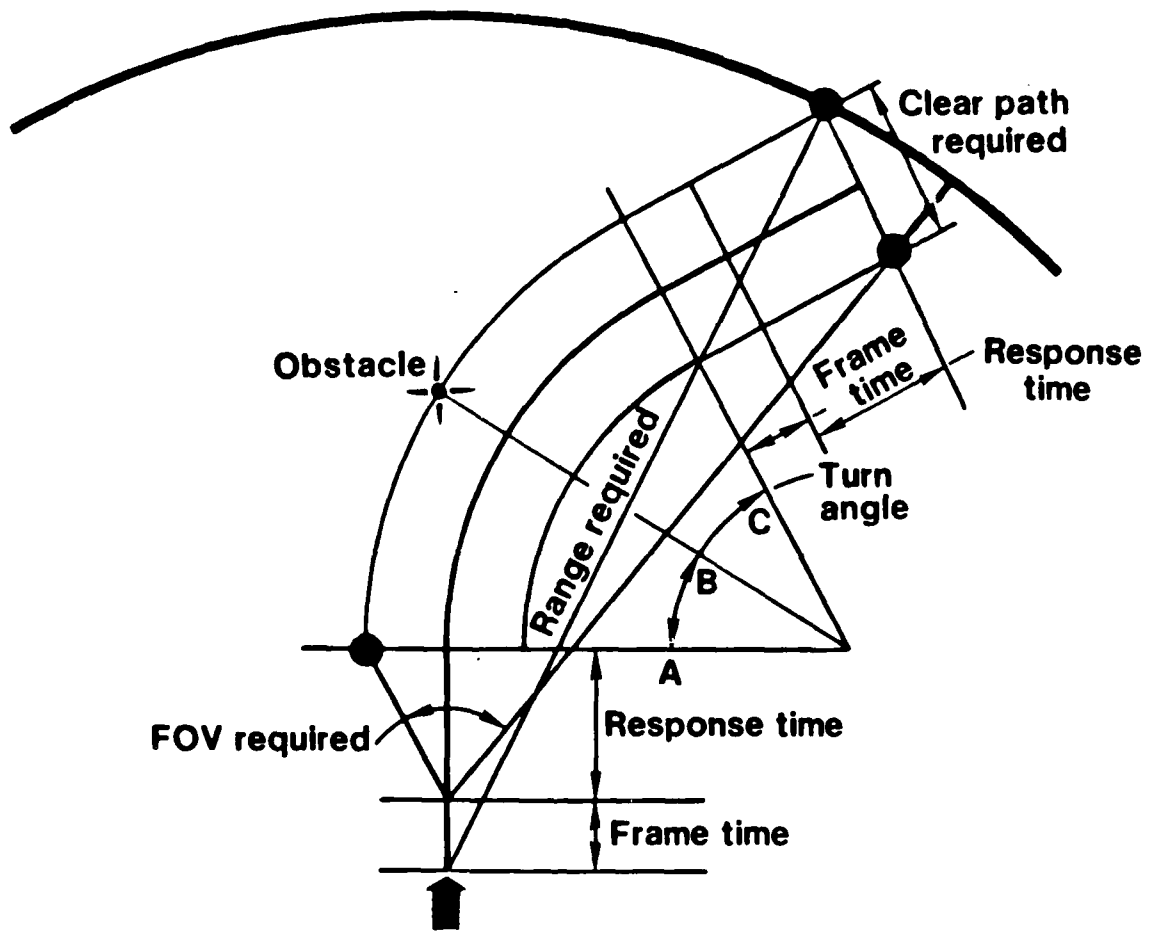


FIGURE 6.7 ENROUTE TURN MANEUVER

- Bank angle = 30 deg
- Response time = 2.5 sec
- Frame time = 1.5 sec
- Clear path = 150 ft

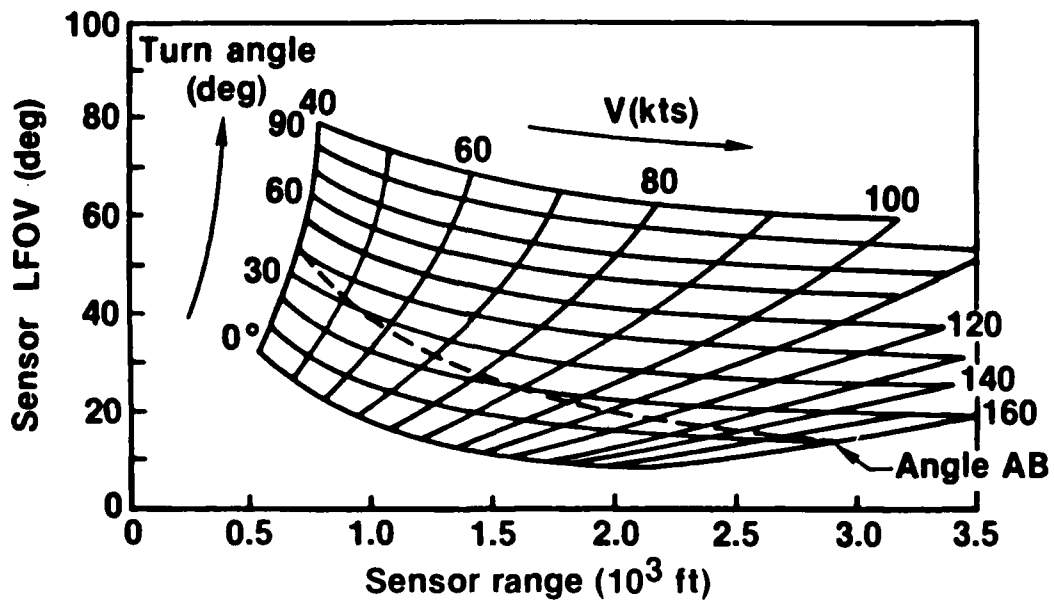


FIGURE 6.8 WWLODS FOV AND RANGE REQUIREMENTS FOR ENROUTE TURN MANEUVER

- Bank angle = 30 deg
- Response time = 2.5 sec
- Frame time = 2.5 sec
- Clear path = 150 ft

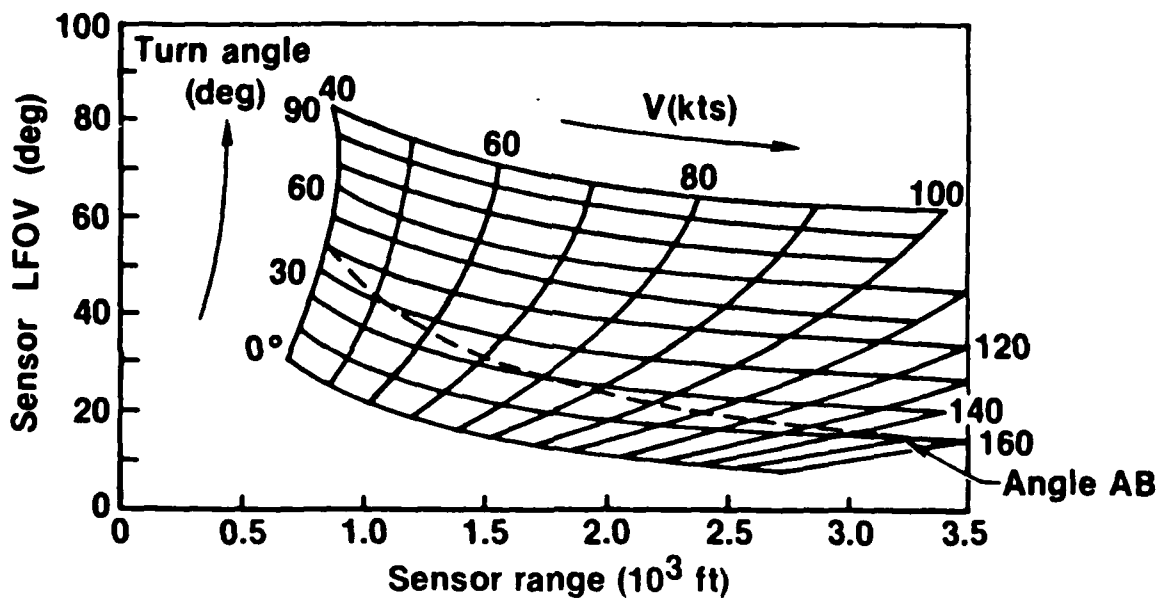


FIGURE 6.9 WWLODS FOV AND RANGE REQUIREMENTS FOR ENROUTE TURN MANEUVER

miss distance. The S-turn has no LFOV requirements beyond those of the clear window desired, but requires longer sensor range than the stopping maneuver used in the NOE mode because the S-turn is performed at constant speed. Other maneuvers, such as climbing turns, could also be used. Within the scope of this contract it was not possible to investigate all of these possibilities. The maneuvers described above represent the limiting cases in terms of sensor requirements and therefore are used to establish the boundaries within which the tradeoff studies used to select the three recommended approaches discussed later are performed. However, the use of these maneuvers in the tradeoff studies does not constrain the user of the WWLODS to these maneuvers in actual use. More severe maneuvers, such as transient pullups, would provide higher speed capabilities or greater safety margins, but an evaluation of their benefits would require the use of a 6-degree-of-freedom flight simulation which is beyond the scope of the present program.

The SOW requires that P_D , the probability of detecting a wire or wire like obstacle in a single resolution element, be a minimum of 0.9, and that P_{FW} , the probability of a false warning of such an obstacle, be in the range of 0.05 to 0.01. The latter criterion is closely related to the signal processing techniques used. In the case of a wire against a sky background, the criterion for the existence of a wire is a series of pulses which generate no return followed by one or more pulses which do generate a return. In this situation, P_{FW} is very low. The other criterion for recognizing a wire is the return of two signals from a single pulse, such as would result from a wire separated from the terrain background by a distance comparable to the spatial pulse length $c\tau$ where c is the speed of light and τ is the pulselength. However, it has been demonstrated experimentally at UTRC that when bare ground is illuminated at an angle close to grazing incidence, double returns can be obtained from sufficiently short pulses even though there is no obstacle in the beam. The reason for this is illustrated in Fig. 6.10. The diameter of the beam at range R is equal to $2R\lambda/D$ where λ is the laser wavelength and D is the transmitted beam diameter (scanner aperture diameter) and the physical length of the spot where it intercepts the ground is equal to $2R\lambda/D\sin\theta$ where θ is the angle between the beam centerline and the mean slope of the ground. If, as shown in Fig. 6.10, the length of the beam intercept on the ground is long enough compared to the length of the pulse, then the possibility of a double return from the ground exists. This would constitute a false warning signal under the second wire-recognition criterion. In order to avoid this, either the pulse length, τ , must be greater than $4R\lambda/cD \sin \theta$ or the angle $\theta \gtrsim \sin \theta$ must be greater than $4R\lambda/cD\tau$. The resulting relationship between range, grazing angle, and pulse length is shown in Fig. 6.11 for an aperture diameter of 2 in. and in Fig. 6.12 for a aperture diameter of 3 in. Since the vertical field-of-view has been selected to be 20° , if the grazing angle is 1° , then $1/20$ or 0.05 of the field-of-view could possibly return double signals from a single pulse even when there is no obstacle in the beam. This represents a

$$\text{Time of first return} = T_1 = \frac{2R}{c}$$

$$\text{Time of second return} = T_2 = \frac{2(R + d/\sin \theta)}{c}$$

$$\text{Pulse length for double return} > T_2 - T_1 = \tau > \frac{2d}{c \sin \theta}$$

$$d = 2R\lambda/D$$

$$\tau > \frac{4R\lambda}{cD \sin \theta}$$

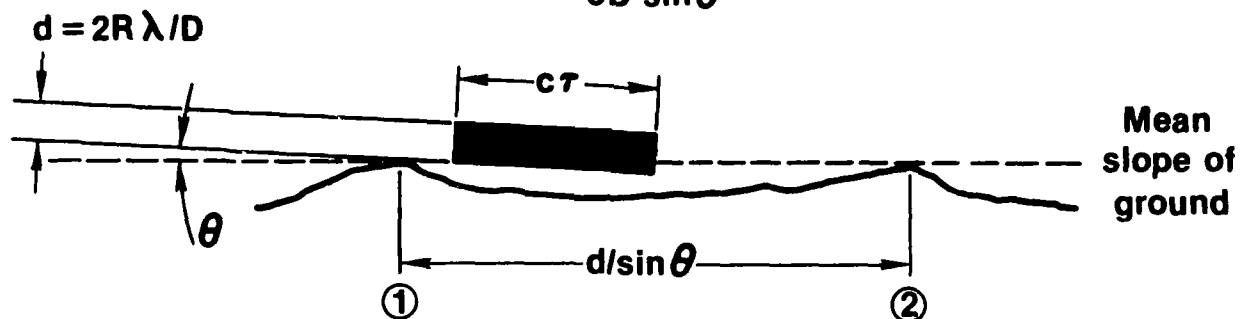


FIGURE 6.10 FALSE WARNING CRITERION FOR PULSE LENGTH

Aperture dia = 2 in.

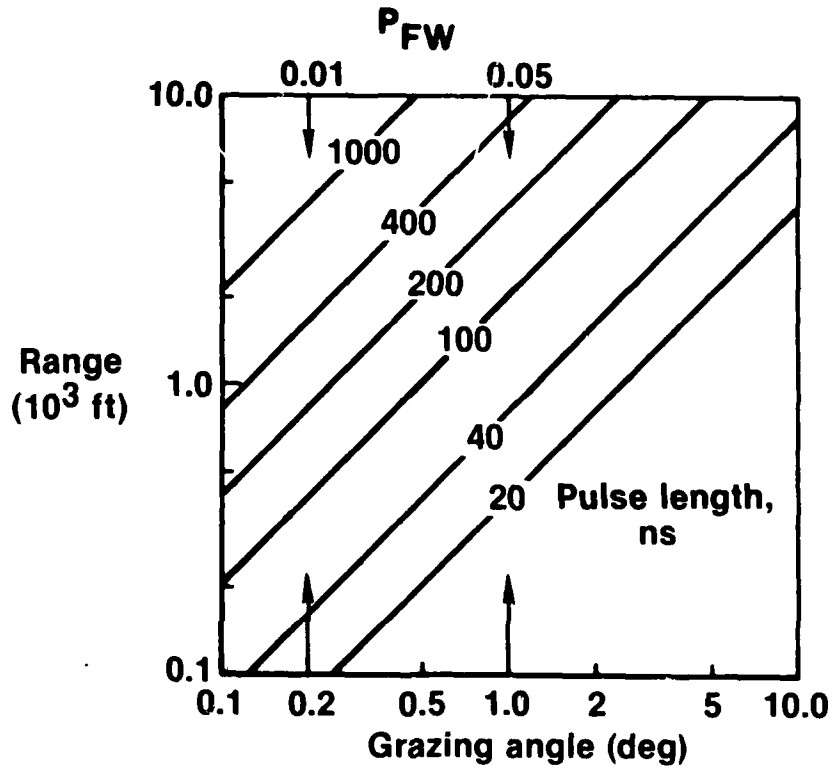


FIGURE 6.11 FALSE WARNING LIMITS ON RANGE AND PULSE LENGTH

Aperture dia = 3 in.

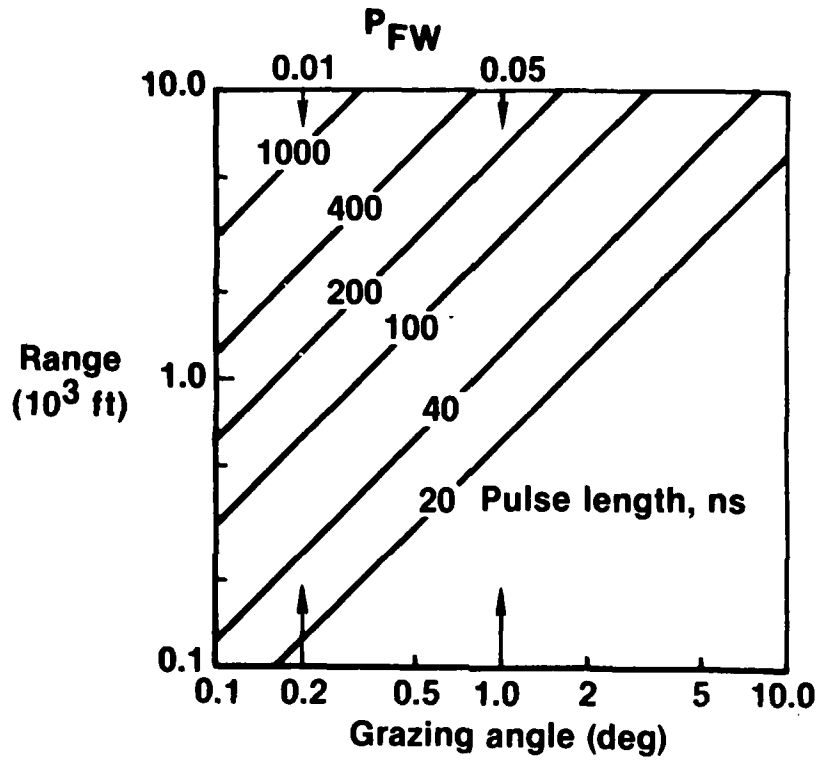


FIGURE 6.12 FALSE WARNING LIMITS ON RANGE AND PULSE LENGTH

possible false warning probability, P_{FW} , of 0.05. Similarly, a grazing angle of 0.2° represents a potential P_{FW} of 0.01. These conditions represent upper limits to P_{FW} since there is a significant probability that there will be no region within the FOV in which the grazing angle is small, whereas the probability that two such regions could exist within the FOV is relatively small. The use of these criteria in selecting desirable laser pulse lengths will be discussed in Section 9.0.

The final factor which must be considered in setting the sensor performance requirements is the scan pattern. The scan pattern requirements are dominated by the need to fly very close to the ground, at altitudes of 0 to 4 ft, in NOE flight. In this flight regime, small isolated obstacles and low fences are hazards which must be avoided. If the pilot wishes to select a particular clearance height above the ground then the scan pattern must provide a spacing of horizontal lines which is equal to $1/2$ of the selected clearance height, as indicated in Fig. 6.13, because the possibility exists that one scan line could pass just above an obstacle and if the line spacing were set at the selected clearance height the actual clearance could be much less than the line spacing. Thus, the vertical spacing between horizontal scan lines and the selected clearance height vary with the angular spacing between scan lines and range is indicated in Fig. 6.13. This horizontal-line scan pattern will also efficiently intercept the vertical poles which are necessary to support long horizontal wire spans. Vertical scan lines are also needed to intercept wires which may be suspended between supports which are farther apart than the width of the clear window. These lines may be spaced apart at distances on the order of 50 to 100 ft and therefore require vertical scan lines spaced at 1 to 3 deg. at ranges of 1000 to 2000 ft. Efficient scan patterns which meet these general requirements are discussed in more detail in Section 8.0.

Because the FOV is rectangular rather than square or circular and because the helicopter can bank at steep angles in normal operations, it is necessary to compensate for aircraft roll motions by rolling the FOV reference axes in the opposite direction. Most maneuvers will be made with bank angles of 40 deg or less, so that the minimum roll compensation required is 45 deg. However, a structural load factor of +2.5 g allows a bank angle of 66.4 deg to be used, so that roll compensation of up to 60 deg is desirable.

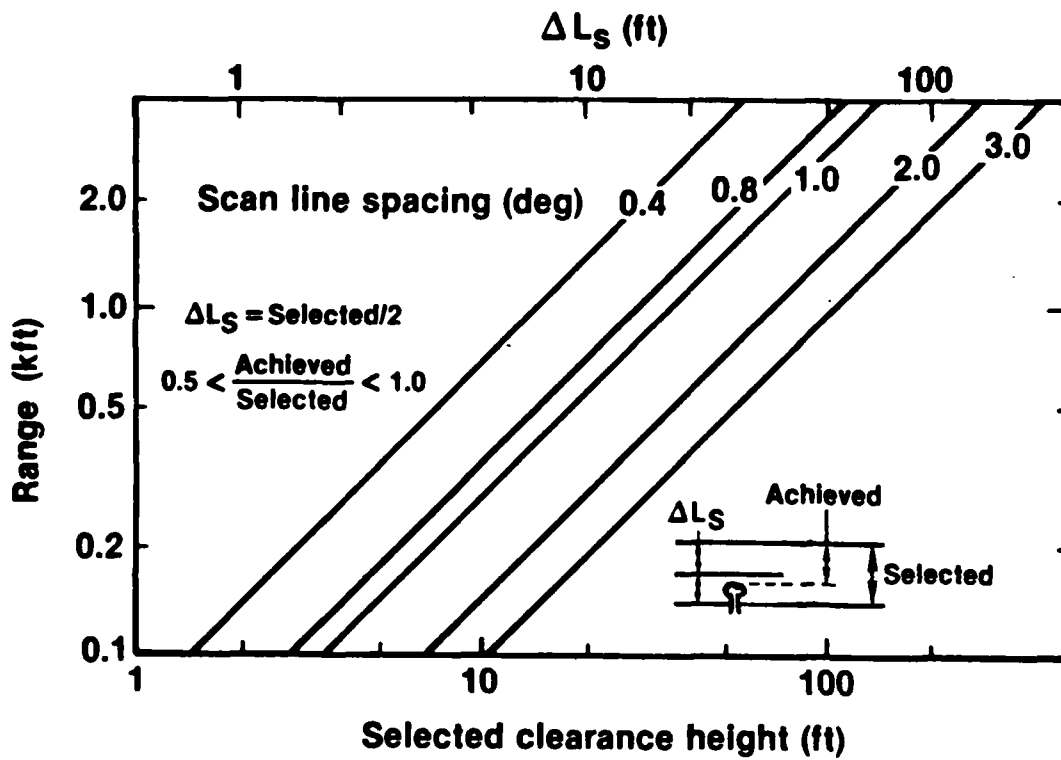


FIGURE 6.13 CLEARANCE HEIGHT

7.0 LASER TECHNOLOGY BASE

Recent development work at UTRC and elsewhere has demonstrated the potential of utilizing high pressure ceramic waveguide structures as a means of realizing an efficient, small, rugged, and air cooled laser gain section. Accordingly, we have used this technology base to estimate the size and weight of a family of CW and pulsed lasers with average output powers ranging from one to thirty watts. The discharge excitation assumed for estimating the power supply weight was CW electric. CW RF excitation is an alternate selection which has promise of providing a simpler laser structure with improved lifetime and with less complication to the power supply. However, at this time, there is insufficient information available to make a reliable determination as to any weight differences between the two excitation approaches, therefore, RF excitation should be carried along as an alternative approach in the WWLODS program.

As part of this contracted effort, experiments were conducted with both Al_2O_3 and BeO square-bore ceramic CO_2 waveguide lasers to determine fundamental performance parameters (Ref. 4). The tests were performed using sealed-off lasers with 36 cm long, 2.3 mm square bores, and 29 cm discharge lengths. Both passive and active Q-switched data were obtained at pulselengths from 30 to 700 ns and PRF's from 10 to 200 kHz. Data were also taken for CW laser operation. These data, together with data from other UTRC programs, form the basis for the scaling laws and the performance comparisons given in Section 9.0.

There are three basic approaches available to realize the pulsed laser format. Active intracavity modulation (Fig. 7.1 (A)) yields the shortest pulses but at the expense of a less efficient laser, increased cost, and complexity. Not to be ignored is the electronic driver for the intracavity modulator, which can require power comparable to the laser excitation. A simpler pulsed laser configuration is realized by employing pulsed RF excitation to realize gain switched spikes at PRF's on the order of 10 to 20 kHz. The major drawback which makes this otherwise attractive approach unusable is the long pulse tail, on the order of microseconds, which inescapably accompanies the narrow gain switch spike, which can be less than a few hundred nanoseconds. The simplest overall pulsed laser candidate configuration is the passively Q-switched laser (Fig. 7.1 (B)). This transmitter approach utilizes an intracavity SF_6 cell to passively Q-switch a CW excited laser gain section. This is a simple, reliable, inexpensive laser which uses a precise selection of laser gain characteristics and SF_6 saturation and recovery characteristics to yield the desired pulsewidth and PRF. PRF's greater than 100 kHz and pulsewidths of 150 to 200 nanoseconds have been demonstrated with this technique. Because it is simple, efficient, and reliable, we have selected the passive Q-switched laser as the baseline pulsed transmitter for the WWLODS.

The laser analysis also provided impetus for consideration of a CW FM laser transmitter format (Fig. 7.1 (C)). In this scheme a CW excited laser is FM chirped,

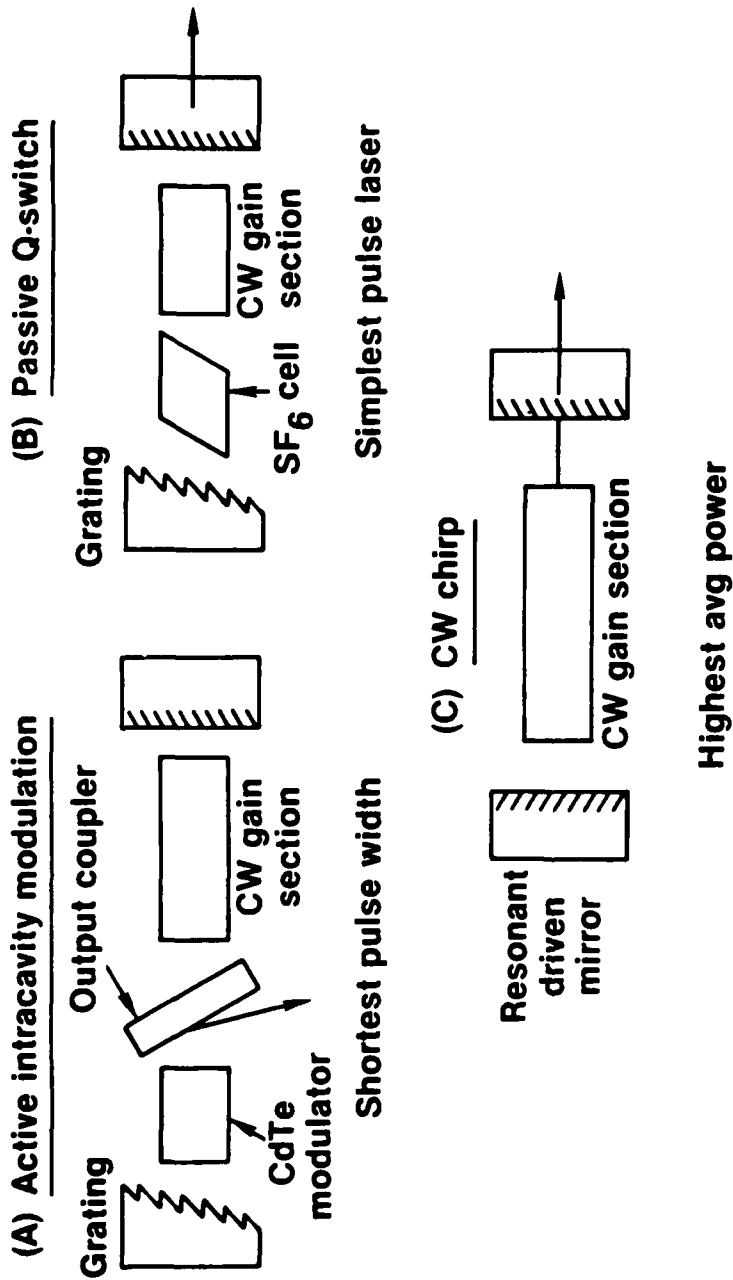


FIG. 7.1 BASIC LASER CONFIGURATIONS

transmitted, and the returned radiation heterodyned with a sample of the current laser radiation; range information being recovered by virtue of the difference in frequency that results from the time delay between the reflected and current laser radiation. This is attractive because it eliminates a separate laser local oscillator and the attendant frequency locking components and, most importantly, it provides a more efficient laser because of the absence of intracavity elements. This difference in efficiency is most pronounced for low power lasers (because of the lower gain-to-loss ratio) and this efficiency could be realized if a simple length tuning modulator (a PZT, for example) is utilized for the modulator. For example, we estimate that a 1 watt average power pulsed laser could yield an 8 watt CW laser if chirped with a PZT. A 10 watt average power pulsed laser, on the other hand, would convert to a 30 watt chirp laser. The above significant advantages must be tempered by the following uncertainties.

- a) It has not been demonstrated that a CW chirp modulation format can be realized with sufficient accuracy to enable wire discrimination to be realized at a pixel rate on the order of 50 kHz.
- b) A signal processor has not been conceived (at least by UTRC) at this date that can discriminate wires at high pixel rates in the presence of the potential Doppler ambiguity that will result from the platform motion and wind-driven background motion of vegetation.

Because of the uncertainties, the FM CW-chirp laser cannot be considered as the baseline laser for WWLODS. However, in order to evaluate the upper bound of the potential performance improvements, range calculations were done assuming ideal signal processing of the FM CW signal, i.e., no loss in SNR due to processing ambiguities. These results are given in Section 9.0. The potential system performance improvements that could result from its higher power are sufficiently attractive (as discussed in Section 9.0) that it is recommended that this laser be carried as an alternative approach that would be selected if the above problems were solved.

The technology considerations involved in choosing laser design approach are summarized in Table 7.1. The implications of the technology choices on laser weight are illustrated in Fig. 7.2. The primary factor is the power in the CW laser discharge (scale A). This determines both the power supply weight (scale B) and the dimensions of the ceramic discharge tube. The tube dimensions determine its weight (scale C). The spread in the weights in Fig. 7.2 corresponds to the range of conditions from a benign laboratory environment (bottom of band) to a severe military environment (top of band). Commercially available waveguide lasers can be obtained that fall on this bottom line. The top line corresponds to a very conservative preliminary design study done by UTRC. For the weight estimates used in Section 9.0, the weight of the ceramic tube was taken at the middle of the band shown in Fig. 7.2. The laser power that is obtained for a given weight of tube plus power supply is read from scale D for the FM CW chirp laser and from scale E for the passively Q-switched laser.

**TABLE 7.1 SUMMARY OF
LASER TECHNOLOGY CONSIDERATIONS**

	CW chirp	Passive Q-switch	Active Q-switch
Weight	Lightest	Nominal	Heaviest
Complexity	Least	Nominal	Greatest
Wire discrim.	Uncertain	Demonstrated	Demonstrated
Efficiency	Highest	Nominal	Poorest
Cost	Cheapest	Nominal	Greatest
Conclusion	1) Needs more study and field test 2) Risk = Modul. and signal processing uncertainties 3) Attractive alternative approach	1) Lowest development cost and time 2) Risk = Higher weight and cost than CW chirp 3) Baseline approach	Not competitive

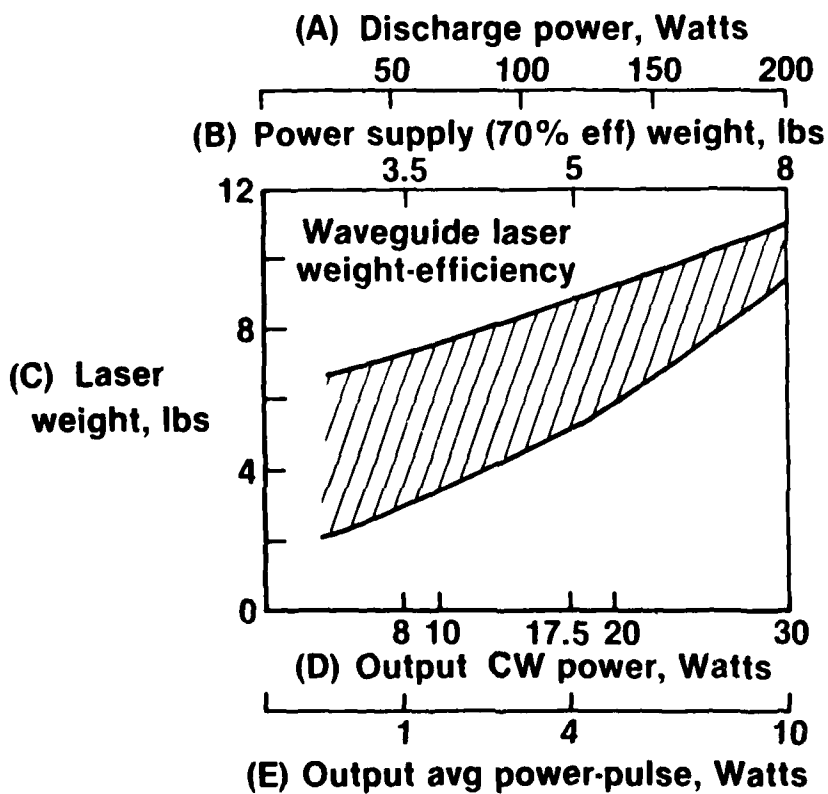


FIG. 7.2 LASER WEIGHT CONSIDERATIONS

8.0 SCANNER DESIGN STUDY

The scanner requirements are determined by the mission analysis of Sections 5.0 and 6.0. A baseline set of requirements, selected as a compromise between the desired capabilities identified in the analysis and the practical limits on scanner mechanisms, is shown in Table 3.1. These requirements were used as a standard of comparison in selecting candidate scanner mechanisms. A discussion of the salient features of the WWLODS scanner candidates is presented in Section 8.1, and a discussion of dither mechanism candidates in Section 8.2. Dither mechanisms are used to produce small, high frequency scan motions which must be superimposed on some scan patterns in order to fill in long narrow gaps in their basic pattern. Section 8.3 contains the results of tradeoff studies comparing the various scanner candidates and Section 8.4 summarizes the results which led to the selection of a baseline scanner for a more detailed investigation and the parameters of the detailed baseline design.

8.1 Scanner Candidates

The scanner study considered the design and performance parameters and the scaling relationships of five scanner candidates: (1) dual rotating wedges (1 pair); (2) dual rotating wedges (2 pair); (3) a dual wedge (1 pair)/turret combination; (4) a ball joint scanner, and (5) a variable wedge scanner. These candidates, which are described in the following subsections, were selected for their large aperture (2 in. - 4 in.) and potential for rapid scan.

Rotating Wedges - 1 Pair

The beam deflection resulting from a dual wedge scanner, diagrammed in Fig. 8.1, is based on the refraction of light by a prism. Although the exact deviation of the output beam, relative to the input beam, of a prism, is a function of the angle of incidence, an approximation for the deviation, δ , of a prism in air, is given by:

$$\delta = (n - 1) \alpha$$

where n is the index of refraction of the prism material and α is the apex angle of the wedge. For 10.6 micron wavelength applications, the optimum material choice is Germanium because of its high refractive index (4.0). A number of other materials were checked for this application, but all had both lower indices of refraction and poorer index-to-density ratios. The latter means that even if a larger angle prism were used to achieve the same deflection with a lower index material, the wedge would be heavier than the Germanium wedge.

The use of two identical wedges, rotated by torquers and programmable by encoders and a servo loop, allows the output beam to be directed to any angle from zero to approximately 2δ compared to the input beam direction. This agility, with

Table 8.1
SCANNER REQUIREMENTS

Field of view:	20° El x 30° Az minimum, 20° El x 60° Az desired
Field of regard:	40° El x 30° Az minimum, 40° El x 60° Az desired
Scan pattern coverage:	
Max. El. spacing	0.5° - 1.0°
Max. Az spacing	3.0° - 4.0°
Frame time:	2.5 sec maximum
Frame rate:	Determined by scan pattern and velocity
Scan velocity:	Determined by laser PRF and resolution element overlap or by torquer limits
Output beam diameters:	2, 3, & 4 in.
Roll compensation:	
Minimum	± 45°
Desired	± 60°

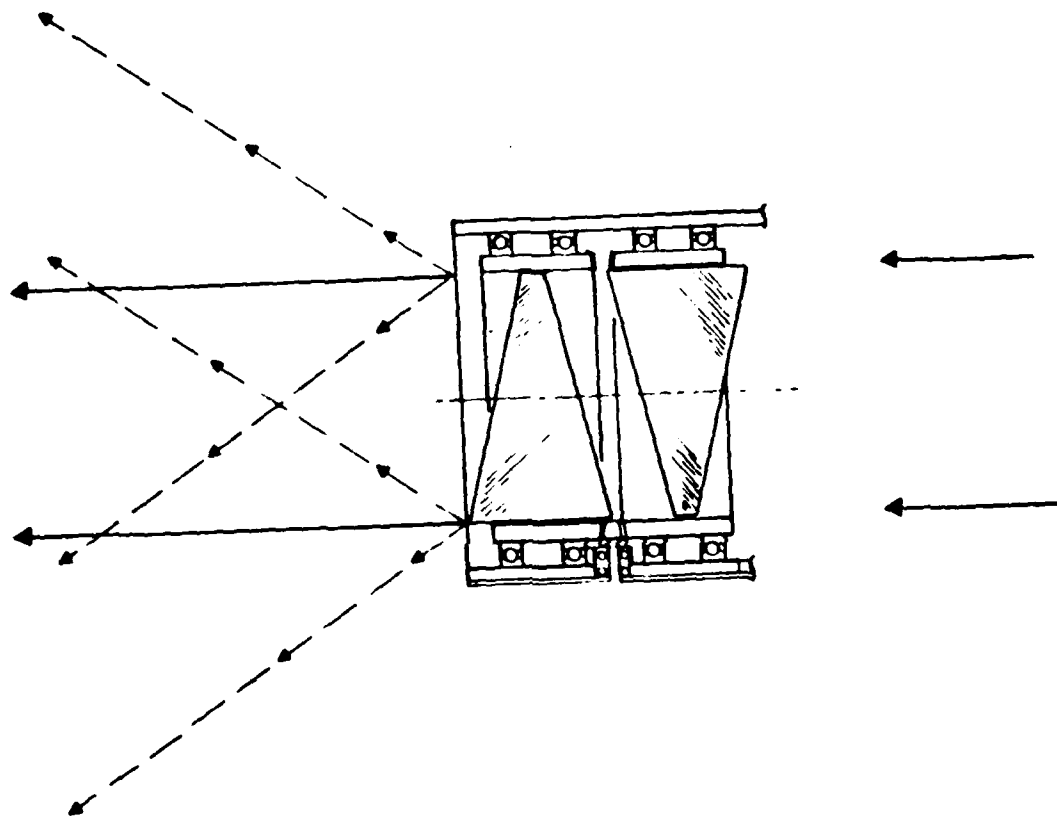


FIGURE 8.1 1-PAIR DUAL WEDGE SCANNER

proper programming, allows any scan pattern to be synthesized, although some patterns will have much larger torque requirements than others. The programmable nature of this scanner also means that pitch and roll compensation may be incorporated into the scan pattern commands so that no additional mechanism is required in order to provide this capability. The torque requirements, must, however, be examined for each case.

Rotating Wedges - 2 Pair

The 2-pair wedge scanner, diagrammed in Fig. 8.2, operates on the same principle as the 1-pair scanner above. The second pair of wedges, does, however, allow additional versatility in the programming of scan patterns and hence the possibility of significantly reducing the torque requirements for a number of scan patterns. For instance if the right wedge pair, marked AZ in Fig. 8.2 is run continuously in a counter-rotating manner, the output beam will be scanned in a horizontal direction and no reversing torques will be required by this wedge pair. The EL pair may then be used to slowly scan the horizontal line up and down with only moderate torques required in reversing the wedge rotations.

Wedge/Turret Combination

The wedge/turret combination scanner, diagrammed in Fig. 8.3, is a combination of the one pair dual wedge scanner with a single dimension scanning mirror and a turret. This combination allows additional versatility in programming scan patterns and hence, the possibility of significantly reducing the torque requirements for a number of scan patterns.

For instance, if the wedge pair of Fig. 8.3 is used to generate a horizontal line scan, the two torquers can run continuously in a counter-rotating manner so that no reversing torques will be required. The pitch mirror is used to slowly scan the pitch turret and rotating wedges up and down to generate an elevation scan. Alternatively, the wedge pair can be used to generate a small, optimized scan pattern and the pitch scan can be used to direct the pattern over a larger Field Of Regard (FOR). In the configuration diagrammed in Fig. 8.3, the angular motion of the pitch turret must be twice that of the pitch mirror so as to keep the wedges and turret centered about the beam. This "divide by two" relationship could be avoided if the pitch mirror and turret are designed to rotate as a unit about the axis of the telescope output beam; however, this would require the turret to ride as an outrigger offset from the pod which would entail additional structure weight.

Ball Joint Scanner

The ball joint scanner, diagrammed in Fig. 8.4, is a moving mirror scanner which the Norden Systems Division of UTC has found to be particularly suitable for applications which can use a dedicated scan pattern. In general, a moving mirror scanner would not be practical for a programmable or variable scan pattern,

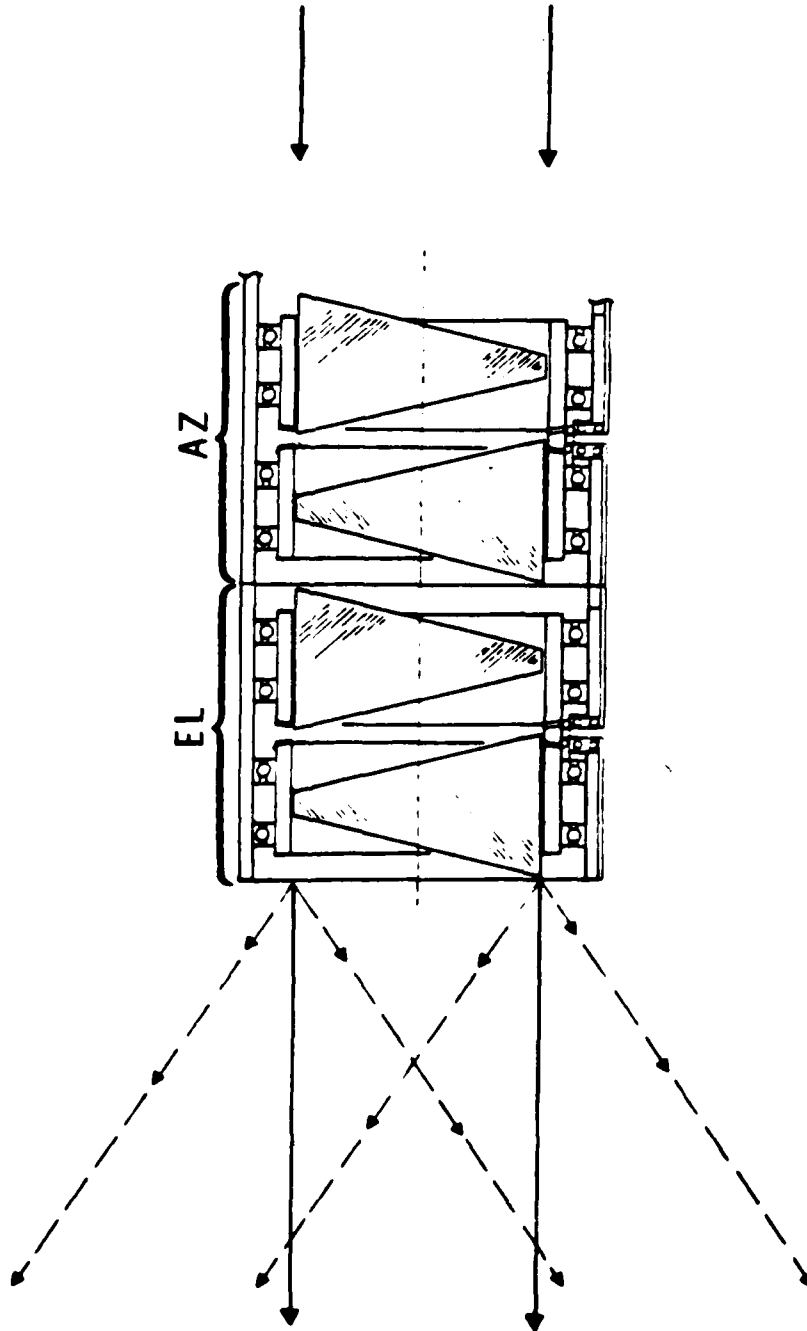


FIGURE 8.2 2-PAIR DUAL WEDGE SCANNER

90-6-17-46

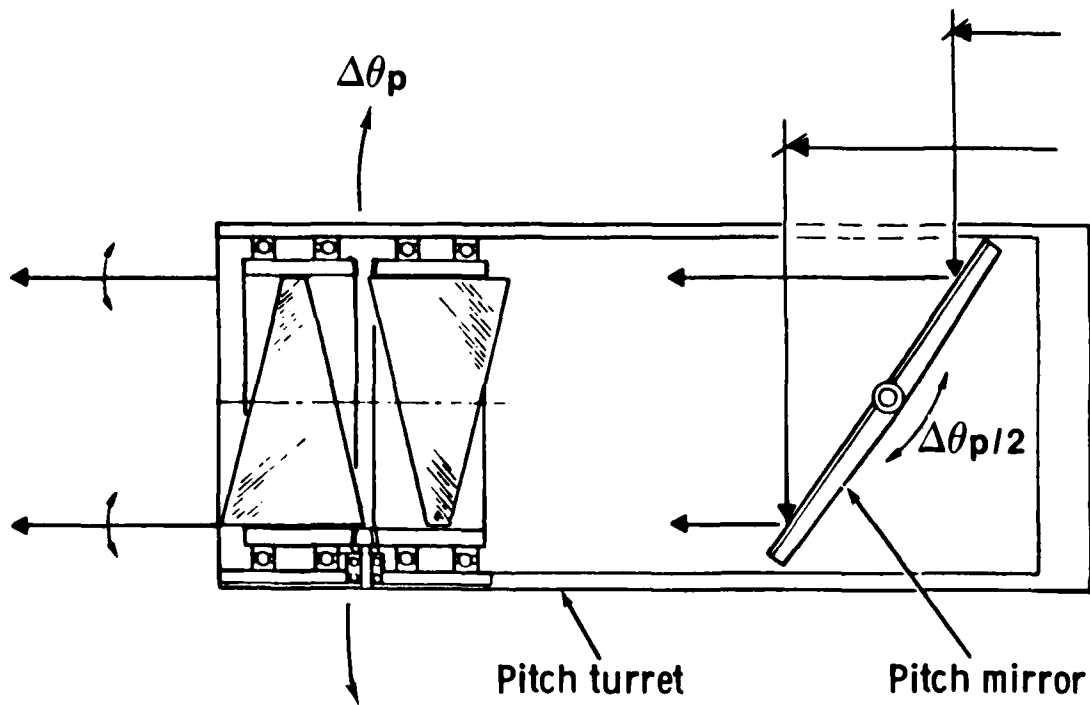


FIGURE 8.3 DUAL WEDGE/TURRET SCANNER

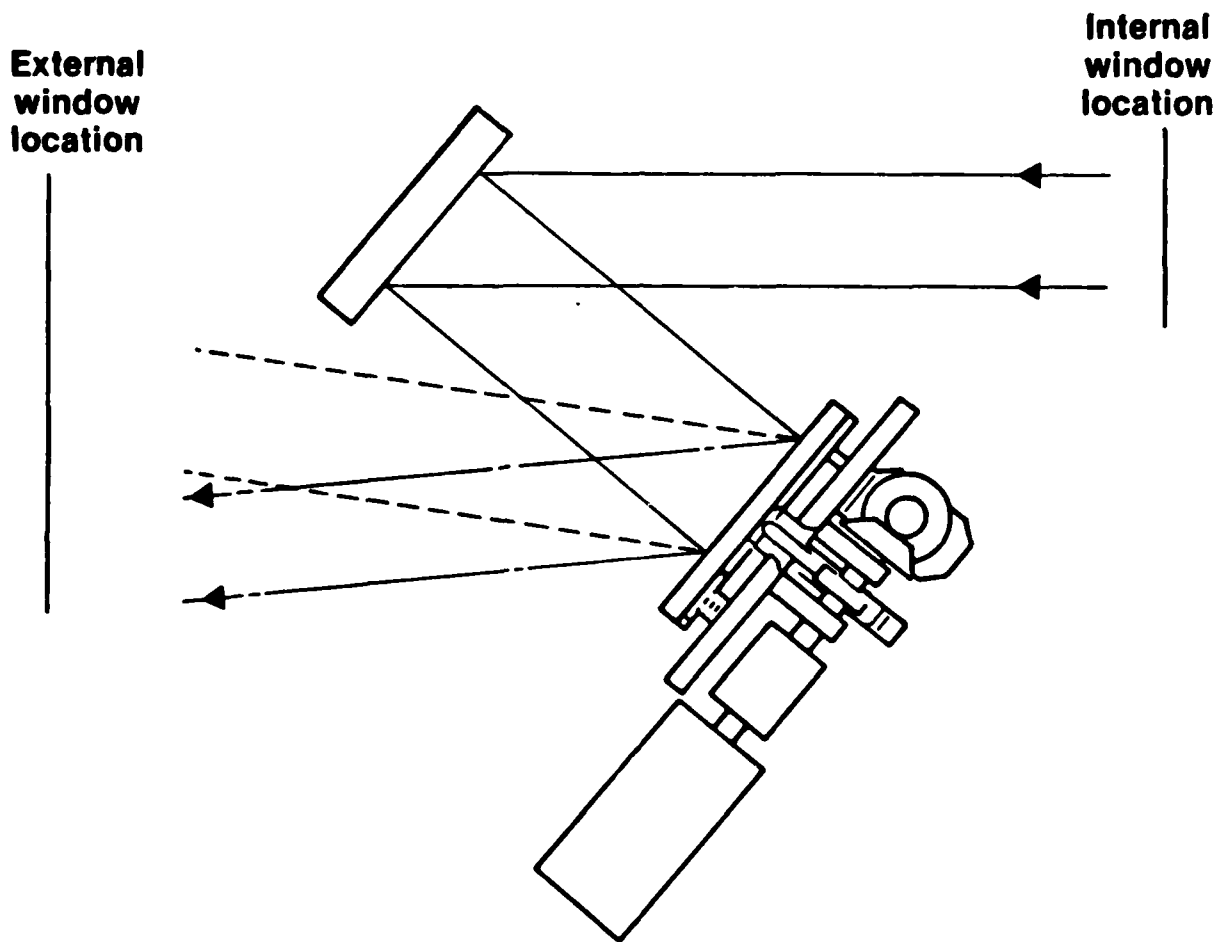


FIGURE 8.4 BALL JOINT SCANNER

except for low scan rates, since some sort of torquers would have to scan the large inertia of the deflecting mirror in two dimensions to provide the desired scan. This would not meet the WWLODS requirements. The ball joint scanner, however, provides the scanning motion by means of cams which drive the mirror about a central ball joint pivot point. Two cams driven from a common drive motor provide an efficient, dedicated scan pattern. For the WWLODS application, which can utilize a dedicated scan pattern, the ball joint scanner is simple and lightweight.

In contrast to the scanners employing rotating wedges, the ball joint scanner requires a window of some sort to keep atmospheric contaminants from the beam expander and laser components. If a window is placed on the output side of the scanner it must be fairly large, if large beams and scan angles are employed. In the wedge scanners, by contrast, the last wedge can also act as a window if care is taken to achieve a seal at the rotary joint. An alternate window location for the ball joint scanner is in the optical train between the turning mirror (top left in Fig. 8.4) and the beam expanding telescope located to the right and out of the figure in Fig. 8.4. In this case, the ball joint mirror and the turning mirror must have environmentally hard coatings which, although not common, do exist according to 10.6 micron mirror coating vendors.

As stated earlier, the ball joint scanner provides a dedicated scan pattern. The particular scan pattern will be discussed in the scanner trade-off section; however, the dedicated nature means that pitch and roll compensation must be provided by adding additional servo motors and mechanical mechanisms in order to superimpose these corrections. This can be done, and the discussion below describes a simple implementation which incorporates both pitch and roll compensation mechanisms.

Variable Wedge Scanner

The variable wedge scanner, diagrammed in Fig. 8.5, is based on the refraction of light by a prism. As discussed above, the deviation, δ , of a thin prism in air is given by:

$$\delta = (n-1) \alpha$$

where n is the index of refraction of the prism medium and α is the apex angle of the wedge. In the variable wedge scanner, the prism medium is a liquid contained between two windows in a flexible cell and the apex angle, α , is varied in order to scan the beam. This type of scanner has been successfully employed in image motion compensation systems where it has the trade name "Dynamens".

In order to be successful for the WWLODS application, this type of scanner requires a high index, transparent liquid for the 10.6 micron wavelength. During

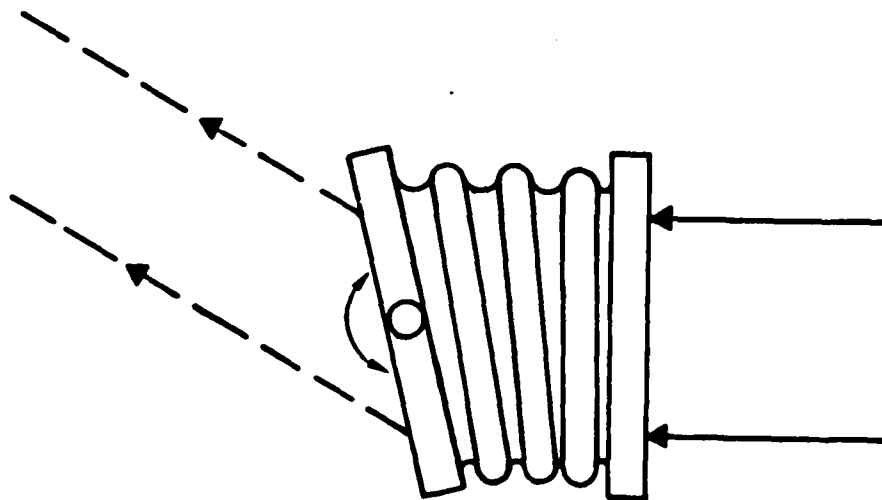


FIGURE 8.5 VARIABLE WEDGE SCANNER

this program, an investigation of fluids which might be applicable identified CS_2 , CCl_4 , C_2Cl_4 and CH_2I_2 as candidates with low corrosive and toxic problems. The analytical chemistry group at UTRC tested the 10.6 micron transmission qualities of the four liquids and found only CS_2 promising from the transmission measurements. The index of refraction listed in the Handbook of Chemistry and Physics for CS_2 is 1.62, which is relatively low compared to that which is desired for implementing a large deviation angle scanner. For this reason, this type of scanner will probably only be useful for small angle scan requirements such as a dither scan to fill in the gaps in the scan pattern of some other type of scanner, such as a rotating wedge scanner. Therefore, the variable wedge scanner was not considered further as a candidate for the main WWLODS scanner.

8.2 Dither Mechanism Candidates

In order to fill in the gaps in raster-type scan patterns, some type of beam dither mechanism may be required. For example, if a scan pattern were generated which consisted of only horizontal scan lines, separated by 0.8° , then long, horizontal wires might go undetected. If a high frequency vertical dither of $\pm 0.4^\circ$ were superimposed on the horizontal scan lines, then the gaps would be filled. The frequency of the dither would, in turn, determine the effective horizontal scan spacing. For a $20^\circ \times 30^\circ$ scan pattern frame which is covered in 1.5 seconds in two interlaced fields, the dither frequency required to provide a 4° effective horizontal scan spacing would be 250 Hz. Similarly, a 0.8° effective horizontal scan spacing would require a 1250 Hz dither scan frequency. It is worth noting that the 0.8° or 4° effective horizontal scan spacing is stated in terms of the output beam scan pattern. If the dither scan is implemented in the optical train before the beam expanding telescope the peak-to-peak scan to be provided by the dither mechanism must be M times greater than the 0.8° to 4° , where M is the magnification of the beam expanding telescope.

Candidates to provide the dither scan, if required, are (1) a variable wedge scanner, (2) a tilting wedge scanner, or (3) a pre-expander galvanometer mirror scanner.

Variable Wedge Dither Mechanism

The variable wedge scanner shown in Fig. 8.5 is one candidate for a dither mechanism. The previous discussion detailed the operating principles for this candidate and indicated that, because of present materials limitations, it is limited to small scan angles such as dither requirements. It does require that the window, bellows and fluid be moved at the dither frequency. For this reason, it is not a preferred approach for a high frequency dither mechanism.

Tilting Wedge Dither Mechanism

The basic elements of a tilting wedge scanner and its operating region are diagrammed in Fig. 8.6. The scanning action results from the fact that the deviation of a prism is dependent on the angle of incidence, θ , of the input beam. The thin prism approximation discussed in earlier sections applies to the minimum deviation region which is the relatively flat bottom portion of the θ vs δ curve in Fig. 8.6. If the prism is operated such that the incidence angle is in the region of operation shown on the curve, the output beam deviation will vary rapidly in response to a rotation of the wedge. This mechanism was initially investigated as a potential scanner mechanism; however, the attainable range of deflection angles was too small. It is, however, a candidate for a dither mechanism.

Pre-Expander Galvanometer Mirror Dither Mechanism

In the pre-expander dither mechanism of Fig. 8.7, a galvanometer mirror is used to dither the beam while it has a small diameter -- prior to beam expansion by the telescope. In this region, the angular dither amplitude must be larger than for a post-expander dither mechanization but the beam is smaller and the angular accelerations are more easily accomplished because inertia of a small diameter mirror decreases as approximately D^3 , while the angular motion increases as D .

In the diagram of Fig. 8.7, relay optics are used to optically couple the galvanometer scanner to the beam expanding telescope in order to overcome field-of-view problems which occur due to beam displacement in a nonrelayed system. Although other combinations of dither and telescope elements are possible, this mechanization serves to illustrate the basic concept of small diameter, low inertia pre-expander scanning of the beam in order to achieve the desired dither scanning.

8.3 Scanner Candidate Trade-Offs

A major task of the WWLODS scanner study was to assess the capabilities, weights and requirements of the candidate scanners in order to provide inputs to the system analysis and aid in the selection of the most promising candidate for a more detailed examination. The following sections summarize the results of these trade-off studies.

Scan Parameters

The scan parameters for the four candidate scanners are summarized in Table 8.2. It is seen that scanners involving rotating wedges have large FOV and FOR capabilities, whereas the ball joint scanner is more limited. This stems

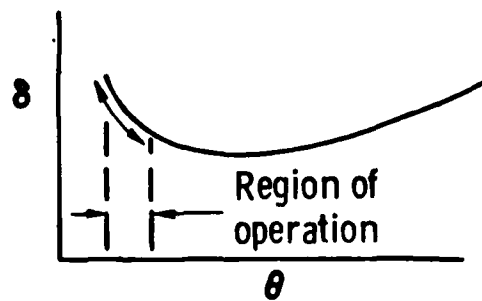
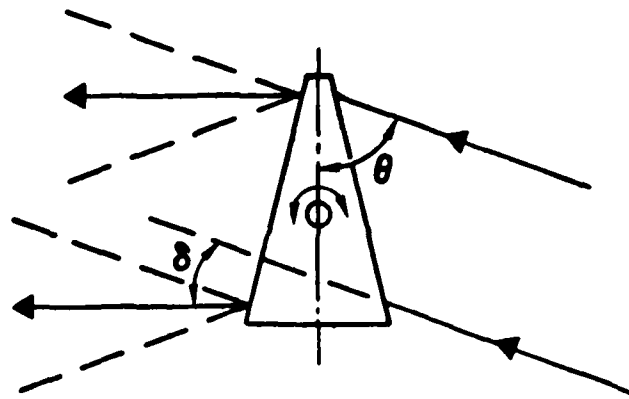


FIGURE 8.6 TILTING WEDGE DITHER MECHANIZATION

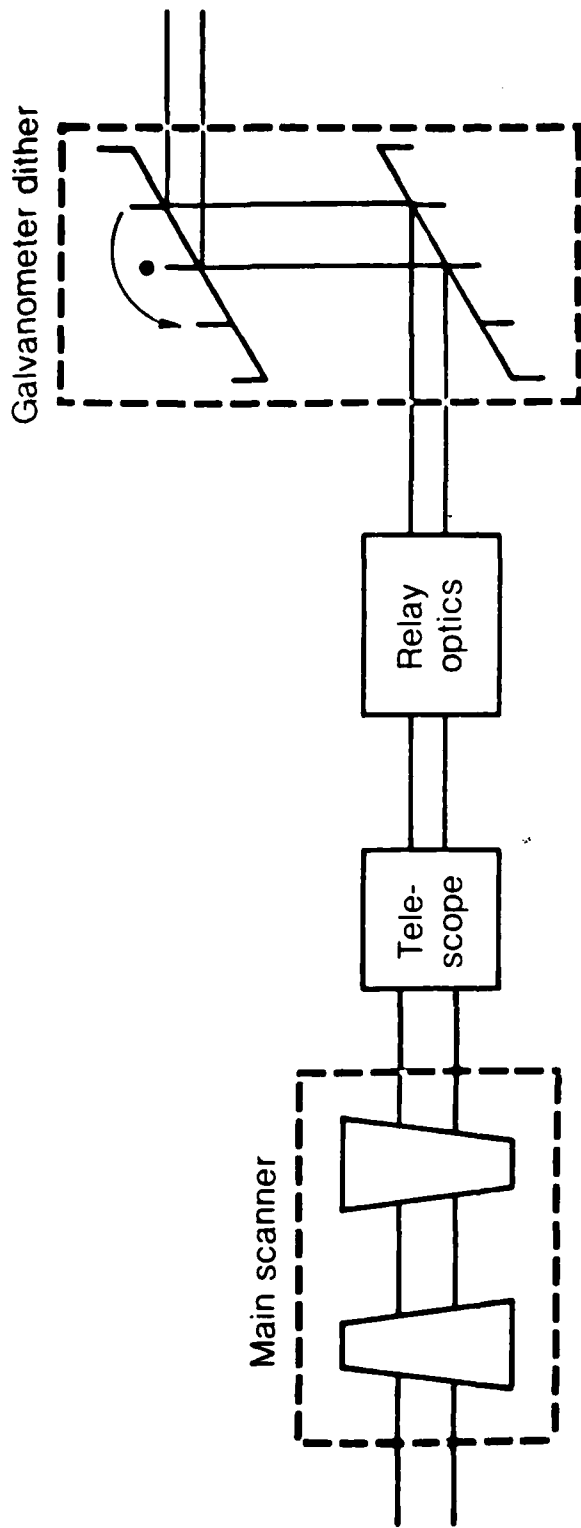


FIGURE 8.7 PRE-EXPANDER GALVANOMETER MIRROR DITHER MECHANIZATION

Table 8.2
CANDIDATE SCANNER TRADEOFFS

CANDIDATE SCANNER	FOV/FOR		FRAME TIME		PITCH/ROLL CAPABILITY	ADDITIONAL WINDOW REQUIRED	NOTES
	± 50°	1-2 SEC	2-4 SEC	4"			
ROTATING WEDGES 1 PAIR	± 50°	1-2 SEC	2-4 SEC		PROGRAMMABLE IN WEDGES	NO	SCAN MAY REQUIRE DITHER
ROTATING WEDGES 2 PAIR	± 50°	< 1 SEC*	< 2 SEC*		PROGRAMMABLE IN WEDGES	NO	SCAN MAY REQUIRE DITHER
BALL JOINT	± 15-30°	< 1 SEC*	< 2 SEC*		ADDITIONAL MECHANISMS REQUIRED	YES	LARGER FOV's REQUIRE LARGER WINDOWS
WEDGE/TURRET COMBINATION	± 50°	~1.25°	~ 2.5°		PROGRAMMABLE IN WEDGES	NO	ENTIRE TURRET MUST BE GEARED TO TURRET MIRROR (2:1 GEAR RATIO)

*LASER PRF LIMITED

from a number of considerations which increase the size, weight and beam clearance problems of the ball joint scanner as the scan field is enlarged. The range of $\pm 15^\circ$ to $\pm 30^\circ$ is not a rigid limit, but simply indicates a practical bound on these designs.

The $\pm 50^\circ$ FOV/FOR limit on the wedge scanners arises from total internal reflection (TIR) problems which are encountered in germanium at the last wedge-air interface. The limit occurs for angles somewhat greater than $\pm 50^\circ$ and thus this value should be taken as an upper practical limit. A ray trace distortion analysis of the large FOV wedge case was made and indicated that although a nearly plane wavefront (WWLODS received beam) passing through a pair of wedges will change to a slightly greater curvature wavefront, the distortion compared to a uniform spherical wavefront, which is suitable for heterodyning, is quite small. Astigmatism changes the divergence of the transmitted beam slightly, but the received beam remains almost perfectly spherical and therefore quite suitable for heterodyning. Thus, large wedge scan angles are acceptable from a beam distortion standpoint.

In the design tradeoff studies (Section 9.0) a maximum laser PRF of 100 kHz was used. The frame time was found to be laser-PRF-limited for most of the scanners considered; however, the single pair dual wedge scanner was limited by the torque capabilities and inertias of standard torquers.

The manner in which the pitch and roll corrections are accommodated requires additional mechanisms for the ball joint scanner; whereas, the wedge scanners accommodate the corrections in the programming of the torquer command signals.

The additional window requirement column highlights the ball joint scanner requirement in contrast to the wedge scanners, which provide their own output window by virtue of the last wedge.

Notes relative to the scan parameters include the fact that wedge scanners require an additional dither scan mechanism in order to preclude long narrow open spaces in the scan pattern. Also, large FOV for a ball joint scanner will require larger, and hence heavier and more lossy, windows for the window-enclosed option.

Scan Patterns

Figure 8.8 displays comparative beam scan patterns for the four candidate scanners. The patterns shown for the one-pair dual-wedge and the wedge-turret combination represent patterns which have reduced torque requirements for wedge scanner pattern generation compared to other dual-wedge scan patterns, such as an X-Y raster pattern centered in the field-of-regard of the wedges. These low-torque patterns use approximately straight horizontal lines which have their end points on the circumference of the field-of-regard. In the wedge-turret combination case, this pattern remains constant and the pitch correction

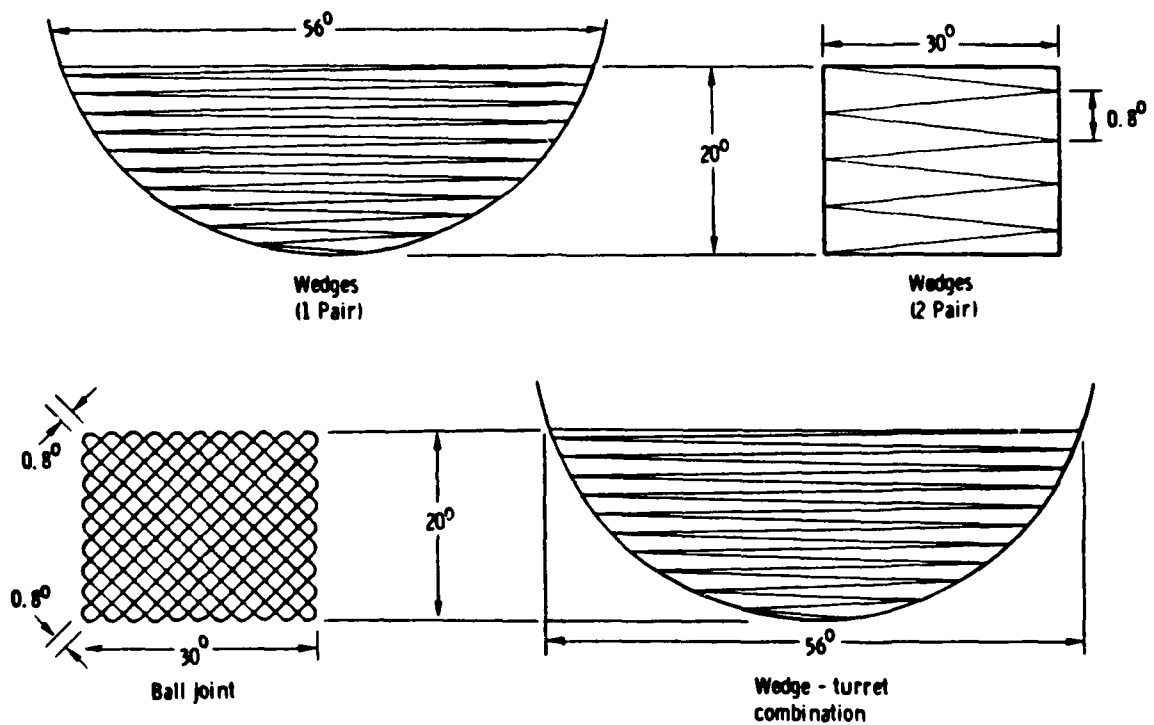


FIGURE 8.8 SCAN PATTERNS

capability of the turret mirror is used to satisfy the pitch correction requirements. In the 1-pair-of-wedges configuration, the pattern shown is for the lowest point in the field-of-regard. As the pitch correction calls for a higher elevation pattern, the pattern, or a trapezoidal approximation thereto, must be synthesized by the commands to the wedge torquers. A benefit of these patterns is the wide scan at the top which can help in looking ahead into turns as discussed in Section 6.0.

The "two pair of wedges" scan pattern is generated by running one pair of wedges (azimuth) in a counter-rotating manner to generate a reciprocating horizontal line scan; the second pair of wedges superimposes an elevation sweep and the pitch correction as required.

The ball joint scan pattern consists of interwoven scan lines which are tilted relative to the horizontal and vertical directions. In the case shown, the scan lines should be tilted at 45° and have a 0.8° spacing. Although other tilts and spacings are possible, this pattern is representative of the ball joint scanner candidate. Pitch and roll corrections must be added by means of additional mechanism.

Weight Versus Clear Aperture

Figure 8.9 presents a parametric comparison of scanner weight as a function of clear aperture for the four candidate scanners. This comparison includes the weights of generic scanner components and the structure to hold those components, but does not include housing weight, which would depend on pod interface and geometry which was not well defined at the point in time when this comparison was made. Also, a dither mechanism was not included in the various wedge scanners since it was not clear if it would definitely be required.

The results of this comparison are that the ball joint scanner has a slight weight advantage for the 2 in. aperture whereas the 1-pair dual-wedge scanner is superior for the 4 in. aperture case. For a 3 in. aperture, the choice between 1 pair of wedges and a ball joint scanner is even. The 2 pair of wedges and wedge/turret combination scanners are much heavier than the other two candidates over most of the aperture range and would only be selected if some feature of their scan pattern became an over-riding consideration.

Weight Versus Frame Time and FOV/FOR

In addition to the weight versus aperture studies detailed in the previous section, an examination of the sensitivity of the weight to changes in frame time and FOV/FOR requirements was made. Table 8.3 summarizes the results of the frame time examination and indicates that the total scanner weight is not a dramatic function of frame time. The N/A notation for a 1 second frame time/1 wedge pair combination indicates that this frame time is not achievable with standard catalogue torquers found during this study.

- Ball joint scanner — external window
- - - - Ball joint scanner — internal window
- · - · Wedge scanner — 1 pair
- Wedge scanner — 2 pair
- Wedge turret combination

(Housing and dither weights not included)

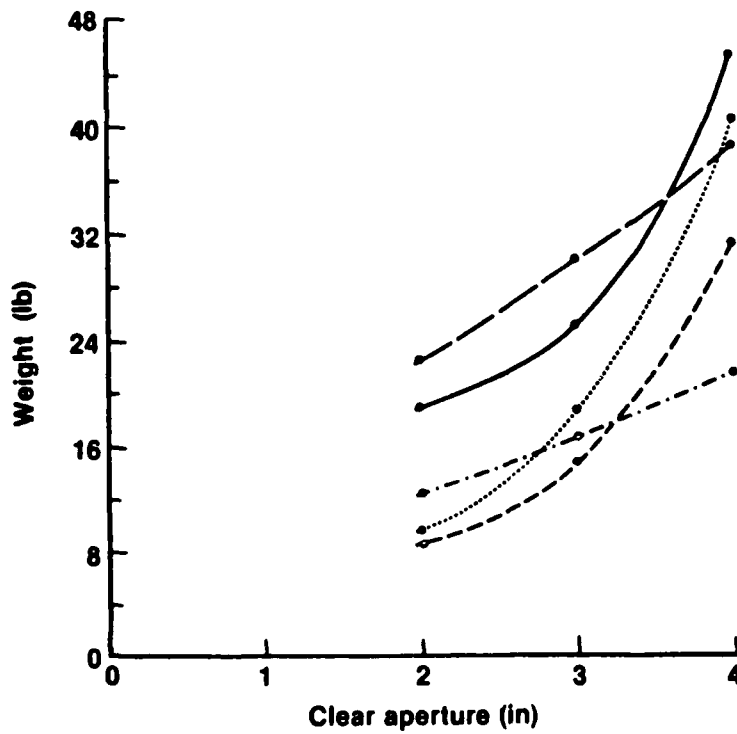


FIGURE 8.9 SCANNER WEIGHT vs CLEAR APERTURE

Table 8.3

SCANNER RELATIVE WEIGHT VS FRAME TIME

Candidate Scanner	1 Second Frame time	2 Second Frame time	4 Second Frame time
Wedges (1 pair)	N/A	1X	0.90X
Wedges (2 pair)	1X	1X	1X
Ball Joint	1.1X	1X	0.97X

The weight versus FOV/FOR examination indicated, as shown in Table 8.4, that the wedge scanner weights are not sensitive to FOV/FOR over the 30° to 50° range whereas the ball joint scanner weight doubles. This dramatic increase is due to larger window, mirror, and structure requirements in order to accommodate the larger scan angles. The weight of the wedge turret combination varies in the same way as that of wedges (1 pair) in Tables 8.3 and 8.4, for the same changes.

Window and Optical Train Considerations

It is desirable to keep the optical train losses to a minimum so that WWLODS range or weather margin may be increased. Figure 8.10 presents a comparison of the one-way losses expected for the four candidate scanners. The peaked shape of the columns representing the wedge scanner configurations arises from the difference in attenuation path across the beam when the two wedges are aligned. In the aligned case part of the beam will pass through the thin portion of two (or four) wedges while the opposite side of the beam will pass through the thick part of both the wedges. Intermediate wedge orientations will produce intermediate losses and loss gradients across the beam. Losses represented in the total bar include not only the absorption losses in the germanium wedges, but reflection losses at the Anti-Reflection (AR) coated wedge surfaces. The AR coating reflection losses were calculated as a function of angle. The only significant coating loss occurs at the last surface and the worst case angle was assumed for comparison purposes. The 2-pair dual-wedge scanner has approximately twice the absorption losses of the 1-pair dual wedge scanner because it has twice the number of wedges and a total of eight AR coatings. Again, only the last AR coating has a significant amount of loss.

The ball joint scanner has losses due to mirror reflections and window absorption. The total column height on the figure corresponds to the case where the ball joint scanner has a ZnS output window, similar to an output window on a FLIR system. The dashed line represents the open pod (internal window) alternative. In this case, a smaller, thinner and more efficient window material is used between the scanner and the beam expanding telescope. Also, the ball joint mirror and turning mirror of Fig. 8.4 must have an environmentally hard coating and the scanner mechanism must be sealed to prevent contamination -- both of which appear to be feasible.

Window material considerations are compared in Table 8.5. The significant items include the fact that ZnS has a loss of 15 percent per cm. However, it is often used because of its good rain erosion properties. Both ZnS and ZnSe are available in large sizes and domed shapes by virtue of a Chemical Vapor Deposition (CVD) process for forming the window blanks.

The lowest loss material is ZnSe; however, it has the highest projected cost and has more of a problem with rain erosion.

Table 8.4

SCANNER RELATIVE WEIGHT vs FOV/FOR

4 in. aperture

Candidate Scanner	30°	45°	60°
Wedges (1 pair)	1X	1X	1X
Wedges (2 pair)	1X	1X	1X
Ball Joint	1X	1.5 X	2X

4 in. aperture

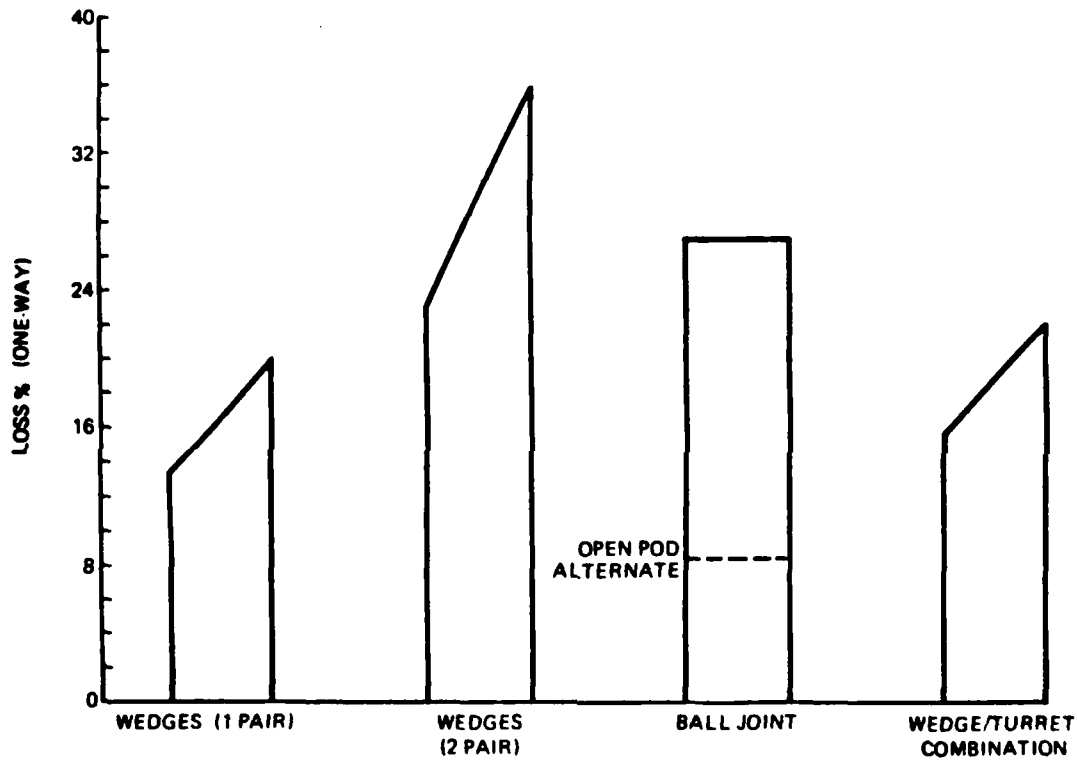


FIGURE 8.10 SCANNER OPTICAL TRAIN LOSSES

Table 8.5
SCANNER WINDOW CONSIDERATIONS

SCANNER	WINDOW MATERIALS	LOSS PER CM	RELATIVE COST	DIAMETER REQUIRED FOR 4" CLEAR APERTURE	COMMENTS
ROTATING WEDGES	GERMANIUM (WEDGES)	2.8%	MODERATE (\$50-\$100/IN ²)*	4 INCHES	ENVIRONMENTALLY HARD AR COATING REQUIRED ON OUTSIDE SURFACE
	ZnS	15%	HIGH (~ \$100/IN ²)*	4 INCHES - 10 INCHES	CHEMICAL VAPOR DEPOSITED (CVD) AVAILABLE FOR LARGE SIZES. RAIN DAMAGE RESISTANT
BALL JOINT	ZnSe	0.05%	HIGHEST (~ \$200/IN ²)*	4 INCHES - 10 INCHES	CVD AVAILABLE FOR LARGE SIZES
	Ge	2.8%	MODERATE (\$50-\$100/IN ²)*	4 INCHES - 10 INCHES	IF OTHER THAN FLAT REQUIRED LARGE VOLUME (\$) OF MATERIAL REQUIRED. Ge IS NOT CVD

*COST ALSO DEPENDS ON THICKNESS REQUIRED

Germanium is available in large sizes, but must have an environmentally hard coating applied to the outer surface. Such a coating is being developed.

Power requirements

Table 8.6 presents a comparison of the power requirements for three scanner candidates having a 2 in. aperture. The single pair of rotating wedges has the highest power requirement since the largest torquers must be used to provide the required angular accelerations. The two-pair wedge scanner requires less power, even though it has four torquers, since two torquers may be low torque and run in a counter-rotating manner. The ball joint scanner has the lowest power requirement since the motor is always running in one direction and the mirror direction changes are supplied by cams.

8.4 Baseline Scanner Selection and Parameters

In Section 9.0, the process of selecting the three recommended design approaches is described in detail. To better define the characteristics of the WWLODS scanner, one system was chosen and a more detailed preliminary scanner design and parameter assessment carried out. For the lowest weight pod configuration, the 2 in. ball joint scanner was selected as the most promising candidate. A mechanical design was prepared for this type of scanner incorporating both pitch and roll compensation capabilities. The following sections detail the parameters of the scanner resulting from this design.

Baseline Scanner Mechanism

The mechanical design for the 2 in. ball joint base line scanner is shown in Fig. 8.11. In this design the main drive motor provides both the azimuth and elevation cam motions. The cams and gear couplings are all contained in an enclosure and a small amount of oil is included for lubrication to reduce wear and friction. The pitch correction is accommodated by a small servomotor which superimposes the desired correction on the elevation cam mechanism. The roll correction is provided by constructing the scanner mechanism in a ring which may be rotated about the ball joint/mirror axis. A second small servomotor is used to rotate the scanner housing relative to its pod mounting surface. This provides the desired roll correction of the scan pattern.

In Fig. 8.11, the large motor cross section is the main drive motor and the two smaller motor cross sections are the pitch and roll correction servomotors. The ball joint appears behind the mirror in the upper left corner. The mirror is

Table 8.6
SCANNER POWER REQUIREMENTS

2 in. aperture

Candidate Scanner	Power Required (W)	Voltage Required
Rotating Wedges 1 pair	184	28 VDC
Rotating Wedges 2 pair	88	28 VDC
Ball Joint	20	115 V, 400 Hz, 3 ϕ

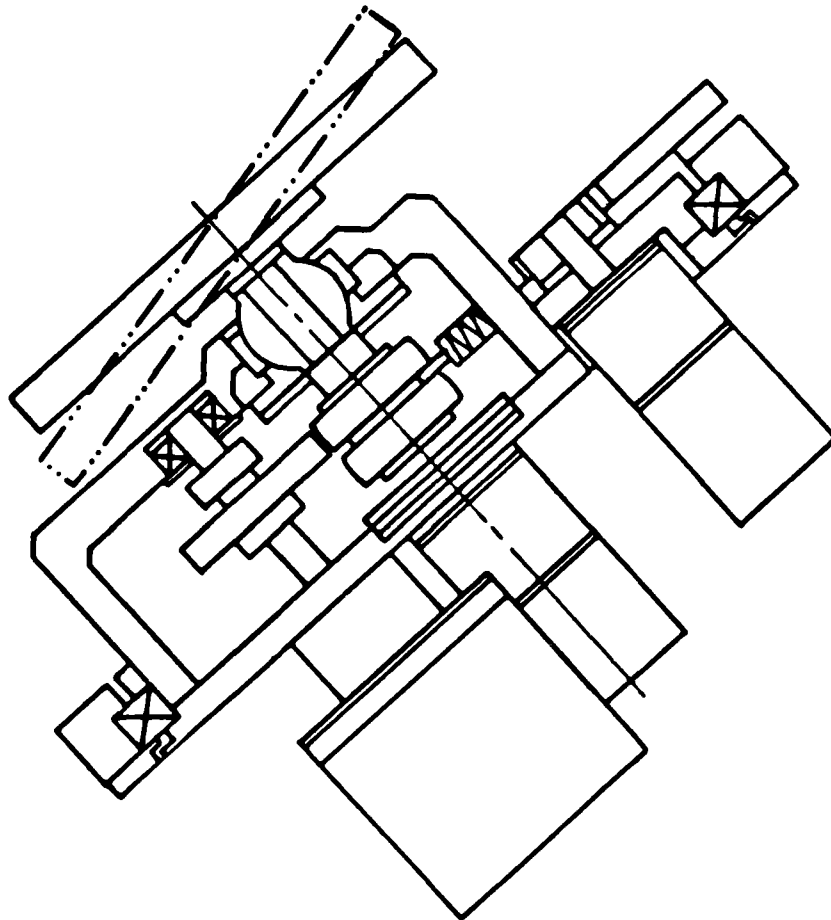


**FIGURE 8.11 2 IN. BALL JOINT SCANNER
MECHANIZATION**

80-6-17-64

bonded to an adapter plate on the rod through the ball joint. All three motors are on the scanner platform and rotate together when a roll correction is applied. This allows a single umbilical to connect to the scanner and no one motor limits the clearance as the mechanism rotates. Thus the scanner unit, in principle, does not have a limit on the amount of roll correction which may be applied.

Scan Pattern and Parameters

The scan pattern which can be generated by the baseline ball joint scanner is shown in Fig. 8.12. The slope of the scan lines, relative to the horizontal, is 15° . This orientation was chosen to yield 0.8° high by 3.2° wide "diamonds" in the scan pattern. This provides a maximum vertical separation of 0.8° at the intersections of the scan lines, and a smaller spacing elsewhere, to ensure that small vertical objects do not escape detection. The wider, 3.2° , horizontal separation ensures that longer horizontal objects, such as wires, will not be missed.

The motors and gear ratios have been selected to cover the complete scan pattern in a 1.5 second frame time, matching the requirement for the signal-integration case of Section 9.0. It is worth noting that the scan pattern is covered in a regular, but not unidirectional (top to bottom or side to side), manner. This means that, for moderate sized objects located toward one edge of the pattern, the update rate will be more than one per 1.5 second frame. By contrast, a horizontal raster scan pattern would update twice in rapid succession for an object near the top or bottom of the frame and then could take 1.5 or 3 seconds to repeat again. The difference between 1.5 and 3 seconds depends on whether or not the 1.5 second frame rate is obtained by interlacing two scan fields.

The notation of 21.2° effective elevation and 30.4° effective azimuth refers to the fact that the sharp diamonds on the ends and top/bottom will be somewhat rounded to maintain reasonable cam features. The effective numbers shown are the AZ and EL coverage estimated to result when this factor is taken into consideration.

Figure 8.13 presents the overall scan parameters of the 2 in. ball joint scanner. The $20^\circ \times 30^\circ$ scan pattern may be pitch corrected $\pm 10^\circ$ for an overall elevation FOR of 40° . The entire pattern and pitch correction may be roll corrected by $\pm 60^\circ$. As pointed out in the previous section, the basic mechanism of the baseline scanner is not limited in roll correction; however, only a $\pm 60^\circ$ gear sector was incorporated into the design in order to hold the weight to a minimum.

Pod Implementation

Although the final scanner/pod design factors in a number of variables including beam expanding telescope design and location, Fig. 8.14 presents one possible pod implementation. The baseline scanner mechanism of Fig. 8.14 is

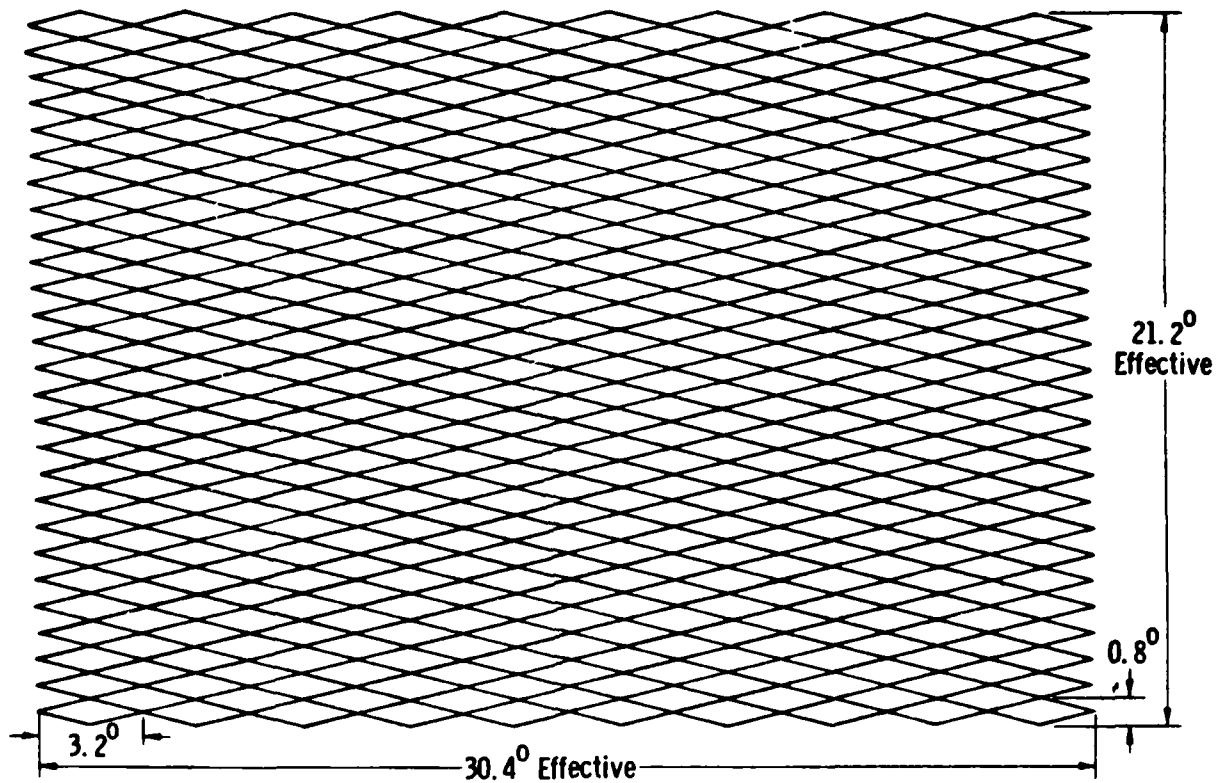


FIGURE 8.12 BALL JOINT SCAN PATTERN

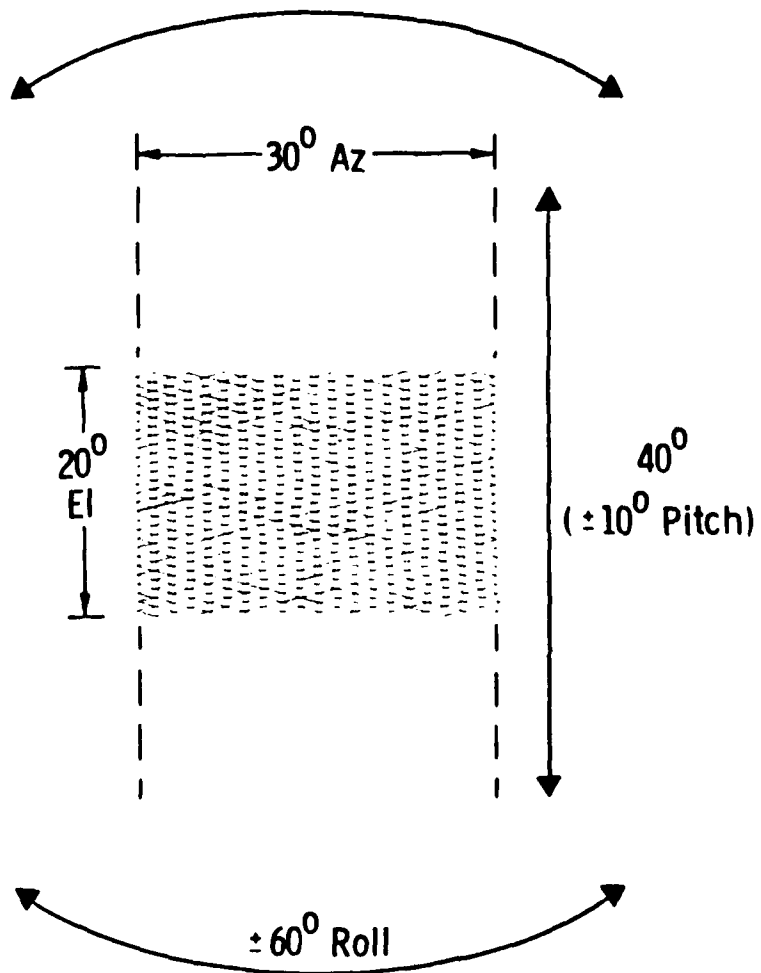
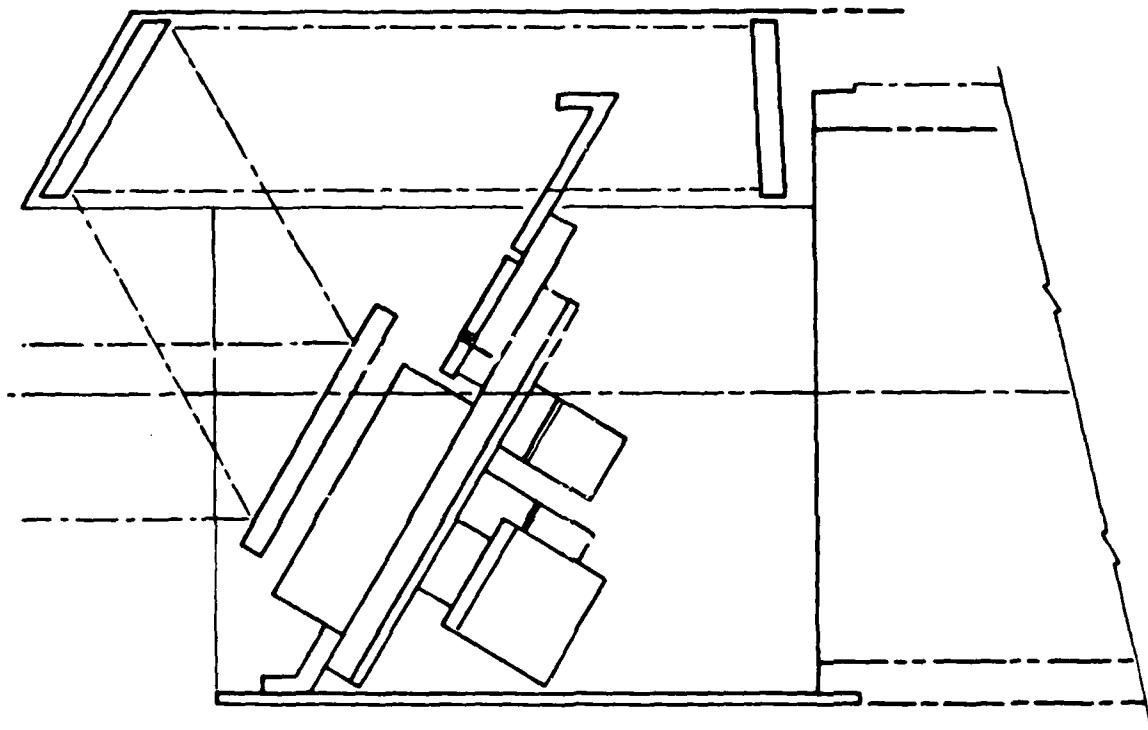


FIGURE 8.1. 2 IN. BALL JOINT SCAN PARAMETERS



**FIGURE 8.14 2 IN. BALL JOINT SCANNER
POD IMPLEMENTATION**

00-8-17-87

mounted on a scanner support ring which is fastened to the inside of the tubular scanner housing shell. The housing shell mates to the main pod, shown in phantom on the right of the figure. In this implementation, the end of the pod is sealed and a window in the middle at the top allows the beam to exit the main pod and enter the scanner section. The turning mirror is located at the end of the pod beam tube from the pod and directed the beam onto the ball joint scanner mirror. The housing shell has a thinner wall than the main pod. It is located outside of the hard point mounting region and does not have the same structural requirements as those imposed on the main portion of the pod.

Baseline Scanner Weight Estimate

Table 8.7 presents a detailed weight estimate for the baseline 2 in. ball joint scanner and housing, for the pod implementation discussed in the preceding section. The first subtotal of 3.2 lbs represents the weight of the basic scan, pitch correction, and roll correction mechanism. The second subtotal of 4.5 lbs includes the housing, mounting, turning mirror and beam window components. The scanner total of 7.7 lbs, although it does not include additional pitch, roll and position readout interface items which would be required for a WWLODS interfacing with a headup display as discussed in Section 9.0, compares very favorably with the 8-10 lbs estimate arrived at during the tradeoff study described earlier (Fig. 8.9).

Table 8.7
**2-IN. BALL JOINT SCANNER
 WEIGHT ESTIMATE**

WEIGHT (LBS)	ITEM
MIRROR	0.18
BALL JOINT	0.04
MAIN MOTOR	0.46
PITCH MOTOR	0.18
ROLL MOTOR	0.18
HOUSING	1.54
CAMS, BEARINGS, HARDWARE, MISC	1.62
MECHANISM SUBTOTAL	3.2
SCANNER SUPPORT RING	0.55
HOUSING SHELL	1.83
BEAM TUBE FROM POD	0.72
WINDOW AND MIRROR	0.30
WINDOW AND MIRROR MOUNTS	0.50
MISC HARDWARE	0.50
HOUSING SUBTOTAL	4.5
SCANNER TOTAL	7.7 LBS*

*ADDITIONAL PITCH, ROLL AND POSITION READOUT INTERFACE ITEMS MAY BE REQUIRED DEPENDING ON FINAL SYSTEM DESIGN. COMBINED WEIGHT OF THESE ITEMS WILL BE LESS THAN 2.3 POUNDS.

9.0 SELECTION OF RECOMMENDED DESIGN APPROACHES

9.1 Selection Procedure

The procedure by which the three recommended design approaches were selected is illustrated in Fig. 9.1. The design analysis of the laser and scanner, described in Sections 7.0 and 8.0, make it possible to determine the total weight of the WWLODS as a function of laser average power (P), type (CW or pulsed), scanner aperture diameter (D), and scanner type. The selection of a detection probability, P_D , a false alarm number FAN, and whether or not integration is performed on the received signal, together with the statistical noise characteristics of the receiver system and the target signatures, determine the signal-to-noise ratio (SNR) required at the output of the detector. The choices of laser PRF, laser P, and scanner D, together with the required SNR ratio then determine the range performance of the WWLODS as a function of power, aperture size, and system configuration. The laser PRF, scanner D, scanner type, and the degree of signal integration together determine the available FOV and T_F . Response time (T_R) is determined by the data gathered in the pilot survey. The combination of range, FOV, T_F and T_R , along with the maneuver requirements established in Section 6.0 then determine the allowable flight speed as a function of the major parameters of the system: power, aperture dia, and configuration. It is then possible to combine the speed vs configuration and the weight vs configuration data to derive plots of speed vs weight for various configurations. A review of these plots is then the basis for the selection of the three design approaches which form the basis of the overall system designs described in Section 9.6.

The system design options considered in this analysis are shown in Table 9.1. The aperture diameters considered were 2, 3, and 4 in. The laser average power ranged from 1 to 10 watts for the pulsed lasers and from 2 to 30 watts for the CW chirp lasers as discussed in Section 7.0. A maximum PRF for the pulsed laser of 100 kHz was established. However, as discussed in Section 8.0, for the 1-pair dual wedge scanner, the PRF was limited to less than 100 kHz by the maximum scan rate. The angular scan rate, $\dot{\theta}$, is a function of the size of the resolution element which depends on the aperture diameter and the PRF:

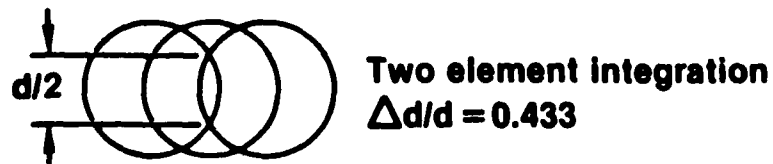
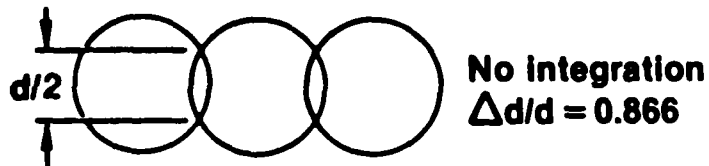
$$\dot{\theta} = F_c (2\lambda/D) \text{PRF}$$

where F_c is the fraction of the beam diameter, d , through which the scan advances between resolution elements. F_c is chosen so that a continuous swath with a width of half the spot diameter is always covered. When there is no integration of the received energy this results in a spacing of 0.866 d as shown in Table 9.1. When the energy from two resolution elements is integrated the spacing is 0.433 d . The SOW specified that the system was to be installed in a UH-60A aircraft. In order to establish a specific framework for system configuration analysis a pod installation was assumed.

Table 9.1
SYSTEM DESIGN OPTIONS

- Aperture diameter
2, 3, 4 in.
- Laser average power
1-10 W Pulsed format
2-30 W CW chirp format
- Laser PRF
Maximum of 100 kHz, scanner limit

- Resolution element overlap



- Pod installation in UH-60A

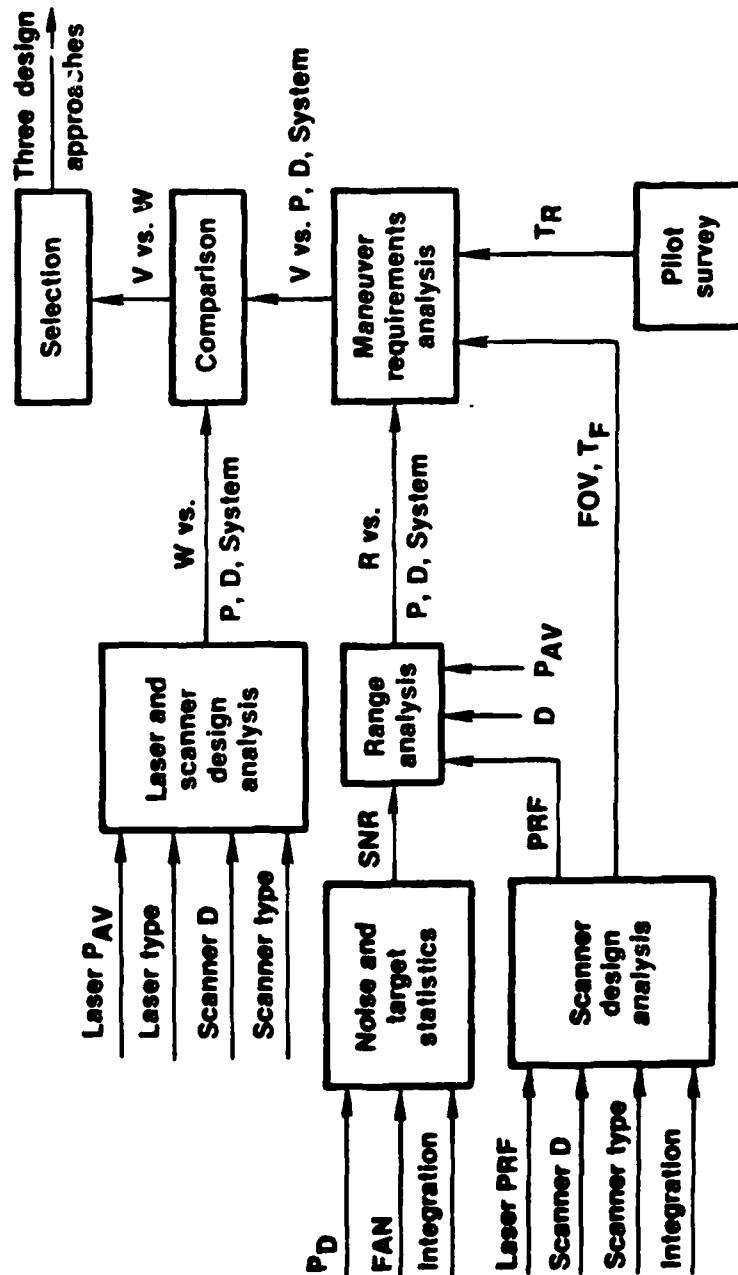


FIGURE 9.1 TRADEOFF/EVALUATION PROCESS

The weight of the laser subsystem is based on analysis and experiment (Ref. 4) and includes consideration of the alternative choices discussed in Section 7.0. The variation of weight with laser power is shown in Fig. 9.2 for the CW chirp laser. These weights include all the elements, including power supplies, that would be required in the pod. Figure 9.3 shows the reduction in power that results when a passive Q-switch is inserted into the laser cavity to convert to CW output to the pulse output format. Figure 9.4 shows the weight of the pod, scanner housing and of the various scanner options as discussed in Section 8.0. A weight allowance of 2 lb has been added to the dual wedge scanner weights given in Section 8.0 to allow for the dither mechanism necessary to fill in the long narrow openings in the dual wedge scan pattern.

The major parameters of the range analysis are illustrated in Table 9.2. The SNR depends on the extinction of the atmosphere (α), the range (R), the laser average power (P), the laser PRF, the aperture dia, and the heterodyne efficiency, η_H . The remaining parameters in the range performance calculation are the cross section of the target, which in this analysis is based on the off-axis signal from a 1/8 in. WD-1 wire, and various system losses including reflection, transmission, and misalignment losses. All of these factors are lumped together in a constant (K) and the value of this constant is determined by flight test data taken in the LOTAWS program (Ref. 2). In the LOTAWS tests the value of η_H was around 0.1. For this analysis a value of $\eta_H = 0.5$ was assumed, based on laboratory measurements which indicate that η_H equal to 0.9 or more should be attainable. The weather conditions required to be examined by the SOW are also listed in Table 9.2 along with the corresponding absorptivities in $(10^3 \text{ft})^{-1}$.

For this analysis a Swerling 2 target was assumed. The Swerling 2 target is a rapidly fluctuating target model and was selected to account for the presence of speckle in the return signal. This is a conservative assumption since other target models have smaller signal fluctuations and therefore require a lower SNR for a given combination of P_D and FAN. The SNR requirements are shown in Table 9.3 for FAN of 10^5 , 10^7 , and 10^9 , P_D of 0.9, 0.99, and 0.999 and for the collection of signal energy from 1 resolution element (no integration) and 2 resolution elements (integration). The time in sec between false alarms (T_{FA}) is roughly equal to FAN/PRF. Two possibilities were evaluated in this analysis. For a FAN of 10^5 and with the use of frame-to-frame correlation of wire hits to reduce false alarms, the effective FAN is 10^{10} and T_{FA} is approximately 27.8 hours. With a FAN of 10^9 and use of information only from a single scan frame $T_{FA} = 2.78$ hours at a PRF of 10^5 Hz. The use of a frame-to-frame correlation along with a FAN of 10^5 requires a lower signal-to-noise ratio than a FAN of 10^9 and therefore gives a longer range capability to the WWLODS. However, since information is required from two frames the delay times involved in the maneuver requirement ($T_f + T_R$) are longer and therefore the allowable speed must be reduced.

CW Chirped Laser

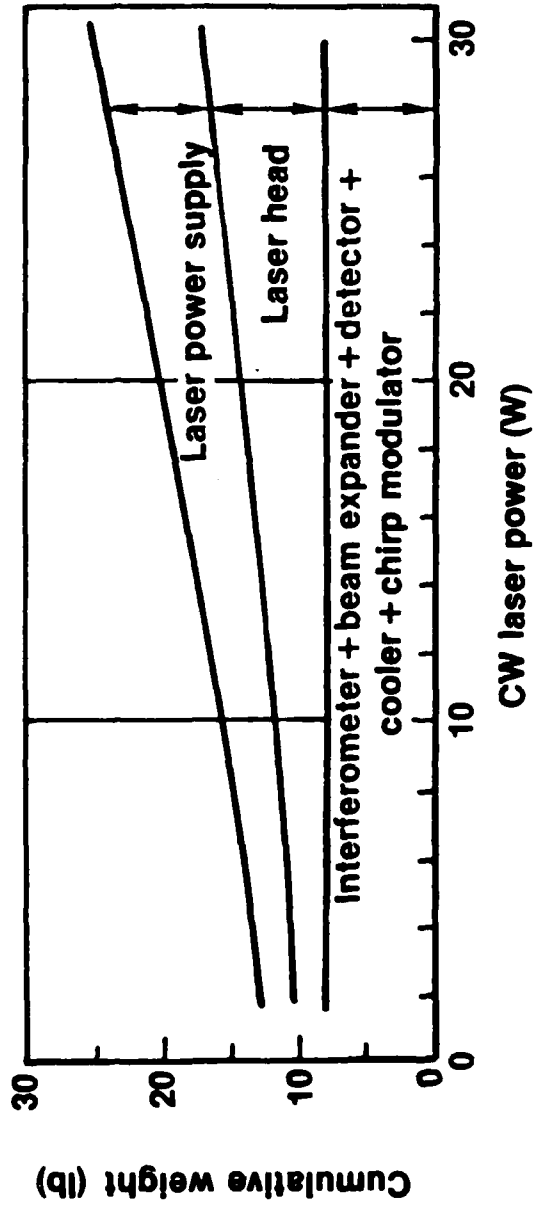
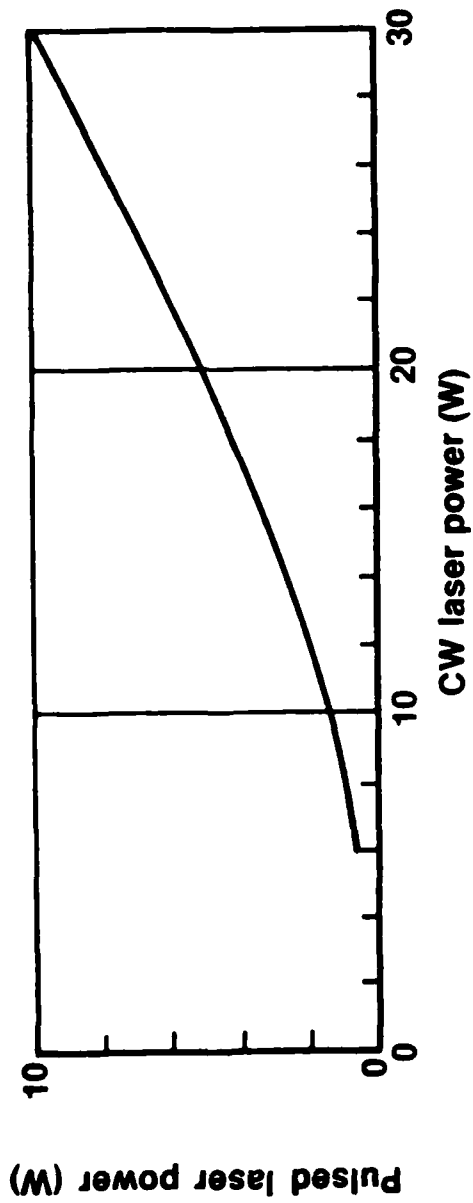


FIGURE 9.2 TRANSCIEVER SUBSYSTEM WEIGHT



**FIGURE 9.3 CW TO PULSED LASER POWER
CONVERSION**

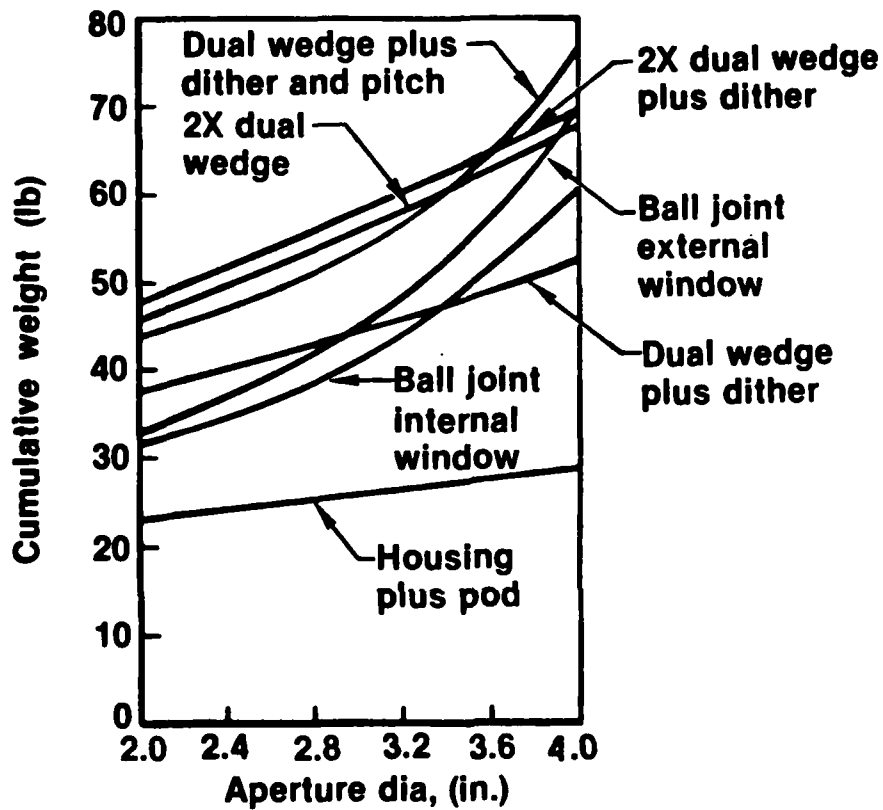


FIGURE 9.4 SCANNER AND POD SUBSYSTEM WEIGHT

Table 9.2
RANGE ANALYSIS

$$\text{SNR} = K e^{-2\alpha R} (P/\text{PRF}) (D/R)^3 (\eta_H)$$

$K = f$ (cross section, losses, etc.)

$K = 446$ for LOTAWS vs 1/8 in. WD-1 wire

α in $(10^3 \text{ ft})^{-1}$	P in W	D in inches
R in 10^3 ft	PRF in kHz	$\eta_H = 0.5$
<u>Weather</u>		<u>$\alpha (10^3 \text{ ft})^{-1}$</u>
Midlatitude summer day		0.10
MLS day + 4 mm/hr rain		0.26
MLS day + 15 mg/m ³ fog (100 m-400 m visibility)		0.70
110F, 85% RH (climatic category 5)		1.00

Table 9.3
SNR REQUIREMENTS

Swerling 2 Target

PD	SNR (dB)											
	0.9				0.99				0.999			
	105	107	109	105	107	109	105	107	109	105	107	109
No integration	20.5	22.0	23.0	31.0	32.5	33.5	41.0	42.0	43.5	41.0	42.0	43.5
Integration	14.0	15.5	16.5	20.0	21.0	22.0	24.5	26.0	27.0	24.5	26.0	27.0

FAN = 10⁵, TFA = 27.8 hr with frame-to-frame correlation (FAN_{eff} = 10¹⁰)
 FAN = 10⁹, TFA = 2.78 hr

9.2 Tradeoff Evaluation

The basic evaluation is performed in terms of the allowable speed corresponding to the stopping maneuver range requirements in NOE flight established in Section 6.0. This is compatible with the use of a simple warning system and it would be available for all the helicopters in the inventory as discussed in Section 5.0.

Figure 9.5 shows the comparison of single-frame detection and frame-to-frame correlation for the case of a 2 in. dual wedge scanner with no pulse integration. Frame-to-frame correlation which has an effective FAN of 10^{10} gives longer ranges, as can be seen from Fig. 9.5, but when the longer frame times are included in the range requirements analysis results of Section 6.0, the allowable flight speed is seen to be either equal to or slightly less than that for a FAN of 10^9 with no frame-to-frame correlation. Figure 9.6 shows that the same results are obtained for a 2 in. ball joint scanner with integration. Based on these results the use of frame-to-frame correlation was not considered further in the analysis since it produces no net increase in allowable speed and would require considerable complexity in the system in order to keep track of wire hits from one frame to the next.

The basic performance capabilities of the WWLODS in terms of system range and the allowable speed for performing the stopping maneuver described in Section 6.0 are shown in Figs. 9.7 to 9.15 for 2 values of rotor tilt, 30 deg and 40 deg, for the configuration options of Table 9.1. Performance is shown as a function of laser power in the range of 2 to 30 watts and is applicable to both CW and pulsed laser formats for the same average power. Performance is also shown for all the weather conditions listed in Table 9.2.

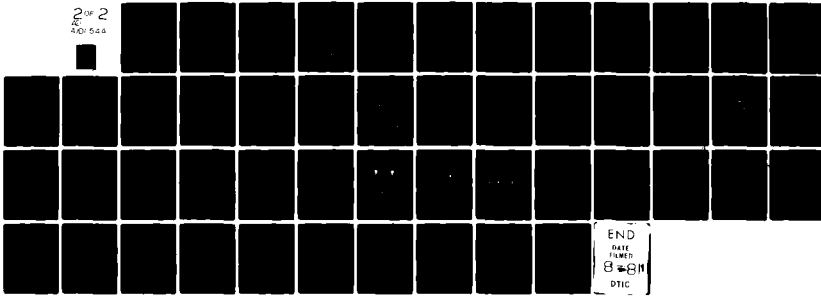
When the speed capabilities of Figs. 9.7 through 9.15 are combined with the weight variations of Figs. 9.2 through 9.4 a speed/weight tradeoff results as shown in Figs. 9.16 through 9.18. Figure 9.16 shows the results for the ball joint scanner with an external window. It has a FOR which is 30° wide by 40° high and a frame size (FOV) which is 30° wide by 20° high. Speed is shown as a function of total system weight for both CW chirp and pulsed lasers. Figure 9.17 shows results for a dual wedge scanner with a field of regard having a dia of 120° and a scan frame 56° wide by 20° high as discussed in Section 8.0. Figure 9.18 shows the results for a dual wedge scanner which has a FOR with a 60° dia and utilizes pitch turret to obtain an effective FOR 58° wide by 40° high and a scan frame FOV 58° wide by 20° high. This system has the same range/speed capabilities as that shown in Fig. 9.17 but has higher weights because of the use of the pitch turret to relieve the acceleration requirements on the wedges as discussed in Section 8.0. This system is an alternate to the dual wedge scanner with the 120° dia FOR and would be considered only if detailed analyses turn up severe limitations due to the wedge scanner acceleration rates required to meet the necessary scan format.

AD-A101 544

UNITED TECHNOLOGIES RESEARCH CENTER EAST HARTFORD CT F/G 17/5
DESIGN APPROACH FOR A LASER WIRE AND WIRE LIKE OBJECT DETECTION--ETC(U)
MAY 81 B B SILVERMAN; H HEYNAU; R J MONGEON DAAK80-79-C-0278
USAAVRADCOM-TR-79-0278-F NL

UNCLASSIFIED

2 of 2
40' 544



END
DATE
FILMED
8-81
DTIC

2 in. Dual Wedge Scanner, No Integration
 Frame Time = 1.25 sec

— FAN = 10^9
 - - - Frame/frame correlation (FAN_{eff} = 10^{10})

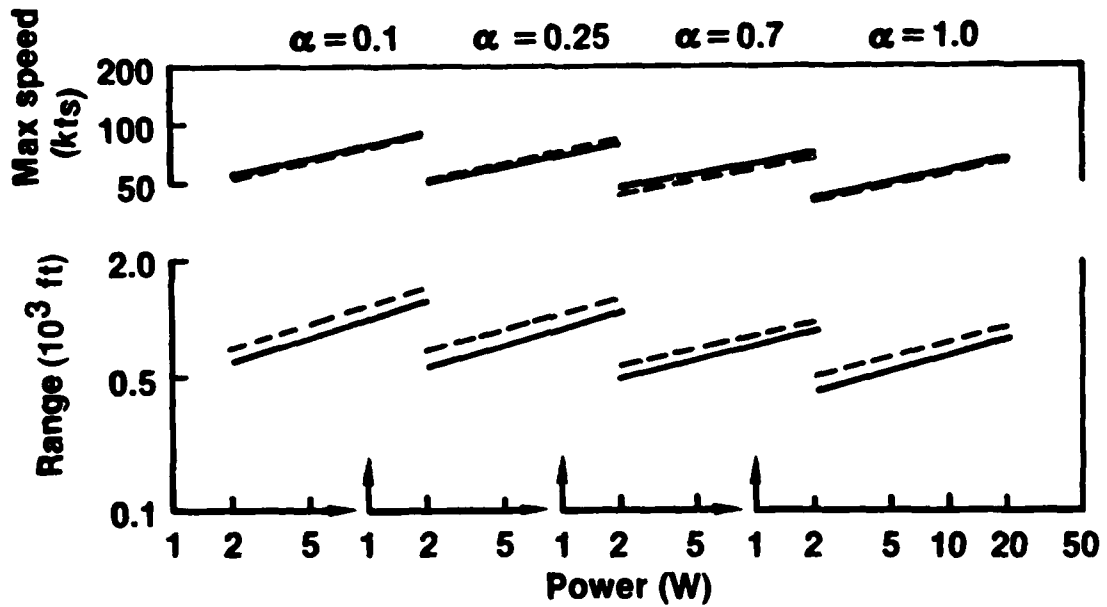


FIGURE 9.5 NOE SPEED/RANGE PERFORMANCE

2 in. Ball Joint Scanner, Integration
 Frame Time = 1.5 sec

— FAN = 10^9
 - - - Frame/frame correlation (FAN_{eff} = 10^{10})

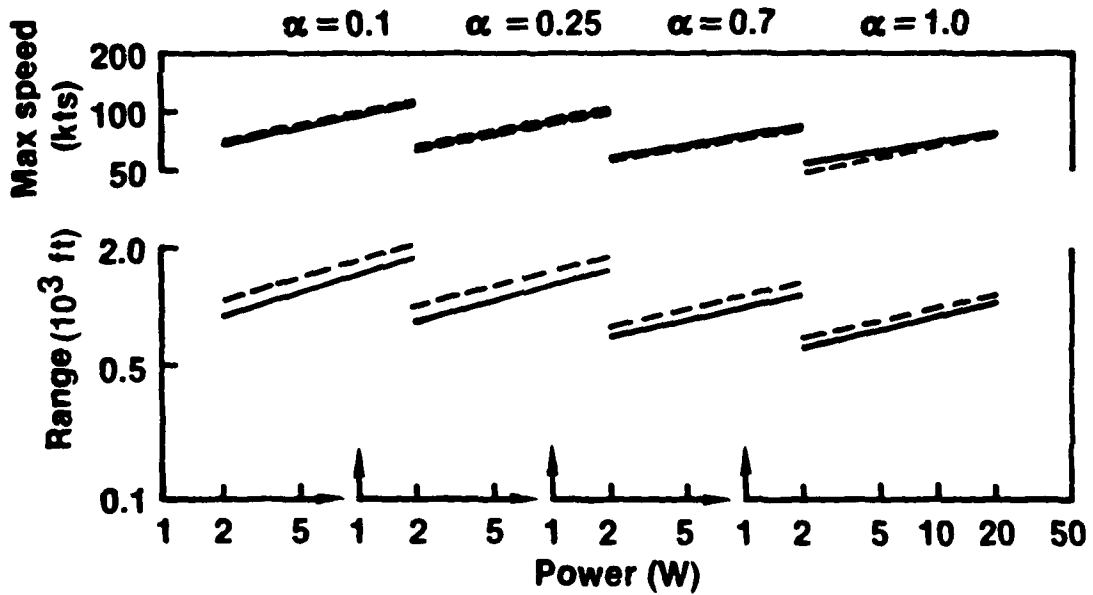


FIGURE 9.6 NOE SPEED/RANGE PERFORMANCE

**2 in. Ball Joint Scanner, No Integration
Frame Time = 0.75 sec**

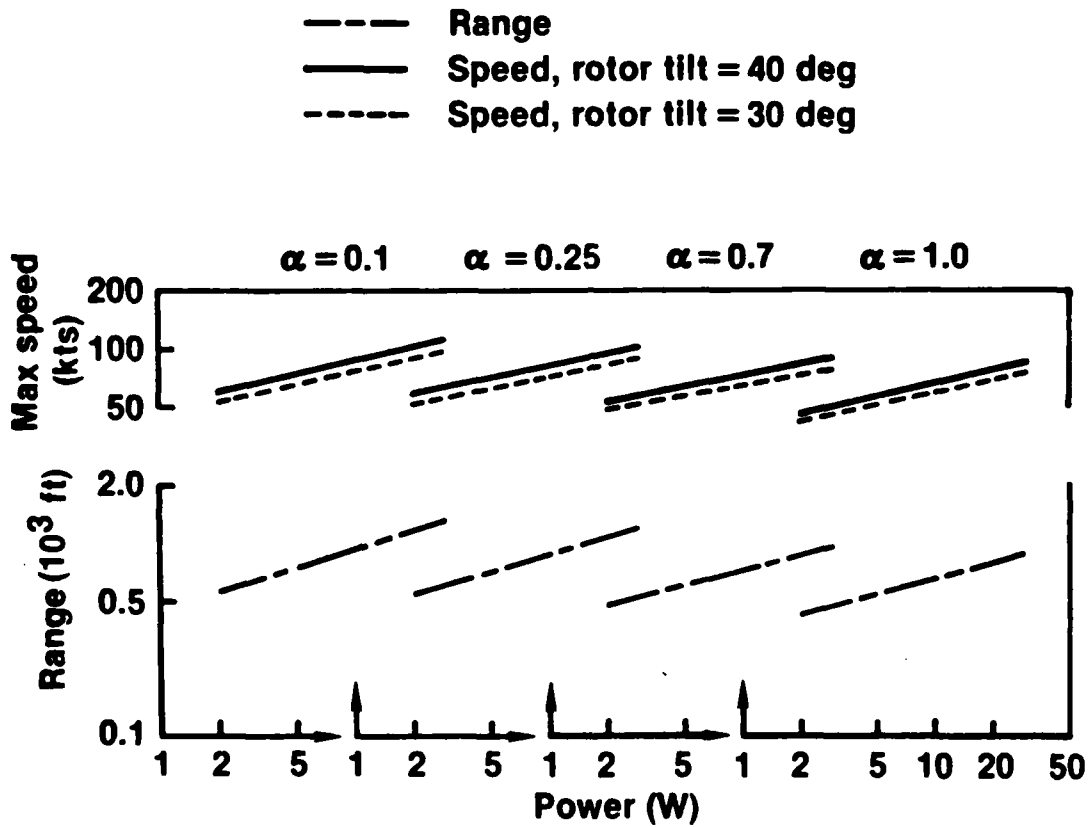


FIGURE 9.7 NOE SPEED/RANGE PERFORMANCE

2 in. Ball Joint Scanner, Integration
 Frame Time = 1.5 sec

- Range
- Speed, rotor tilt = 40 deg
- Speed, rotor tilt = 30 deg

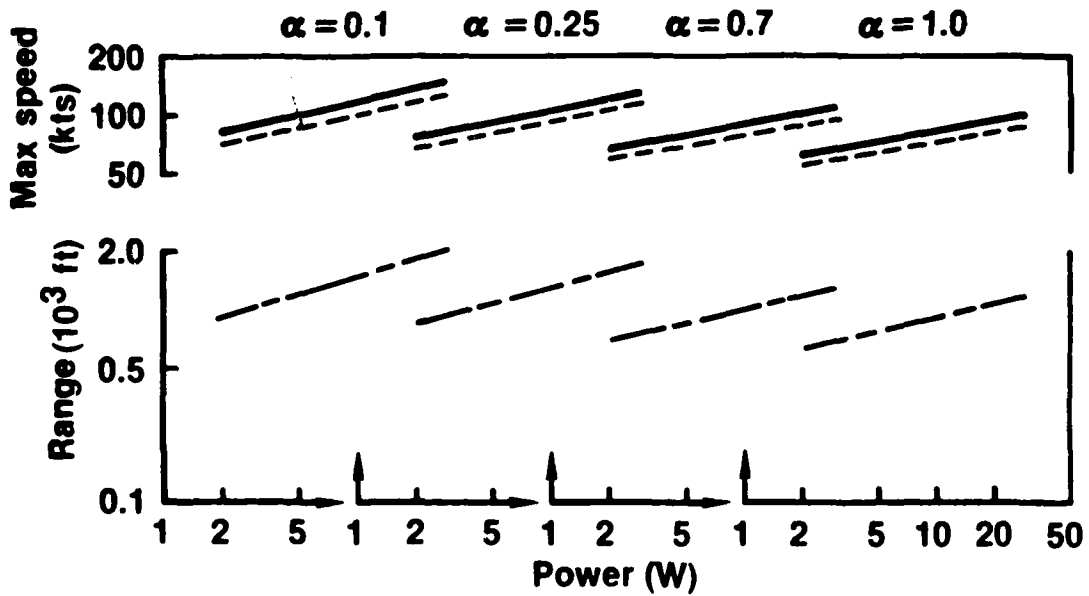


FIGURE 9.8 NOE SPEED/RANGE PERFORMANCE

3 in. Ball Joint Scanner, No Integration
Frame Time = 1.13 sec

- Range
- Speed, rotor tilt = 40 deg
- Speed, rotor tilt = 30 deg

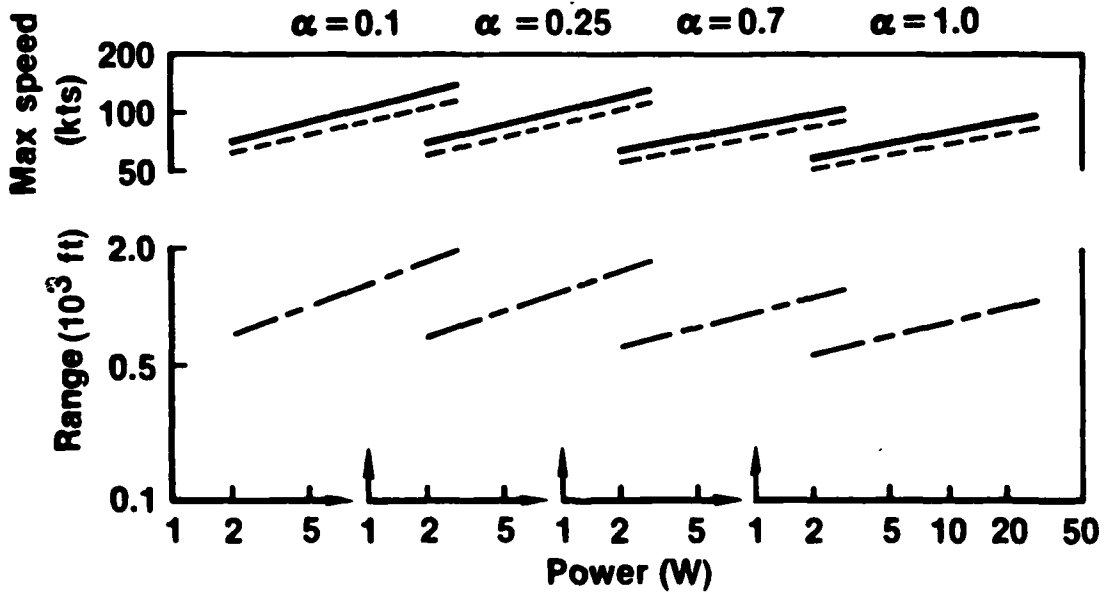


FIGURE 9.9 NOE SPEED/RANGE PERFORMANCE

3 in. Ball Joint Scanner, Integration
 Frame Time = 2.25 sec

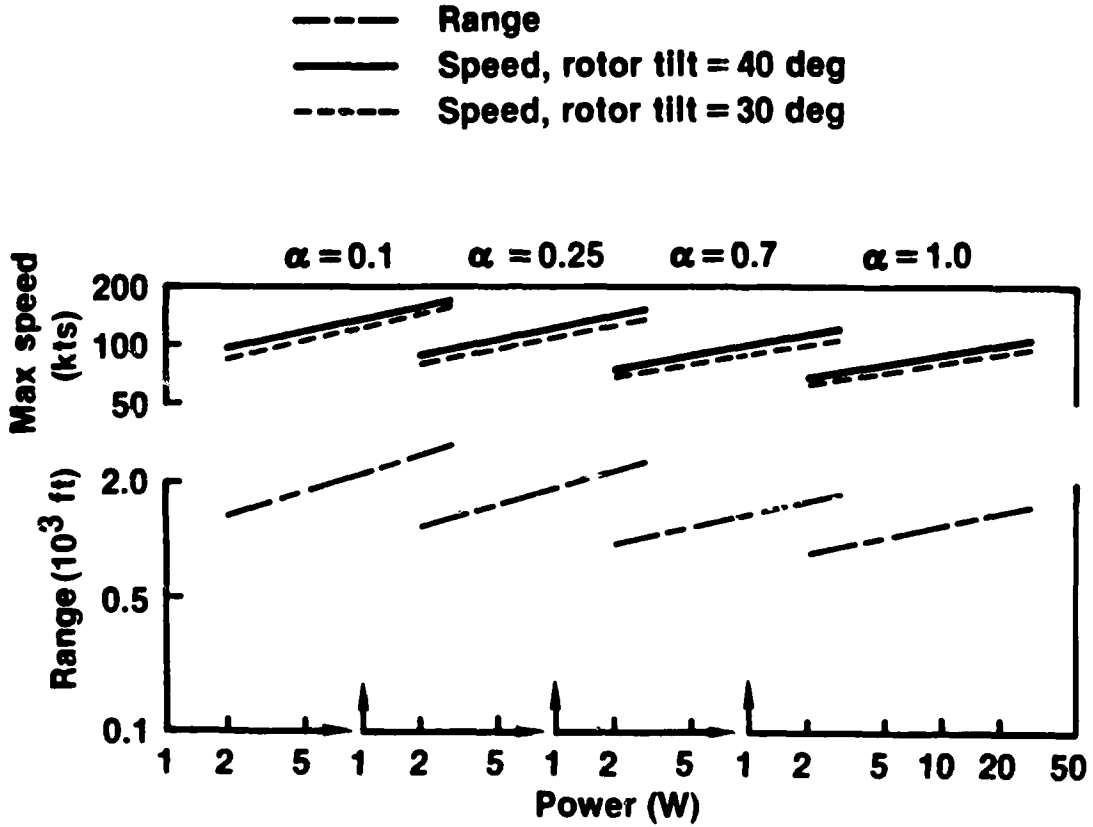


FIGURE 9.10 NOE SPEED/RANGE PERFORMANCE

4 in. Ball Joint Scanner, No Integration
 Frame Time = 1.5 sec

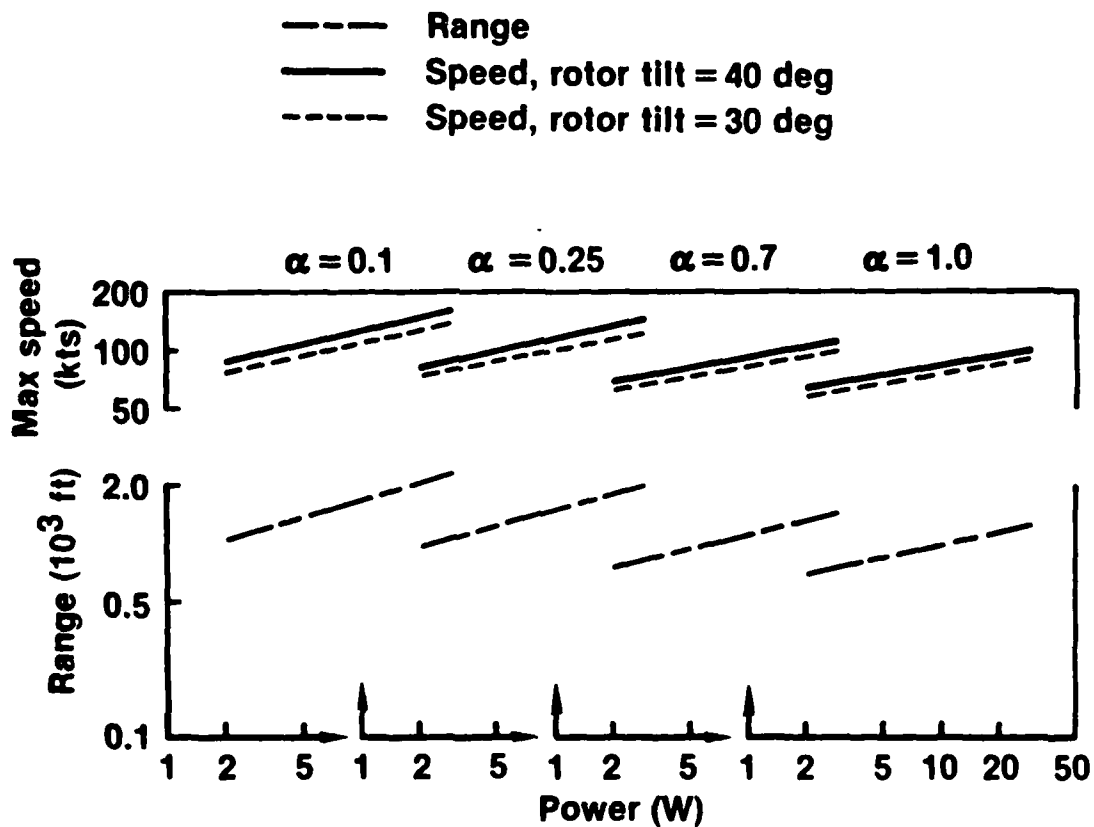


FIGURE 9.11 NOE SPEED/RANGE PERFORMANCE

**2 in. Dual Wedge Scanner, No Integration
Frame Time = 1.25 sec**

- Range
- Speed, rotor tilt = 40 deg
- - - Speed, rotor tilt = 30 deg

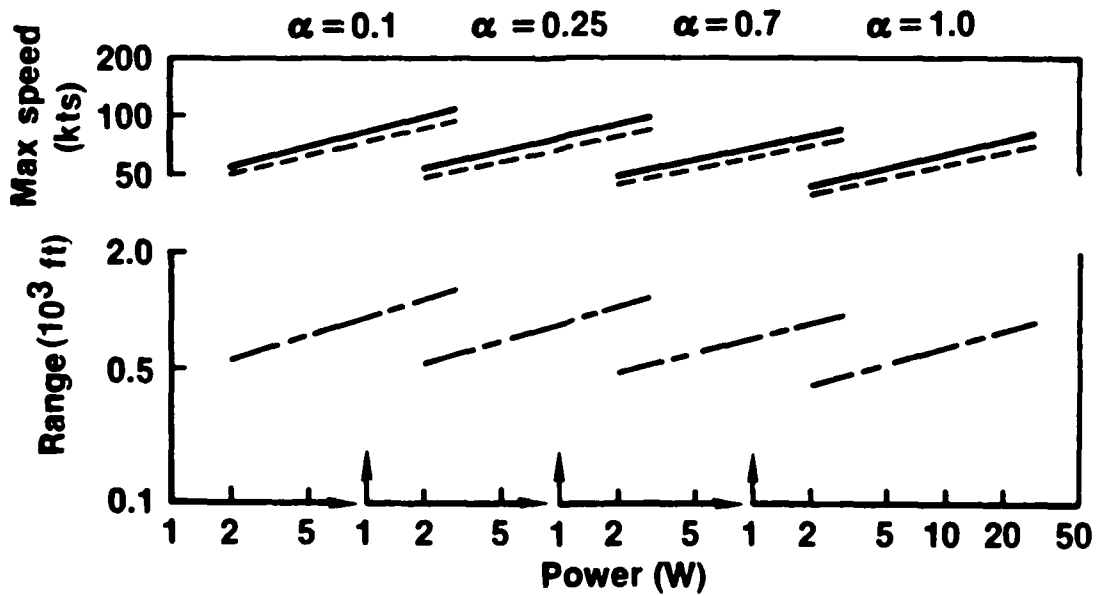


FIGURE 9.12 NOE SPEED/RANGE PERFORMANCE

2 in. Dual Wedge Scanner, Integration
 Frame Time = 2.5 sec

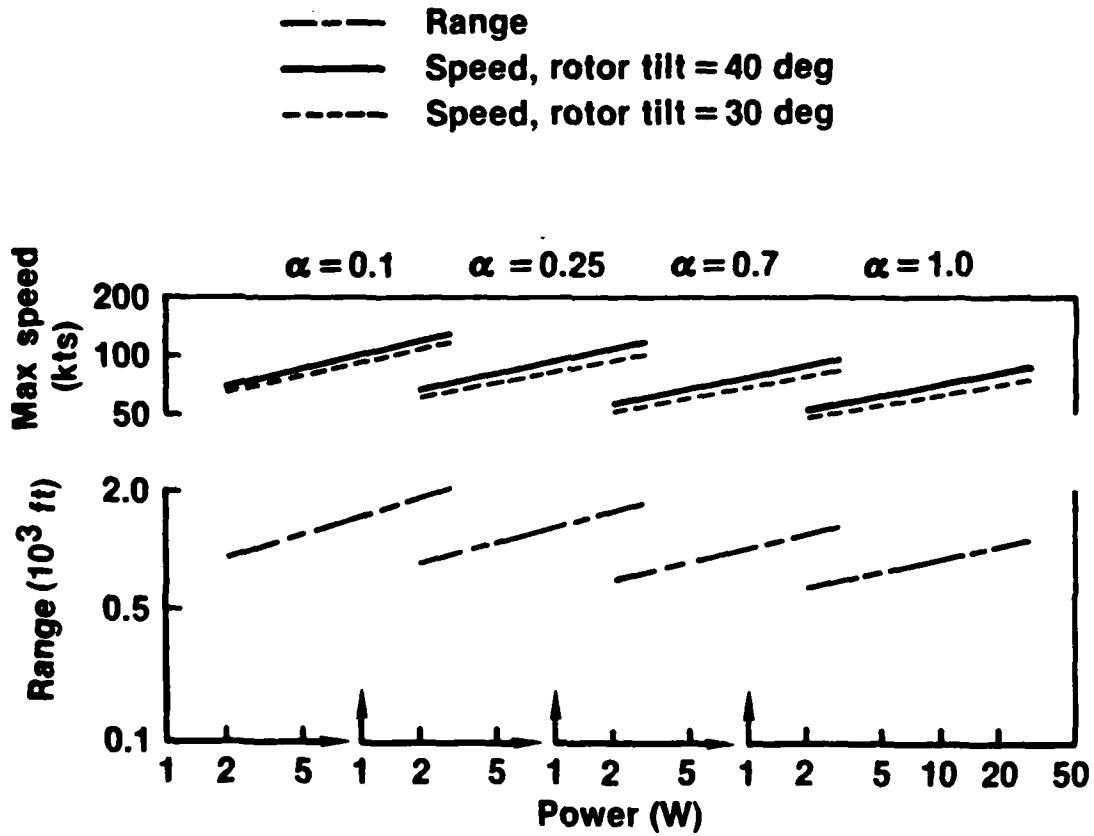


FIGURE 9.13 NOE SPEED/RANGE PERFORMANCE

**3 in. Dual Wedge Scanner, No Integration
Frame Time = 1.9 sec**

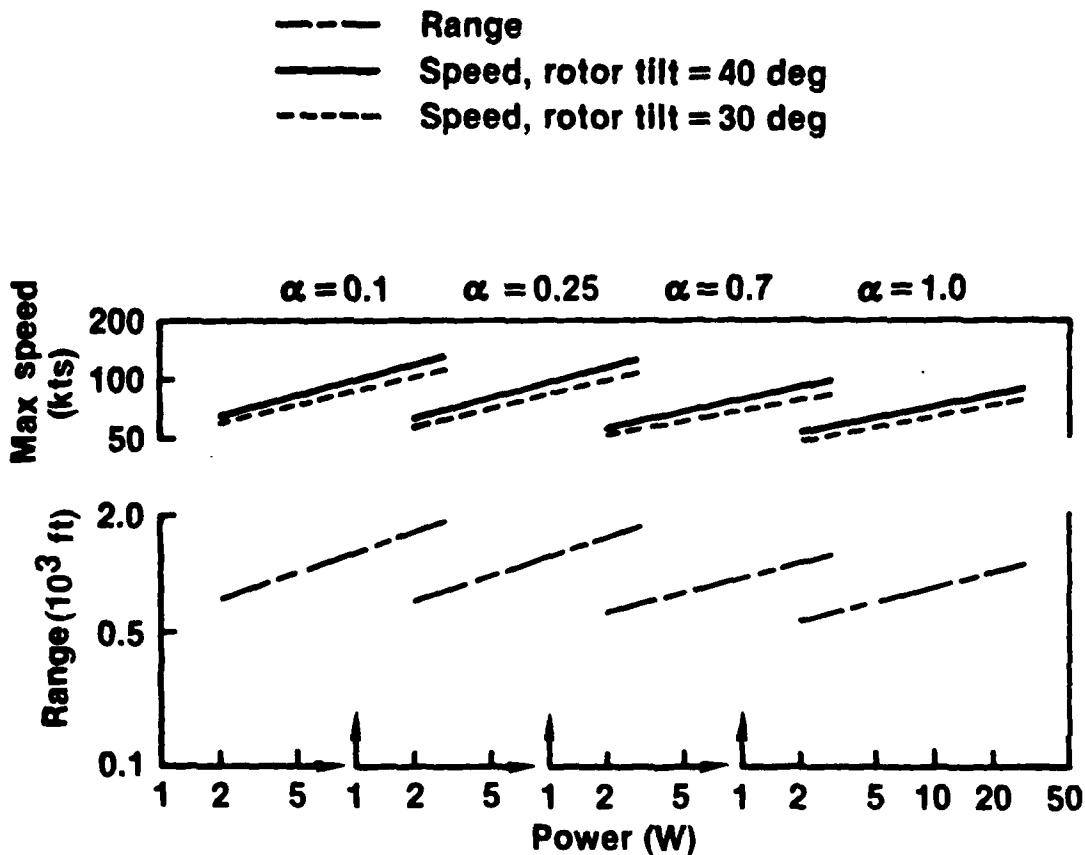


FIGURE 9.14 NOE SPEED/RANGE PERFORMANCE

4 in. Dual Wedge Scanner, No Integration
 Frame Time = 2.5 sec

- Range
- Speed, rotor tilt = 40 deg
- Speed, rotor tilt = 30 deg

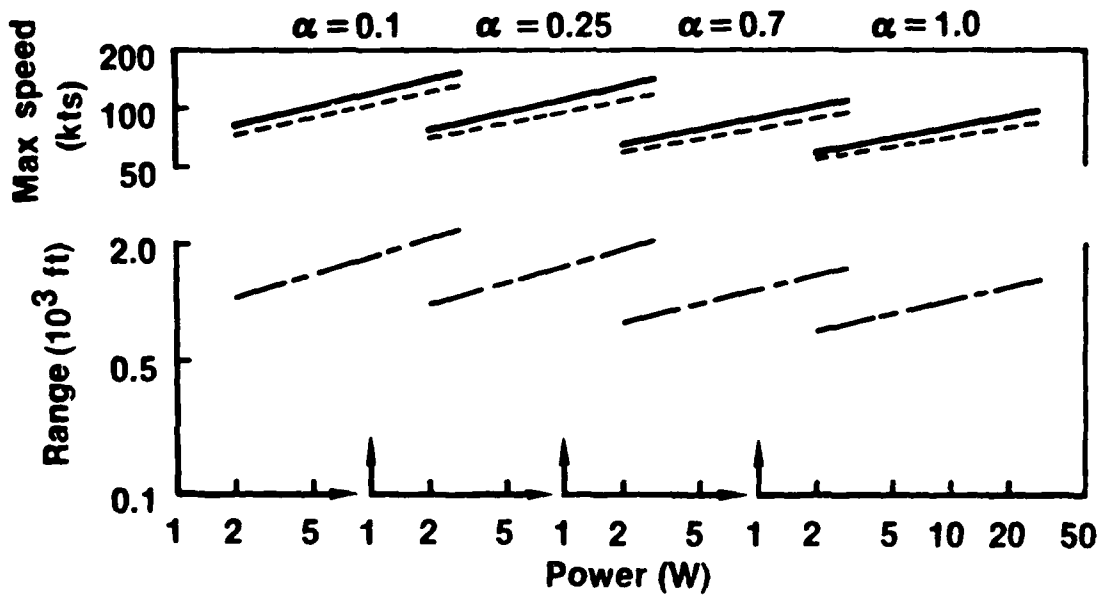


FIGURE 9.15 NOE SPEED/RANGE PERFORMANCE

Ball joint scanner with external window

30 deg W x 40 deg H FOR
30 deg W x 20 deg H FOV

- Pulsed laser
- - - CW laser
- Recommended design approach

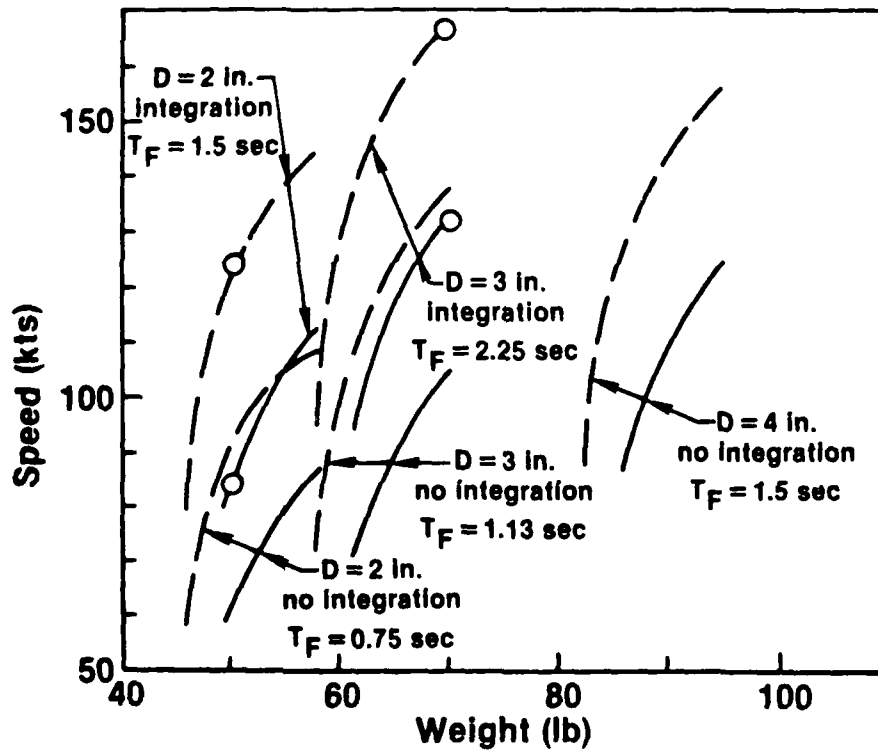
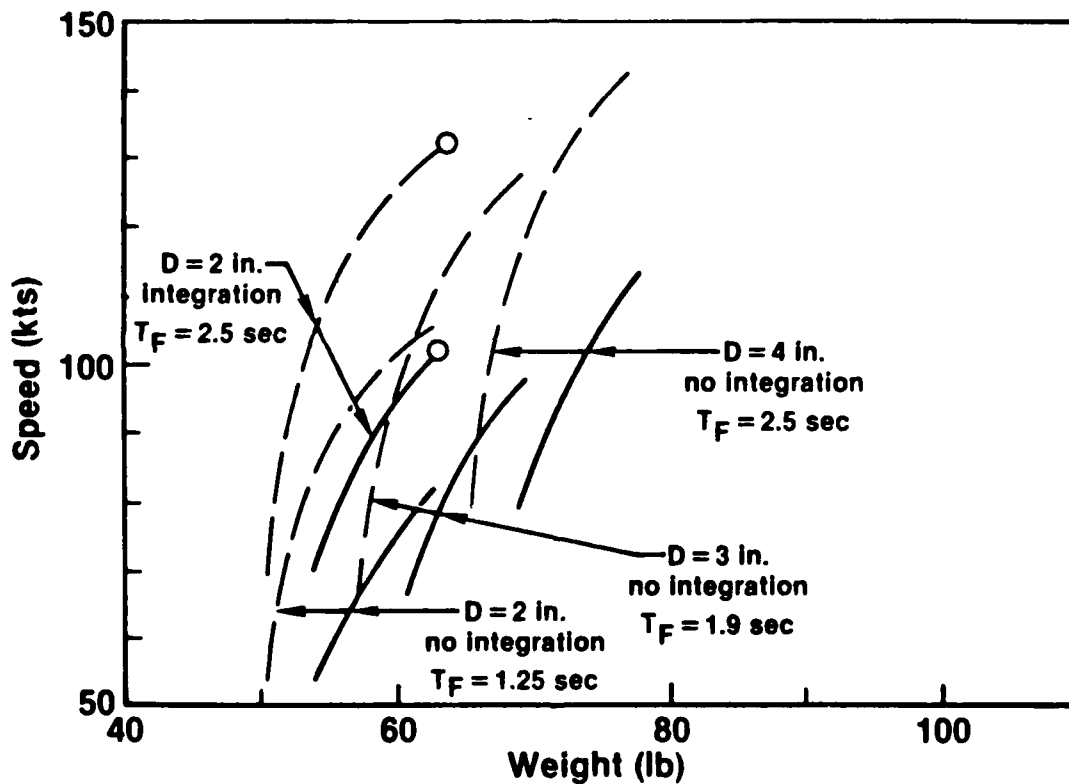


FIGURE 9.16 NOE SPEED/WEIGHT TRADEOFF

**Dual wedge scanner with 120 deg dia. FOR
56 deg W x 20 deg H FOV**

- Pulsed laser
- - - CW laser
- Recommended design approach



**FIGURE 9.17 NOE SPEED/WEIGHT
TRADEOFF**

Dual wedge scanner with 60 deg dia. FOR and pitch turret

56 deg W x 40 deg H FOR
56 deg W x 20 deg H FOV

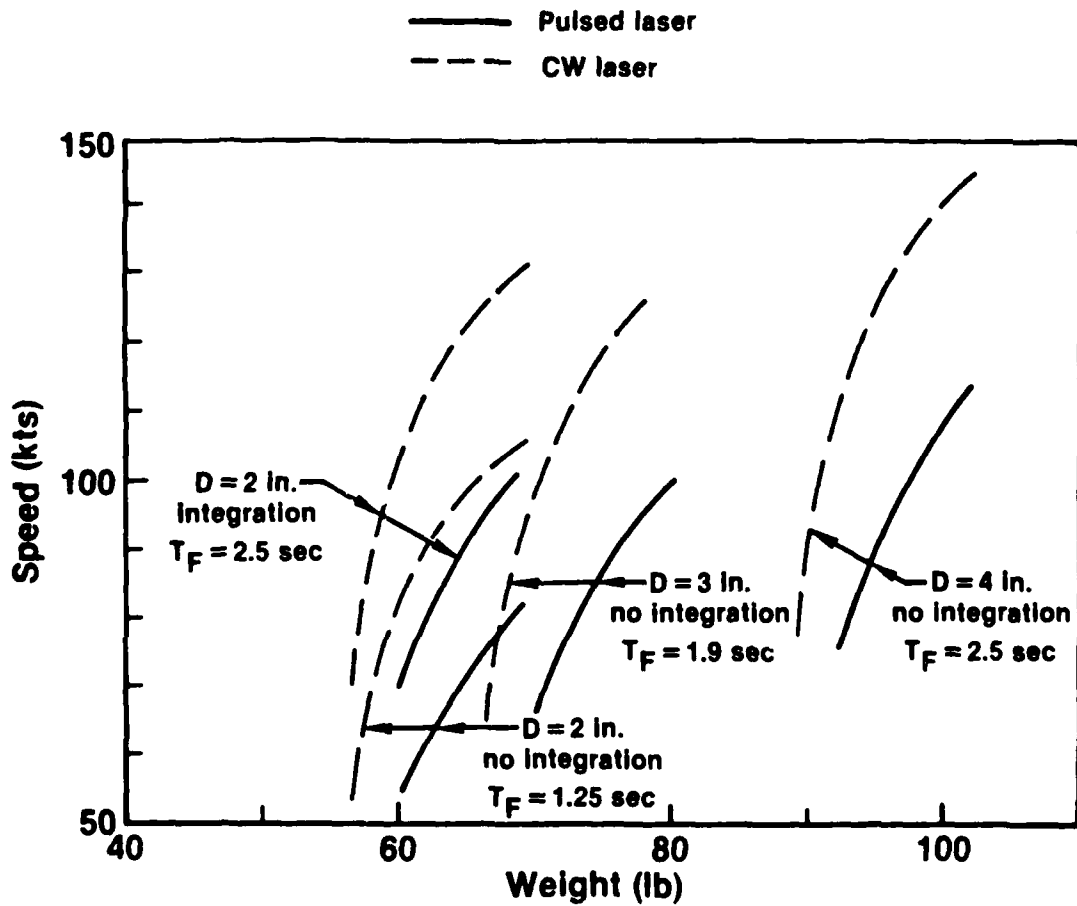


FIGURE 9.18 NOE SPEED/WEIGHT TRADEOFF

One feature common to all the results is that the decrease in required signal-to-noise ratio obtained with integration more than compensates for the increase in frame time so that the highest range and the highest allowable speed is always obtained with integration. However, integration is not used with the 4 in. ball joint scanner or with the 3 or 4 in. dual wedge scanner because the frame time would be larger than the nominal 2.5 sec indicated by the pilots as desirable, as discussed in Section 5.0. As can be seen by looking at the lines for no integration, an increase in scanner dia. results in both an increase in range and an increase in frame time but the net result is an increase in allowable speed capabilities. This would also be true for those cases where integration is used except for the fact that the large diameters cannot utilize integration because the frame time would be longer than 2.5 sec.

9.3 Recommended Design Approaches

The three recommended design approaches are indicated on Figs. 9.16 and 9.17 by pairs of circles. One recommendation is a two-inch ball joint scanner. This is the only system capable of performing useful functions within the weight goal of 50 lb. The two circles indicate the performance capabilities of the CW chirp (upper line) and the pulsed (lower line) lasers. As discussed in Section 7.0, the passively Q-switched pulsed laser would be the baseline design. However, the FM-chirp CW laser would be carried as a parallel development because it would yield superior range and speed capabilities if the modulation and signal processing problems were solved. Thus the anticipated performance of a 50 lb WWLODS with a 2 in. ball joint scanner would fall somewhere between the 2 circled points indicated in Fig. 9.16. The CW laser would have an average power output of 14.5 watts and the corresponding pulsed laser would have an average power output of 2.8 watts.

A second recommended design approach is a 3 in. ball joint scanner with the maximum laser power available, 30 watts for the CW laser and 10 watts for the pulsed laser. It has the highest range and speed capabilities of any of the system configuration options considered in this analysis. However, it also has a weight of 70 lb. This weight could be reduced to 66 lb if the internal window option for the scanner design were chosen. However, the external window is considered as the primary design approach because of its lesser problems with aerodynamics and with the accumulation of water in rain and fog weather conditions.

The third recommended design approach is a 2 in. dual wedge scanner with the laser power at the high end of the anticipated range. It has the highest value of FOR and a 56° wide FOV. These parameters will give it the capability of performing more flexible turn maneuvers than the ball joint scanner, which is limited to a 30° wide FOV, as can be seen from Figs. 6.7 through 6.9. The weight of this system is 63.5 lb which is roughly half way between the weight of the small and large ball joint scanners.

The characteristics of the 3 recommended design approaches are summarized in Table 9.4. As can be seen, the weights of the 3 systems are approximately equally distributed in the range from 50 to 70 lb. In order to reach the 50 lb weight it is necessary to accept low laser powers and the minimum scanner diameter. As a result, this system has the shortest range and the lowest speed capabilities. The primary evaluation parameter in the initial selection process was the speed capability of the helicopter in NOE flight in good weather ($\alpha = 0.1/10^3 \text{ft}$). This performance is always available because it requires no display of position information for the obstacles detected and can be utilized in conjunction with a simple audible warning or flashing light warning system. With a HUD a pilot has the option of performing a popup maneuver (Figs. 6.3 through 6.6) or a turn maneuver (Figs. 6.7 through 6.9). The speeds for performing the popup maneuver are comparable to those for performing the stopping maneuver in NOE flight. For the turn maneuver both the angle through which the flight path is turned and the speed at which the maneuver is performed are important parameters. The wider FOV available with the dual wedge scanner gives it the capability of turning through much larger angles than either of the ball joint scanners. It should be noted that all of these speed capabilities are based on performing the relatively modest maneuvers at constant speed. Higher speeds would be possible in every case if more severe maneuvers such as a transient climb or a steeper bank angle or rotor tilt angle were used.

The degradation in performance as the weather gets worse is also indicated in Table 9.4 for the NOE flight stopping maneuver. Even in the worst weather conditions (fog and 110 F 85% RH) the speed capabilities are still respectable. In the case of fog conditions, the speeds based on the stopping maneuver probably exceed the speed that the pilot could fly to maintain clearance above the ground even if there were no obstacles.

Table 9.4 shows the performance capabilities of the WWLODS for the nominal performance conditions required by the SOW: $P_D = 0.9$ against WD-1 wire. The performance has also been evaluated for a P_D of 0.999 against WD-1 wire and for a P_D of 0.9 against TOW/DRAGON wire. By coincidence the P_D of 0.999 requires an increase in SNR of 10.5 dB and the dia of the TOW/DRAGON wire is 10.5 dB lower than that of the 1/8 in. WD-1 wire. Thus the performance for both of these conditions is the same. The net result is a reduction in range by approximately a factor of 2.25 and the resulting ranges and the corresponding speeds for the NOE stopping maneuver are shown on Table 9.5.

Another requirement of the SOW is that the probability of false warning of wire, P_{FW} , should be a maximum of 0.05 with 0.01 desired. As discussed in Section 6.0 this requirement leads to a relationship between the WWLODS range and the laser pulse length for a pulsed system. The range/pulse length relationship is shown for the 2 in. dia scanners in Fig. 9.19 and the for 3 in. dia scanner in Fig. 9.20. In all cases it can be seen that the nominal pulse length of 150 to 200 nanoseconds discussed in Section 7.0 is compatible with the false warning criterion. The

Table 9.4
**RECOMMENDED DESIGN APPROACHES
 AND PERFORMANCE CAPABILITIES**

Integration, false alarm time = 2.8 hr
 40 deg rotor tilt, 30 deg bank angle, + 1.5g pullup, 0.0g pushover

Scanner type Diam Frame Time	System wt. (lb)	Laser power (W)		Range (ft) $\alpha = 0.1 /$ 10^3 ft	Maximum speed (kts)					
		CW	Pulsed		$\alpha = 0.1 / 10^3$ ft		NOE			
					Turn max θ / V	Popup $\theta_G = 0$	$\alpha = 0.25$	$\alpha = 0.7$	$\alpha = 1.0$	
Ball joint D = 2 in. TF = 1.5 sec	50.0	14.5		1650	deg/kts					
		2.8			30/85	115	124	110	92	85
Dual wedge D = 2 in. TF = 2.5 sec	63.5	30		2100	20/60	65	80	68	64	
		10			80/75	140	130	118	94	86
Ball joint D = 3 in. TF = 2.25 sec	70.0	30		3100	70/60	100	92	76	70	
		10			30/120	V_{max}	170	150	120	102
				2200	30/90	150	120	98	86	

Note: Higher speeds are possible if more severe maneuvers are used.

Table 9.5
SPECIAL PERFORMANCE CAPABILITIES

(a) Against WD-1 wire with $P_D = 0.999$
 (b) Against TOW/DRAGON wire with $P_D = 0.9$
 Dia = 0.011 in. = -10.5 dB re 1/8 in. WD-1 wire
 Midlatitude summer day, $\alpha = 0.1/10^3$ ft
 40 deg rotor tilt

Scanner	Laser power (W)	Range (ft)	NOE speed (kts)
	CW		
	Pulsed		
Ball joint Dia. = 2 in. $T_F = 1.5$ sec.	14.5	740	68
	2.8	440	41
Dual wedge D = 2 in. $T_F = 2.5$ sec.	30	940	73
	10	670	55
Ball joint D = 3 in. $T_F = 2.25$ sec.	30	1380	100
	10	980	77

Aperture dia = 2 in.

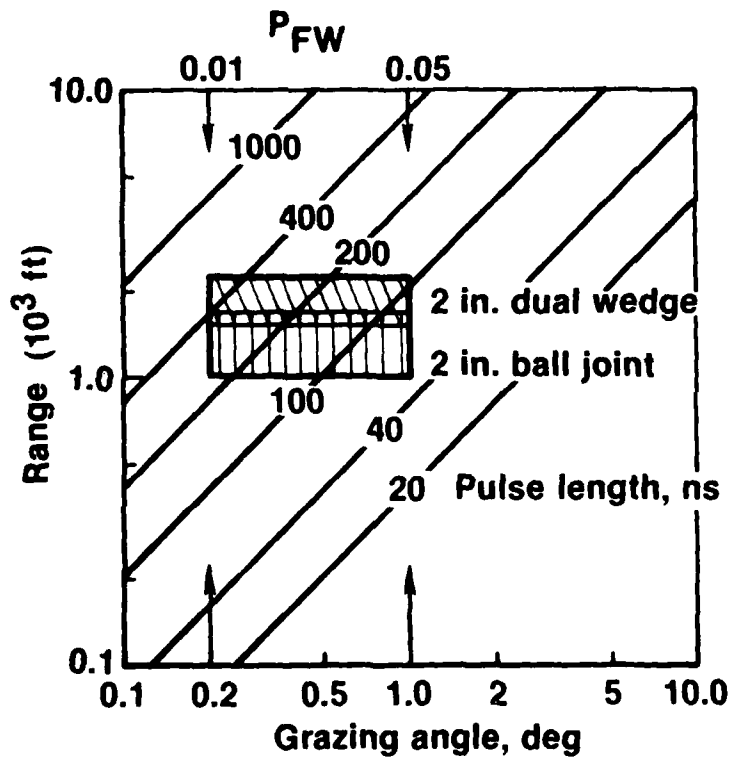


FIGURE 9.19 FALSE WARNING LIMITS ON RANGE AND PULSE LENGTH

Aperture dia = 3 in.

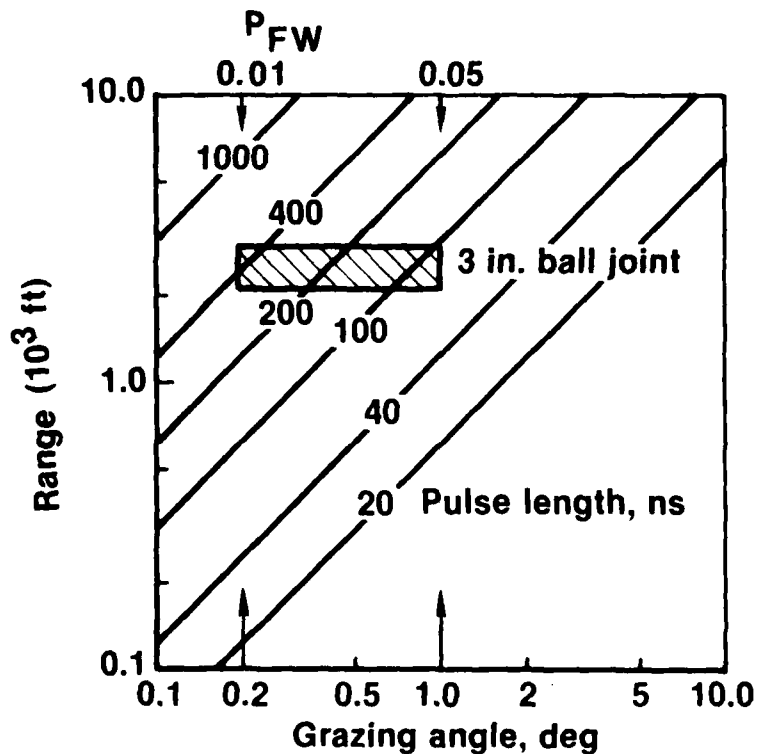


FIGURE 9.20 FALSE WARNING LIMITS ON RANGE AND PULSE LENGTH

question of wire discrimination for the CW chirp system is an unresolved signal processing issue at this time.

The ability of the WWLODS to operate in cross-wind conditions is a function of the width of the field-of-view. The crab angle θ_{CR} is a function of the cross wind velocity V_C , and the velocity over the ground V_G :

$$V_C = V_G \tan \theta_{CR}$$

The crab angle also depends on the available width of the field-of-view, LFOV, and the width of the clear window required for pilot safety, W:

$$\theta_{CR} = \frac{LFOV - W}{2} \quad (2)$$

For the minimum acceptable window width (\dot{W}) of 24° defined by pilot preferences (see p. 16 and Fig 5.1), Eq. (2) results in crab angles of 3° for the ball joint scanners and 16° for the dual wedge scanner. Substituting in Eq. (1), $V_C = 0.05241 V_G$ for the ball joint scanners, and $V_C = 0.28675 V_G$ for the dual wedge scanner. The resulting crosswind capabilities are shown as a function of ground speed in Fig. 9.21. It can be seen that the wide field-of-view of the dual wedge scanner gives it a much greater ability to accommodate crosswinds than does that of the ball joint scanner.

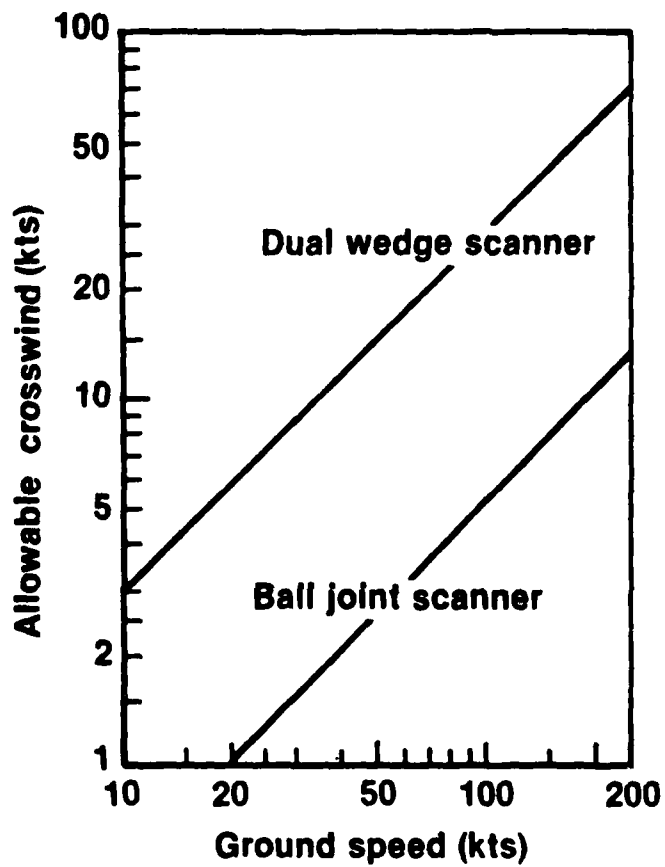


FIGURE 9.21 CROSSWIND CAPABILITIES

9.4 Preliminary Design Concepts

For each of the recommended designs, a preliminary conceptual layout was made to establish the geometrical relationships of the major subsystems, the mechanical and optical design requirements, the weight buildup of the complete system, and the envelope dimensions. Pods constrained to mate with an external location on the UH-60A were designed in all cases.

The 2-in. dual-wedge-scanner WWLODS is shown in Fig. 9.22. The front section of the pod is axially symmetric to accommodate the dual wedge scanner. Immediately behind the scanner is the interferometer volume which contains the germanium duplexer, 1/4 wave plate for polarization control, beam-expanding telescope, receiver including detector, dewar, and cooler to maintain the detector at 77 K, and the required folding and alignment mirrors. The transmitter and local oscillator waveguide lasers, built in a common ceramic block, and the laser power supplies and pulse modulator frequency control and air cooling components are arranged in the aft section of the pod.

The major structural element is the interferometer housing, indicated by the crosshatching in Fig. 9.22. The lasers are rigidly mounted to the rear of this housing, so that it maintains the critical alignments and provides the stiffness necessary to place the structural resonances at a frequency on the order of 300 Hz, which is well beyond the primary helicopter vibrational forcing functions. Mounting points are shown spaced as required for a standard external stores assembly. An installation on the stub wing of the UH-60A is shown in Fig. 9.23. This installation suffers a FOV loss in the upper right quadrant due to shielding by the aircraft fuselage. The compact size and simple shape of this design would also allow mounting in the nose avionics bay, which would eliminate the shielding limitations but would require rearrangement of the existing equipment in current aircraft.

The pod and its contents would be built to conform to approved military specifications. Its weight breakdown and overall dimensions are shown in Column 1 of Fig. 9.24. Also shown in Fig. 9.24 are the major characteristics of the other two recommended designs. As indicated in Fig. 9.24, the ball joint scanner designs require larger windows and more folding mirrors than the dual wedge scanner. Because the WWLODS must be capable of mating with all the helicopters listed in Table 5.1, signal processing elements to convert the receiver output to input signals for the various display options, and cable connections to the prime power supply in the aircraft would have to be custom designed and therefore have not been included in the weight breakdowns of Fig. 9.24. It is estimated that the total weight of these items would range from 2 to 6 lbs. All installations would require a control box containing 1 circuit card, switches and indicators, with an estimated weight of 1 lb, and 1 to 3 lbs of cables. These components could trigger an existing audible or flashing light signal for a total weight of 2 to 4 lbs. To generate a more complex display to indicate the quadrant in which the detection occurs (as discussed in Section 10) would require 1 additional card to read coarse LOS position from the

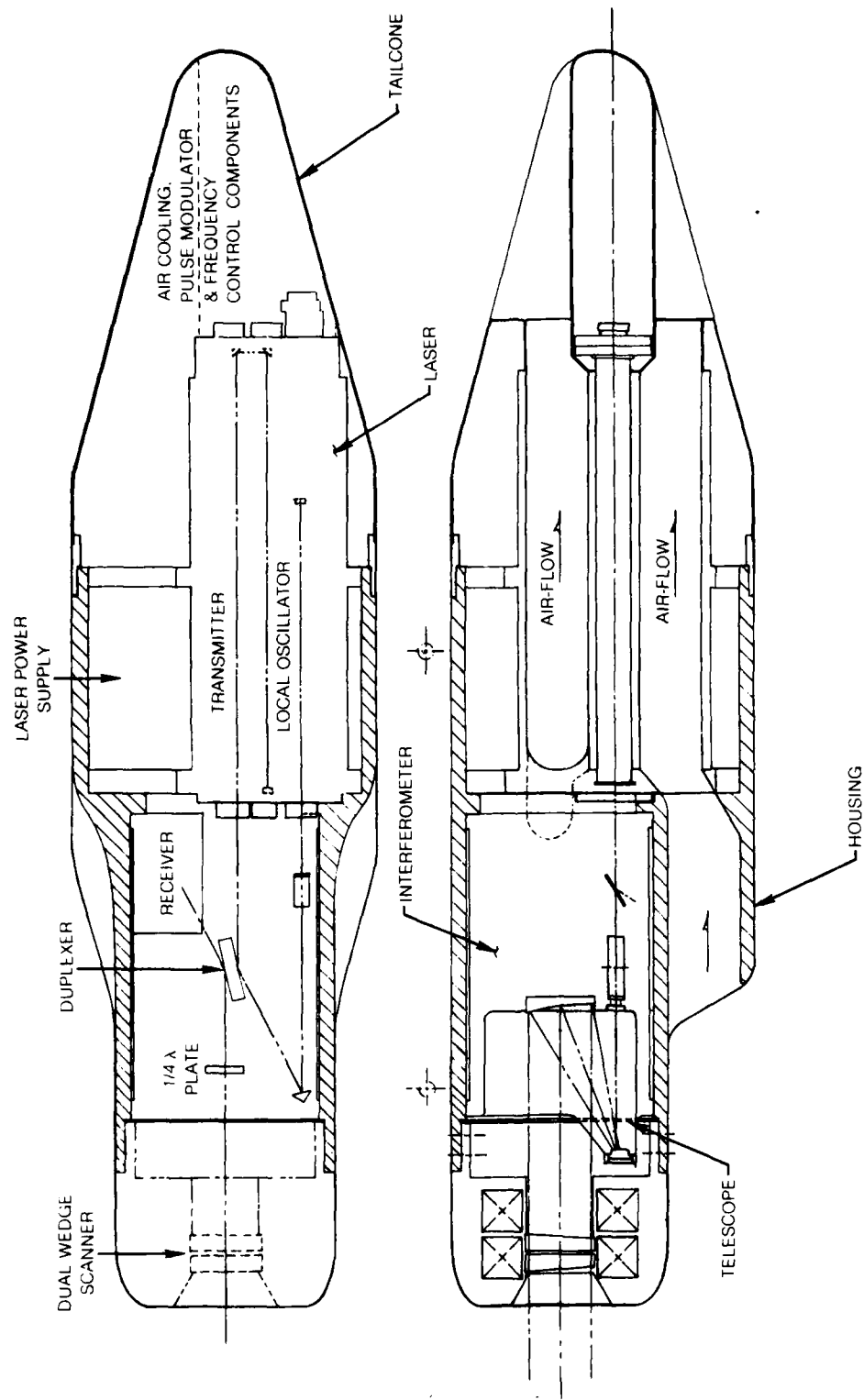


FIGURE 9.22 PRELIMINARY DESIGN CONCEPT FOR 2-in. DUAL WEDGE SCANNER WWLODS

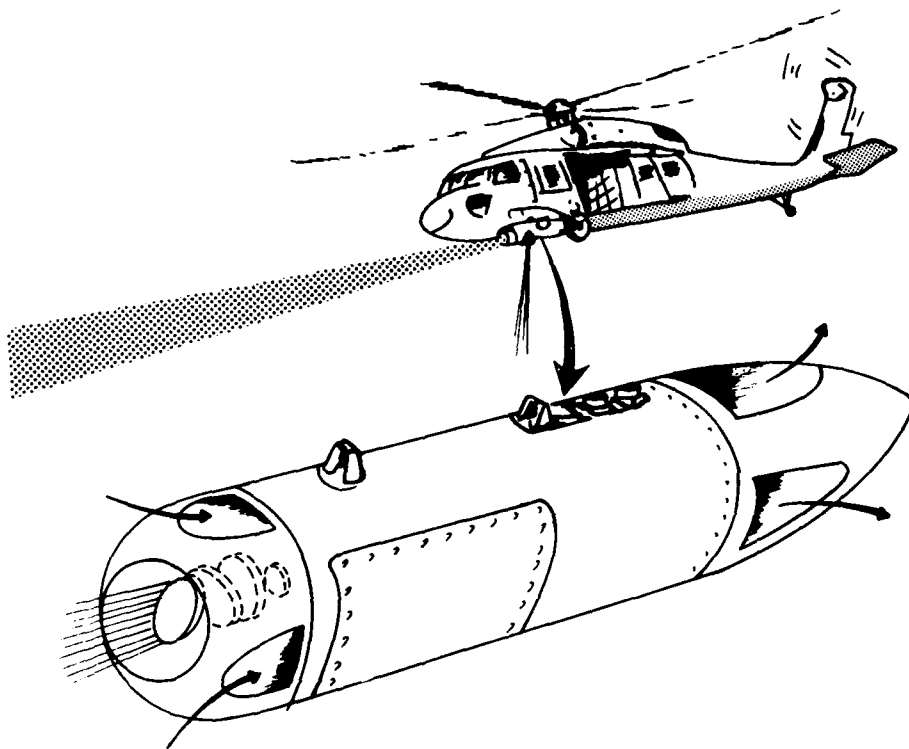


FIGURE 9.23 WWLODS INSTALLATION

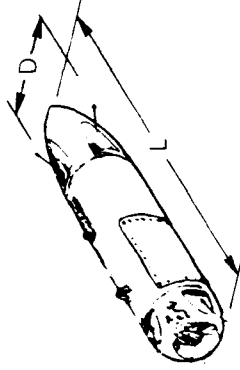
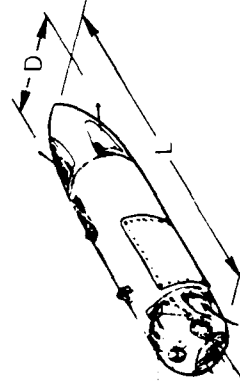
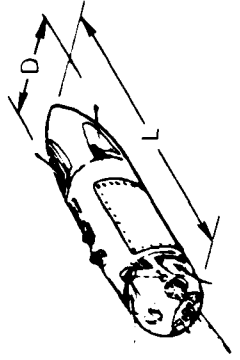
	 2 in. WEDGE	 3 in. BALL JOINT	 2 in. BALL JOINT
WEIGHTS (lbs)			
LASER	11.1	11.1	6.7
LASER POWER SUPPLY	9.0	9.0	6.0
INTERFEROMETER	8.0	9.0	8.0
SCANNER	12.5	18.5	9.6
POD & REMAINING COMPONENTS	22.9	22.9	20.2
TOTAL	63.5	70.5	50.5
LENGTH (L)	36.0 in.	40.0 in.	30.0 in.
DIA D	8.5 in.	8.5 in.	8.5 in.

FIGURE 9.24 POD DESIGN SUMMARY

scanner and a four-light display such as that in Fig 10.2, and would have a total weight of 3 to 5 lbs. To interface with an existing video display or HUD would require 3 additional cards and would result in a total weight of 4 to 6 lbs.

Most of the items in the WWLODS are standard materials, catalog items, or nearly identical to elements of existing systems such as LOTAWS. The laser, however, would be a new development. Therefore, a preliminary design of the laser was made, major parts were detailed using alternative material and fabrication techniques (aluminum and steel; casting, forging, and extrusion; and welding, bonding, and bolting). Vendor quotes were obtained on major parts, including the BeO laser channels, to provide a basis for estimating both the practicality of the design and the production cost.

10.0 PROGRAM PLANS, RISKS AND COST ESTIMATES

Program plans have been formulated to cover the time between the 6.2 program end and the time of Initial Operational Capability (IOC). These plans have been broken down into 6.3B, 6.4, and production segments. Two alternative plans have been developed entailing two levels of risk, one lower and one higher. Both plans are designed to yield a WWLODS with performance as required by the mission and a system meeting all mil specs; the risk involved is in meeting the program schedule, weight, size or cost goals.

10.1 6.3B Program

The objective of the 6.3B program is to demonstrate the performance of the complete system and of all the subsystems. The major elements of the 6.3B program are shown in Table 10.1. At the beginning of the 6.3B program, it is necessary to perform a detailed concept formulation and design of the complete system so as to arrive at a quantitative definition of the parameters of all of the subsystems.

Major Issues

The baseline design, which derives from demonstrated technology, is the passively Q-switched pulse laser with electric discharge excitation. For this approach, the issue is obtaining the highest possible efficiency, within the limits set by the large intracavity losses introduced by the Q-switch, so as to obtain the highest possible output power. As discussed in Section 7.0, an alternative development would be directed at the production of a CW chirp laser with RF excitation because of its promise of high output power. The issue in the development of this laser is the accuracy with which the chirp modulation can be maintained and the impact which any errors in modulation would have on the signal processing. The power supply to drive either the RF or electric discharge laser is a straightforward development problem whose only issue is minimization of weight. Frequency controls are required for the transceiver, but these are straightforward systems which have already been demonstrated at adequate performance levels in the LOTAWS program.

The scanner selection from among the three recommended design approaches would be made in the detailed design activity. In the case of the ball joint scanner, the major issues are the design and cost of the window. For the external window the erosion resistance of the Anti-Reflection (AR) film and the cost of relatively large windows are the issues. For the internal window option the aerodynamic disturbance which may be introduced by a forward facing opening is a potential problem. For the dual wedge scanner the preferred design approach requires a FOR with a 120 degree angle and a FOV with dimensions roughly 20 degrees high by 56 to 60

Table 10.1
MAJOR ELEMENTS OF 6.3B PROGRAM

<u>Element</u>	<u>Issue</u>
● Detailed concept formulation and design	Quantitative subsystem definitions
● Laser <ul style="list-style-type: none"> • Pulsed, RF, 1-10W • CW chirp, RF, 2-30W • Power supply • Frequency controls 	Efficiency Modulation Weight
● Scanner <ul style="list-style-type: none"> • 2 in. ball joint } • 3 in. ball joint } • 2 in. dual wedge 	Window, water film Wedge accelerations, water film
● Interferometer <ul style="list-style-type: none"> • Beam expander • Duplexer • Telescope • Detector • Frequency monitor 	Open vs. closed cycle cooling
● Package	Multiple installations
● Signal processing <ul style="list-style-type: none"> • Pulsed • CW chirp 	● Wire discrimination/false warning <ul style="list-style-type: none"> • Pulse length vs. false warning • Frequency domain processing
● Display <ul style="list-style-type: none"> • Audio • Up-down, left-right } • HUD 	Pilot interface
● Integration	DTI
● Flight test	OTI

degrees wide, which is programmable to various locations within the field of regard. The issue in this case is the magnitude of the accelerations required for the wedges in order to meet the scan programming requirements and the availability of adequate torquers. This issue would have to be addressed in the detailed design stage. For all scanners an issue which must be addressed is the possibility of forming a film of water on the outside surface in rain or fog conditions. A design which will not permit the formation of water films must be found since the l/e absorption length of water at 10.6 μm is approximately 10 microns, and the WWLODS cannot tolerate such a large transmission loss.

Noncritical Issues

The interferometer comprises the beam expander, duplexer, transmit/receive telescope, signal detector and the detector(s) to monitor the laser frequency. A configuration based on the successfully demonstrated LOTAWS arrangement is expected to be more than satisfactory for this application. The only issue to be resolved in the detailed design stage is the question of whether an open-cycle Joule Thompson refrigerator or a closed cycle Stirling cryopump should be used to cool the detectors. The tradeoff is between initial cost and weight versus reduced weight and life cycle costs.

Packaging would be a straightforward problem if the WWLODS were to be used on only a single vehicle. However, the five vehicles on which the anticipated use of the WWLODS is based, do not have common mounting hard points or even good locations available for a pod. A pod installation which would fit all 5 helicopters also has potential limitations in terms of compatibility with helicopter Center of Gravity (CG), limitations. Thus, an option which would have to be considered in a detailed design stage would be the use of self contained packages which could be located in the various helicopters in the most optimum way.

The main issue in the signal processing subsystem is the ability to discriminate wires from background objects without creating false warnings. If a pulsed laser format is used, this issue resolves into a tradeoff between pulse length and false warnings resulting from grazing incidence on extended targets such as ground or treetops. For the CW chirp laser, signal processing will be done in the frequency domain rather than in the time domain as is the case with the pulsed laser. In addition to the range/Doppler ambiguity common to chirp radars (but resolvable) the major uncertainty is wire discrimination. It is possible that a loss in effective SNR would occur in frequency domain processing and this issue would also have to be addressed in the detailed concept formulation and design phase.

Development of the interface between the display and the pilot would be a major issue in the 6.3B program. Display options range from a simple audio warning, to a slightly more complex four-light display that would give up-down and left-right information, to a head-up display which would give synthetic scene data to the pilot. A hypothetical scene in which a wire warning would occur is shown in Fig. 10.1. With the audio warning, the pilot's only option is to stop. A very simple display which would be mounted on top of the instrument panel glare shield and therefore would

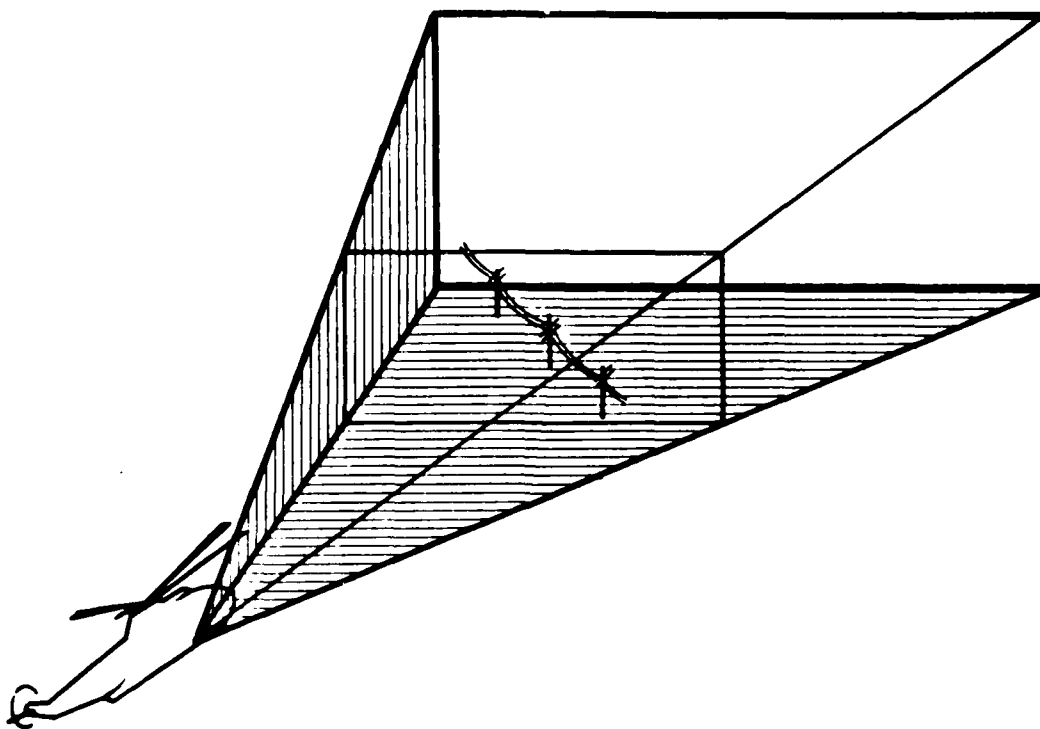


FIGURE 10.1 HYPOTHETICAL SCENE

always be in the pilots field-of-view without requiring him to look away from the outside world, is illustrated in Fig. 10.2. This would consist of four lights which would tell the pilot which quadrant the obstacle or obstacles lie. Additional information could be provided by having the light corresponding to the closest obstacle flash or by having the light flash when the range to the obstacle was equal to or less than a value which could be chosen by the pilot and set into the system. This display would give the pilot the option of maneuvering over or around the obstacle rather than stopping, provided that he can identify the obstacle visually.

All the pilots interviewed agreed that if a HUD is available they would prefer the type of display shown in Fig. 10.3. The symbology used here is similar to that which is familiar to pilots from the VSI/EMADI/EADI instruments currently in use and all of the data required for forming this display is available to the WWLODS as discussed in Section 5.0. In this display format all the obstacles detected in a given frame would be displayed. They are shown as circles in Fig. 10.3. Those closer than a threshold value of range, which would be input by the pilot, would be flagged as indicated by the arms on the two right-hand obstacle symbols and the closest obstacle would be indicated by either a flashing symbol or a filled in symbol as indicated by the far right symbol in Fig. 10.3. The position of the velocity vector relative to the horizon would also be displayed and in addition a symbol which would be representative of the actual dimension of the rotor of the helicopter at the range of the closest obstacle would also be displayed. A numerical indication of the range, say in hundreds of feet, would also be shown to the pilot. The operation of this kind of display, in a typical flight profile, is illustrated in Fig. 10.4. When the helicopter is at position 1, frame 1 is generated showing obstacles A and B with A being closer and nine units of range away. The size of the aircraft symbol indicates that the helicopter could fly between obstacles A and B if the pilot wished to. If the pilot continues his right turn, position 2 and frame 2 indicate that all three obstacles are within the field-of-view of the WWLODS and that the closest obstacle, obstacle A, is five range units away. At position 3 (frame 3) obstacle A has gone out of the field of view, obstacle B is two range units away and the flight path is almost parallel to the line of B and C. The helicopter will pass to the right of the obstacle C with adequate clearance.

Under the ground rules established in Section 5.0, the audio and flashing light display options are usable on all the aircraft in Table 5.1, and do not interfere with any existing displays. The preferred display can be superimposed on any HUD and would therefore be usable on the AAH and AH-1S, and also on the ASH if it has some form of HUD. The use of the EADI, which could accept and present the preferred display format, is not acceptable because it is a heads down instrument.

The two remaining activities in the 6.3B program are system integration, which is necessary to assure that a flyable item will be produced at the end of the 6.3B

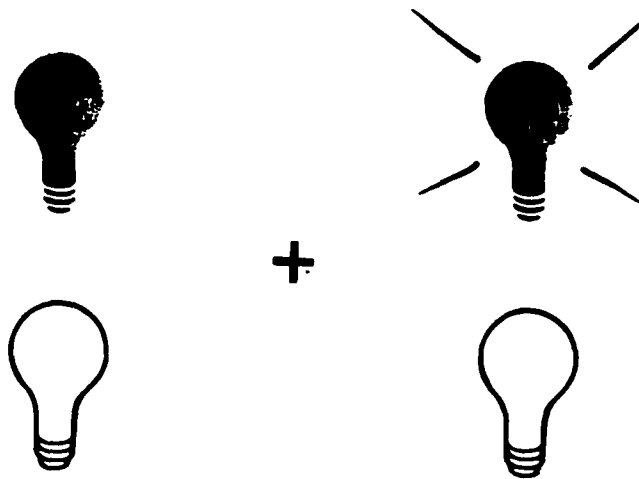


FIGURE 10.2 MINIMUM DISPLAY OPTION

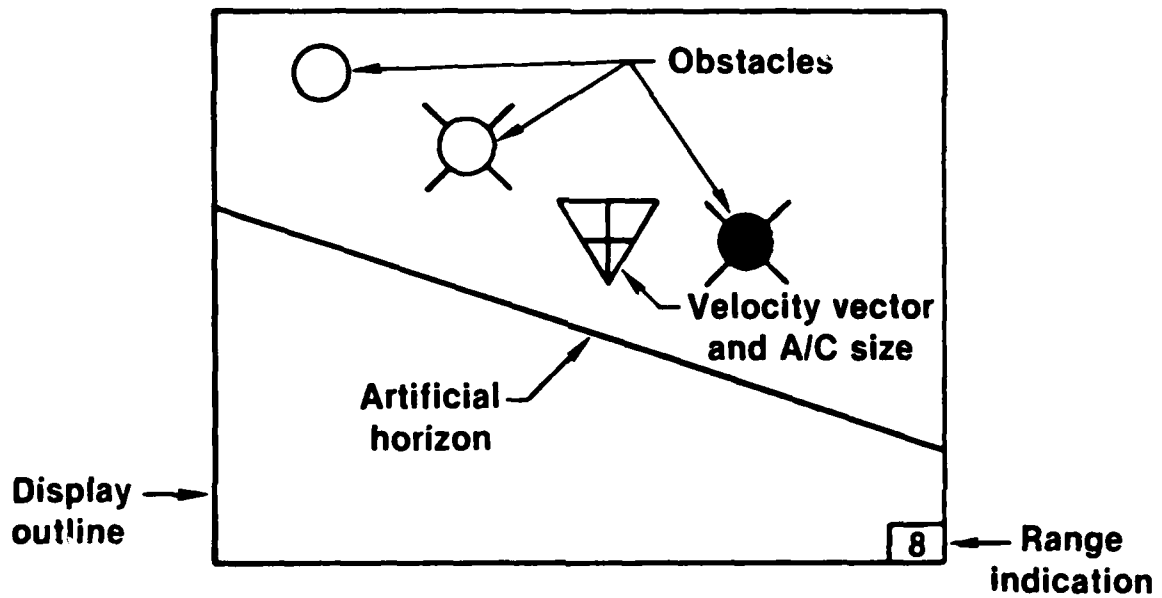


FIGURE 10.3 PREFERRED DISPLAY

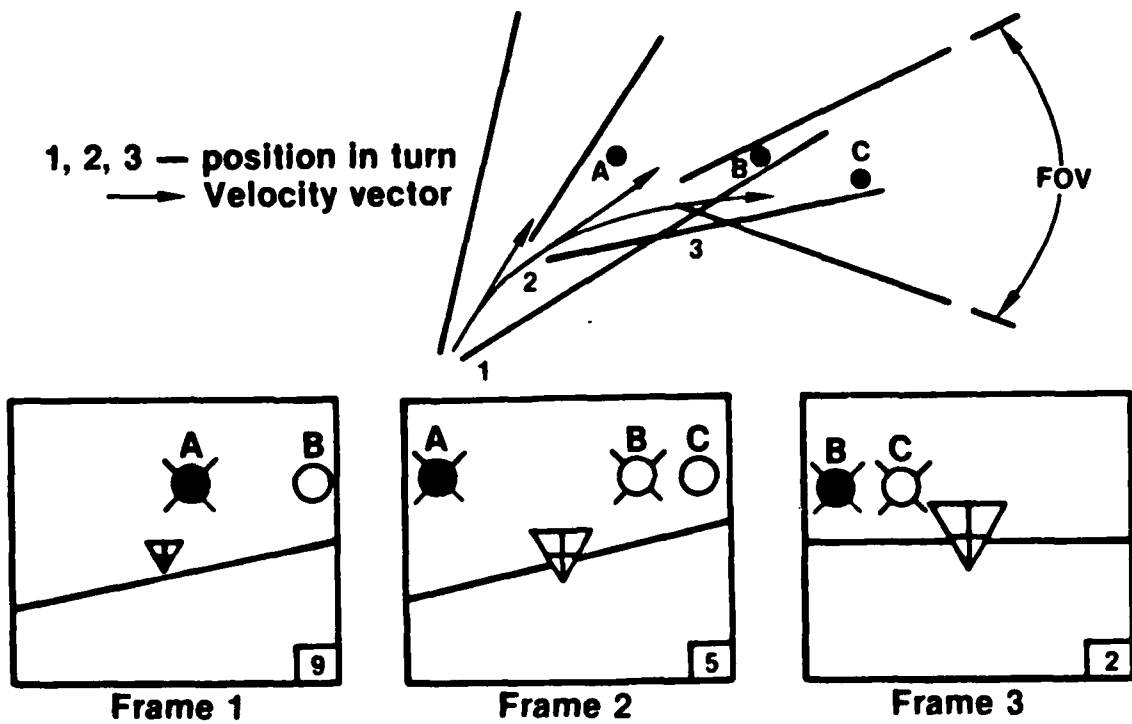


FIGURE 10.4 DISPLAY PRESENTATION OF A TYPICAL FLIGHT PROFILE

program and which is the end item which is examined during Development Test I (DT I) for Army approval. Provision of a flight test program is necessary to verify the actual performance of the system and to satisfy the Army requirements for Operational Test I (OT I).

The structure of the 6.3B program activities is illustrated in Fig. 10.5. The elapsed time for this program would be 24 months. A great deal of parallel activity is performed during this time and the integration activity which assures that all these separate design and development activities are properly interfaced is an important element of the program. Also note the element labeled display/pilot interface. This activity should be performed using a computer-driven cockpit simulation and would require the cooperation of Army flight personnel. It would be an important element in the determination of the actual display type.

10.2 6.4 Program

The elements of the 6.4 program are shown in Table 10.2. The objective of the 6.4 program is to release to the manufacturing activity a complete definition of all the parts and procedures required to manufacture, install, maintain and operate the system. A number of constraints exist in the 6.4 program which are not found in the 6.3B program; in addition to meeting the performance requirements, the 6.4 program must use mil spec parts and must meet the weight, cost and "ilities" goals. Timely completion of approval procedures and making of decisions are both necessary in order to meet the schedule and cost goals. The elements of the 6.4 program listed in Table 10.2 are shown in a time-phased manner in Fig. 10.6. The process of engineering design and of the redesign to correct any shortcomings found in the testing programs results in the creation of specifications and drawings for parts to be manufactured and for purchased parts and materials lists. In the course of the 6.4 program, six to eight complete WWLODS units would be fabricated, assembled and tested. A variety of qualification demonstrations would be performed to verify that the WWLODS will survive in the Army operational environments. The test conditions involve various combinations of temperature, humidity, vibration, shock and altitude and would be performed at the component (box), subsystem, and system levels. One or more of the preproduction units would be operated in a reliability demonstration to establish the Mean Time Between Failures (MTBF) of the components and of the complete system. Another unit would be required to demonstrate the maintainability of the system and to establish maintenance procedures. One early activity is the development of a number of program plans including: safety, reliability, Quality Assurance (QA), Electromagnetic Compatibility (EMC), Survivability/Vulnerability (S/V), Nuclear Hardness Assurance (NHA), and Integrated Logistics Support (ILS). These plans impact both the design of the system and the procedures used in the 6.4 program testing and later in the production program. Nuclear survivability criteria are met by conducting a Nuclear Hardness Assurance (NHA) program in accordance with a NHA plan during the 6.4 program. This is a detailed design activity and cannot be fully defined at this time.

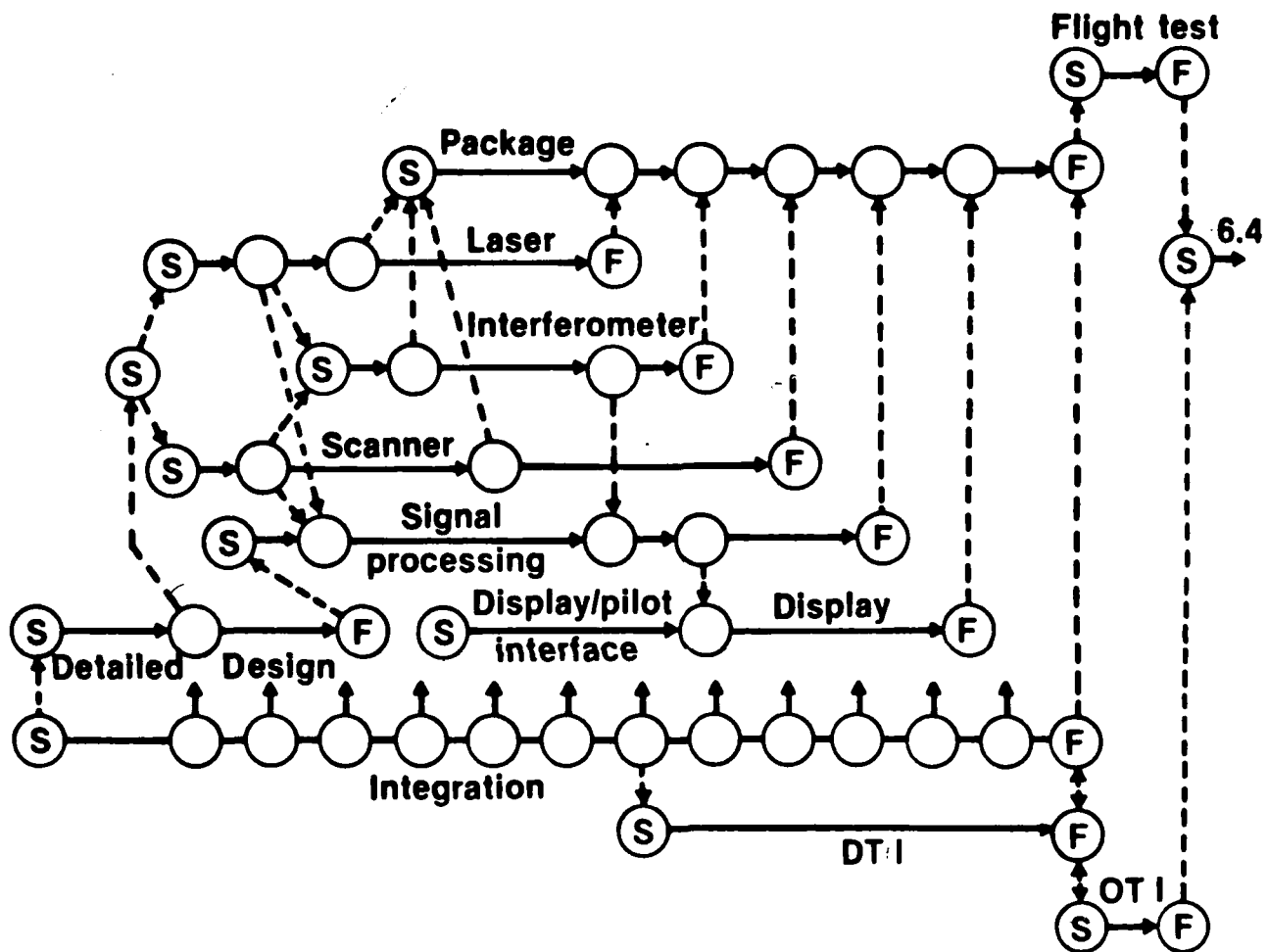


FIGURE 10.5 6.3B PROGRAM STRUCTURE

Table 10.2

6.4 PROGRAM

- **Objective:** Release definition to manufacturing
 - **Constraints:** Performance, mil specs, weight, cost, schedule, approvals/decisions
-
- | ● Elements | ● Outputs |
|---|---|
| ● Eng. design/redesign | ● Dwgs, specs, parts and matls. lists |
| ● Fab. and assem. | ● 6 - 8 complete units |
| ● Qualification demos. | ● Environ. survivability |
| ● Reliability demos. | ● MTBF |
| ● Maintainability demos. | ● Maintenance procedures |
| ● Safety, reliability, QA, EMC, S/V, NHA, ILS plans | ● Design and procedures |
| ● Prod. tooling design | ● Dwgs, specs, parts and mat'ls. lists |
| ● Acceptance test sys. design | ● Dwgs, specs, parts and mat'ls lists |
| ● Publications | ● Operator's and maintenance handbooks, record dwgs, specs, parts and mat'ls lists, reports and data on all demos, nomenclature |
| ● DT II | ● Army acceptance |
| ● OT II | ● Army acceptance |

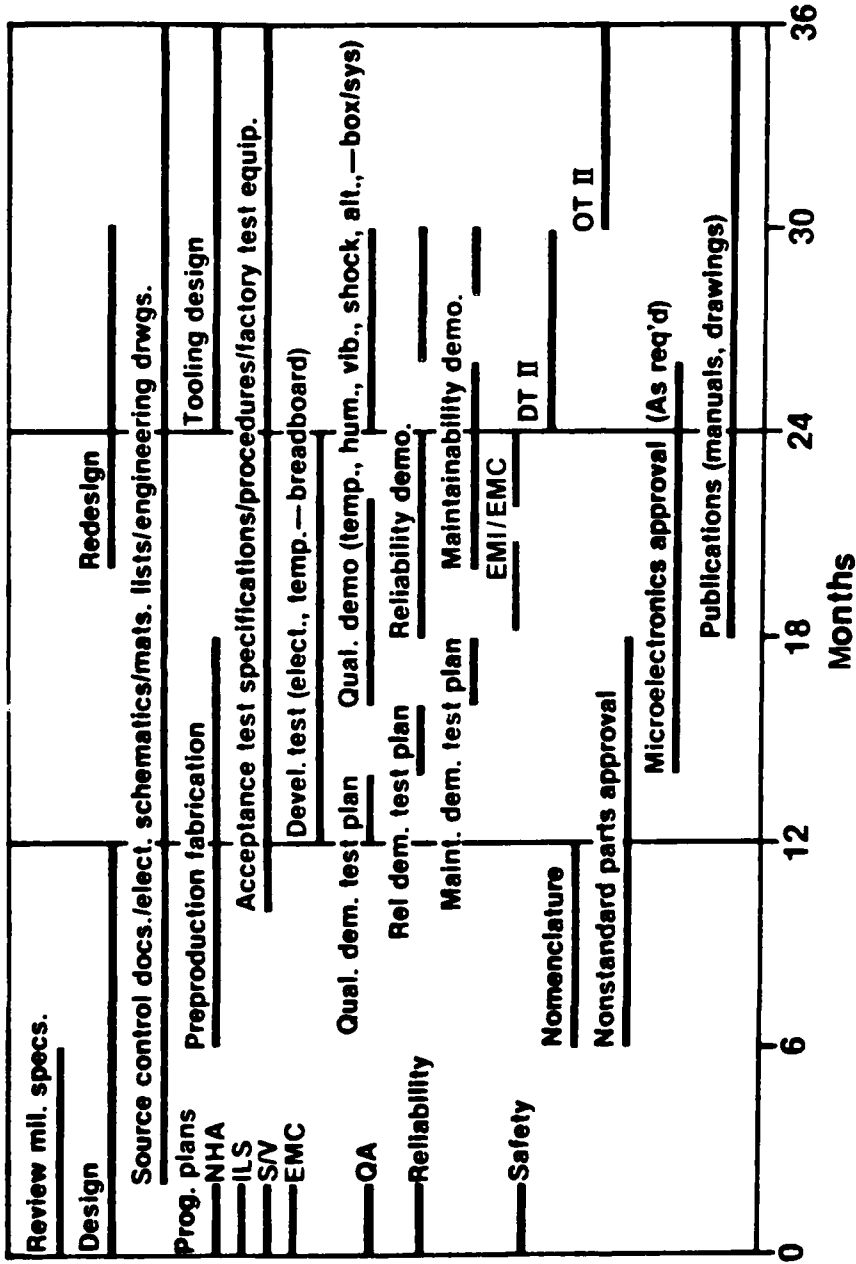


FIGURE 10.6 6.4 PROGRAM SCHEDULE

However, it can be observed that except for the laser, all the components of the WWLODS (window, optics, electronics, wiring, structure, etc.) are very similar to those of current FLIRs and will therefore have very similar nuclear survivability properties. The laser itself is mostly BeO, along with some mirrors, actuators, and electronics. BeO is used as a moderator in some nuclear reactors, and is therefore very hard in the nuclear survivability sense. The other laser components are similar to FLIR components (optics, actuators, etc.) and will therefore have similar hardness. Heterodyne detection systems are inherently harder than passive detection systems because the local-oscillator-induced detector current will swamp nuclear-induced detector currents up to a level much higher than that which would completely hide the signal in a passive detection system. Thus, the nuclear survivability of the WWLODS can be expected to be at least as good as that of the other systems on board the helicopter, and probably better.

Design of the production tooling or at least some of the major elements in the production tooling would be started in the 6.4 production program. A major activity in the 6.4 program is the design of procedures and equipment for factory acceptance testing. A large number of publications are generated during the 6.4 program. These include: the operator's handbook and the maintenance handbook; a record set of drawings, specifications, and parts and materials lists; reports and data from all the demonstration tests; and a nomenclature list. Development testing and operational testing (DT II and OT II) are also required for Army acceptance procedures in the 6.4 program.

10.3 Program Risks

The overall schedule of the lower risk program is shown in Fig. 10.7. The program is shown as starting at the beginning of FY1981. The 6.3B program runs for 24 months and culminates with the completion of DT I. A three month flight test program meeting the requirements of OT I follows and the 6.4 program begins immediately thereafter. The Required Operational Capability documentation (ROC) would have been produced prior to this time. The 6.4 program follows the schedule shown in Fig. 10.6 with DT II being completed in 30 months and OT II at the end of 36 months. This carries the program through the first quarter of FY1986. A six month period for the Development Acquisition In Process Review (DEVA IPR) by the Army is allowed, at the end of which production begins. The first production item is delivered 18-months after the beginning of production, in the first quarter of FY1988. A period of 6 months is allowed for Initial Production sample Testing (IPT) to meet Army requirements and a further 3 months for field installation checkout and field crew familiarization with initial production units. Fabrication of aircraft installation kits, which would be done under a separate contract, runs in parallel with the production activities. This program results in an IOC at the end of FY1988. This is a low risk program in the sense that the risks of missing the schedule, weight, or cost goals are low, provided of course, that unnecessary delays in approvals and decisions by the Army are not incurred and that adequate allowance for inflation is made in the cost estimates.

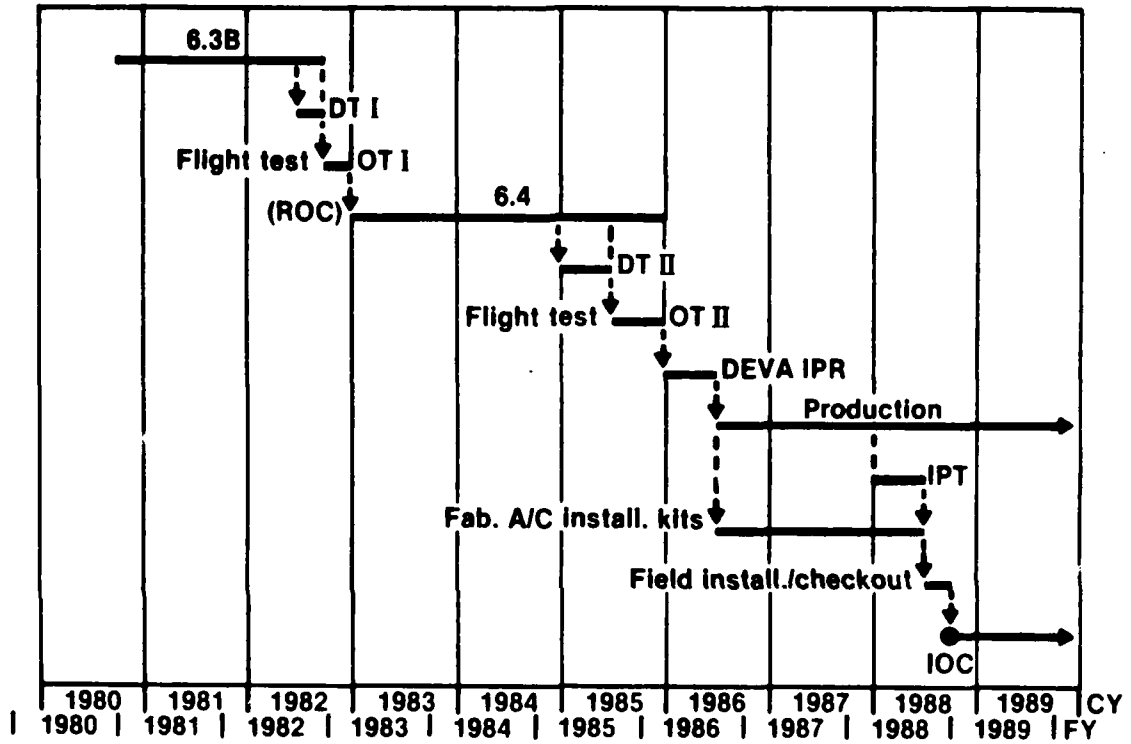


FIGURE 10.7 LOWER RISK PROGRAM

A program schedule that entails higher risk but has a much earlier IOC is shown in Fig. 10.8. In this program the detailed design, performance configuration, engineering design, preproduction fabrication, conformation to mil specs, and the other requirements of Tables 10.1 and 10.2 are accomplished in an augmented 6.3B + program. Because of the many simultaneous activities, communication among the various groups involved can be very good and both the time and cost of the 6.3B + program can be less than those of the sequential 6.3B and 6.4 programs of the lower risk option. The schedule in Fig. 10.8 calls for a 33 month 6.3B + program. In this higher risk program, DT I and OT I are not conducted. DT II occurs in the last 6 months of the 6.3B + program. OT II begins after 30 months and takes 6 months, ending at the end of FY1983. A 6 month DEVA IPR follows, and production is started upon DEVA IPR approval. Fabrication of aircraft installation kits also starts at about this time. The first production unit is delivered 15 months after production starts. A 6 month IPT is conducted in parallel with a 4 month OT IIA which includes field installation and checkout, field crew familiarization and flight testing. IOC occurs at the end of FY1985 and a 6 month Production Validation In Process Review (PV IPR) starts at this time. The risks in this program are primarily in the area of schedule and weight. Because of the overlapping testing and decision making tasks, and the compression of the 6.3B + and production programs, the possibility of the schedule slipping 12 to 24 months (20 to 40 percent) exists. However, even in the worst case, the IOC would be 1 year earlier than in the sequential lower risk program. The compressed program would also cost less up to the time of the first production unit delivery. The greatest risk is that the compressed program would yield a WWLODS weight that would be 10 to 20 percent higher than that for the longer program. This would also entail a roughly 10 to 20 percent higher production cost in constant dollars, but if the IOC can be pushed forward by 2 to 3 years as indicated by the proposed schedules of Figs. 10.7 and 10.8, the actual cost in then-year dollars may be less for the compressed program option.

10.4 Program Costs

An estimate of the cost of the development program and of subsequent production costs (in constant 1980 dollars) was made for the total WWLODS, including the pod structure and all its contents, on the basis of similar size and weight radar and electronic systems produced by UTC's Norden Systems subsidiary. The results of this estimate are shown in Fig. 10.9. In the range of pod weight from 50 to 70 pounds, the development cost is estimated at \$2.5 to \$4M, depending on the size of the system, and the production cost averaged over 4000 units ranges from about \$20 to \$30K over the same range of sizes. The first unit costs would range from \$70 to \$110K. These costs are based on current radar and similar electronic systems experience. The cost prediction technique used does not distinguish between standard and accelerated program schedules. Items which are not normally found in such systems, such as the cooled detectors and the precisely machined and

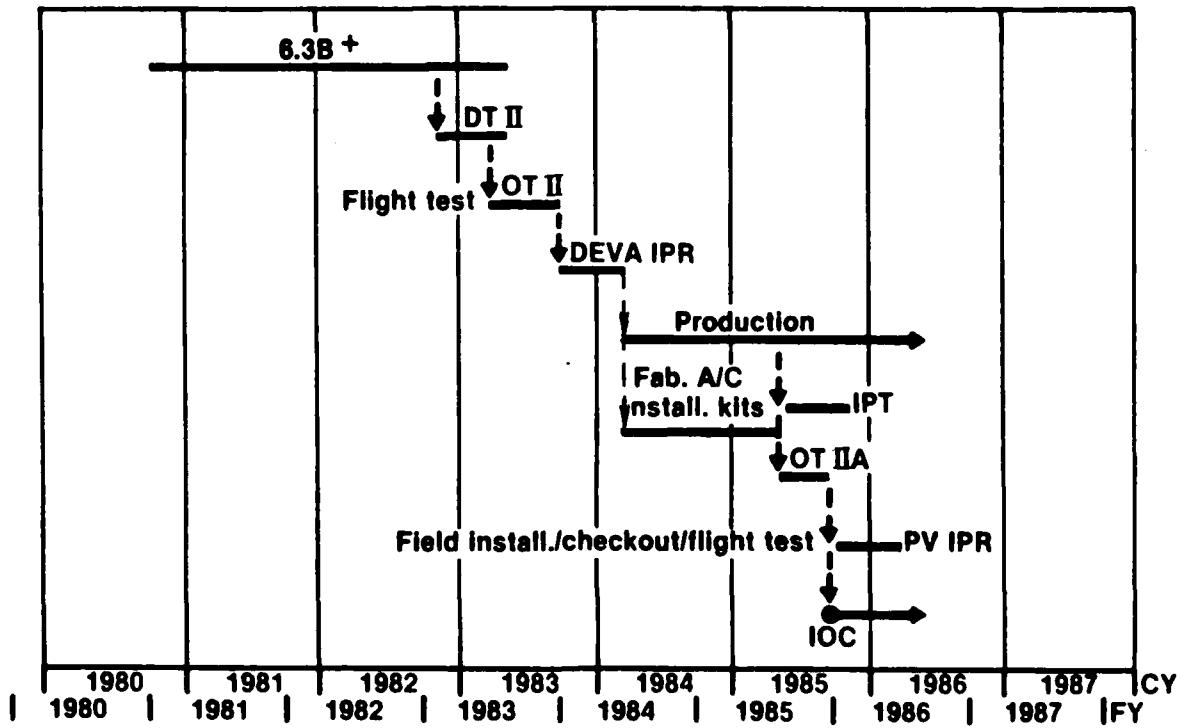


FIGURE 10.8 HIGHER RISK PROGRAM

Based on radar experience
Constant 1980 dollars

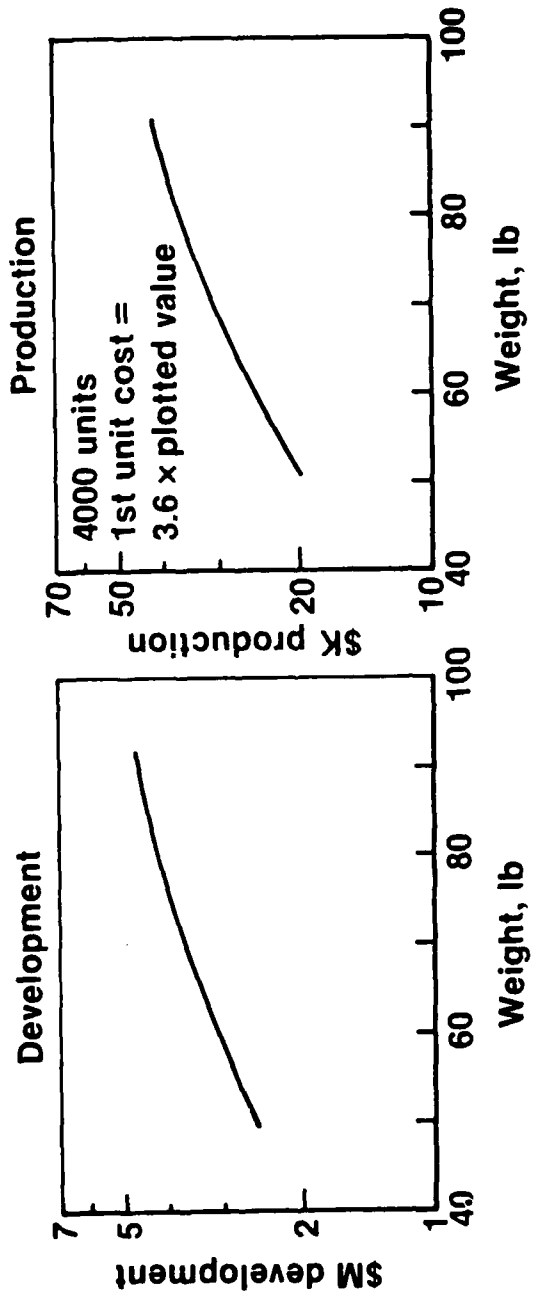


FIG. 10.9 ESTIMATED COST OF WWLODS

vibrationally hardened ceramic laser would probably add fixed dollar amounts to these estimates. Based on current UTRC experience, the laser design and cost study described in Section 9.3, and vendor estimates of the costs of detectors and cryogenic refrigerators, this additional cost would range from \$5 to \$20k, depending primarily on the market for detectors at the time of purchase and the productionizing evolution of the laser. Thus, the \$50k cost goal for the WWLODS appears to be achievable.

The cost of cables, controls, and display interface equipment discussed in Section 9.4, which would be in the aircraft, would range from \$2 to 4k.

11.0 REFERENCES

1. Employment of Army Aviation Units in a High Threat Environment. Field Manual No. 90-1, Headquarters, Department of the Army, Washington, D. C.
2. DelBoca, R. L., et al.: The Development and Testing of a Laser Obstacle Terrain Avoidance Warning System (LOTAWS). 7th DoD Conference on Laser Technology, 8-10 June, 1976.
3. Mongeon, R. J., et al.: Multifunction Coherent CO₂ Laser Radar for Airborne Tactical Operations (U). Meeting of IRIS Specialty Group on Active Systems. 28-29 October 1980 (Confidential).
4. Final Test Report, Contract No. DAAK80-79-C-0278. United Technologies Research Center.

1 June 1980

AVRADA

DISTRIBUTION LIST FOR TECHNICAL REPORTS
(In-House and Contract)

This is the standard distribution list for technical reports under the cognizance of your activity. It supersedes the list dated 1 Oct 76. For information on distribution policy call the STINFO Office, Ext. 52184.

Additional addressees, except foreign nationals, may be added at the end of the list at the discretion of the cognizant office. Before adding an address, however, consider the intent of the distribution statement applied to the report. (See DOD Dir 5200.20)

Classified reports will be distributed on a "need-to-know" basis, with special attention to the transmission controls on distribution of classified reports by contractors to non-government addressees.

DETACH THE LIST AND USE AS A REPRODUCIBLE MASTER FOR PRINTING

101	Defense Technical Information Center ATTN: DTIC-TCA Cameron Station (Bldg 5) Alexandria, VA 22314	314	HQ, Air Force Systems Command ATTN: DLWA/Mr. P. Sandler Andrews AFB Washington, DC 20331
012		001	
104	Defense Communications Agency Technical Library Center Code 205 (P. A. Tolovi) Washington, DC 20305	403	CDR, MIRCOM Redstone Scientific Info Center ATTN: Chief, Document Section Redstone Arsenal, AL 35809
002		002	
200	Office of Naval Research Code 427 Arlington, VA 22217	404	CDR, MIRCOM ATTN: DRSMI-RE (Mr. Pittman) Redstone Arsenal, AL 35809
001		001	
206	Commander Naval Ocean Systems Ctr ATTN: Library San Diego, CA 92152	408	Commandant US Army Military Police School ATTN: ATZN-CDM-CE Fort Mc Clellan, AL 36205
001		003	
212	Command, Control & Comm Div Development Center Marine Corps Development & Education Comd Quantico, VA 22134	417	Commander US Army Intelligence Ctr & School ATTN: ATSI-CD-MD Fort Huachuca, AZ 85613
001		003	
214	CDR, Naval Air Systems Comd Meteorological Dept (Air-553) Washington, DC 20361	418	Commander HQ Fort Huachuca ATTN: Technical Reference Div Fort Huachuca, AZ 85613
001		001	
217	Naval Air Systems Command Code: Air-5332 Washington, DC 20360	419	Commander US Army Electronic Proving Ground ATTN: STEEP-MT Fort Huachuca, AZ 85613
004		001	
219	Dr. T. G. Berlincourt Office of Naval Research (Code 420) 800 N. Quincy St Arlington, VA 22217	422	Commander US Army Yuma Proving Ground ATTN: STEYP-MTD (Tech Library) Yuma, AZ 85364
001		001	
300	AUL/LSE 64-285 Maxwell AFB, AL 36112	432	Dir, US Army Air Mobility R&D Lab ATTN: T. Gossett, Bldg 207-5 NASA AMES Research Center Moffett Field, CA 94035
001		001	
301	Rome Air Development Ctr ATTN: Documents Library (TSLD) Griffiss AFB, NY 13441	437	Deputy for Science & Technology Office, Asst Sec Army (R&D) Washington, DC 20310
001		002	
313	Armament Development & Test Ctr ATTN: DLODL, Tech Library Eglin Air Force Base, FL 32542	455	Commandant US Army Signal School ATTN: ATSH-CD-MS-E Fort Gordon, GA 30905
001		001	

456 Commandant
US Army Infantry School
ATTN: ATSH-CD-MS-E
001 Fort Benning, GA 31905

461 CDR, Rock Island Arsenal
ARRCOM
ATTN: JARRI-LR-Y
001 Rock Island, IL 61299

466 CDR, US Army Combined Arms
Combat Developments Activity
ATTN: ATCACC
003 Fort Leavenworth, KS 66027

470 Director of Combat Developments
US Army Armor Center
ATTN: ATZK-CD-MS
002 Fort Knox, KY 40121

474 Commander
US Army Test & Eval Comd
ATTN: DRSTE-CT-C
001 Aberdeen Proving Ground, MD 21005

475 CDR, Harry Diamond Lab
ATTN: Library
2800 Powder Mill Road
001 Adelphi, MD 20783

479 Director
US Army Human Engineering Lab
001 Aberdeen Proving Ground, MD 21005

483 Director
US Army Materiel Systems Anal Actv
ATTN: DRKSY-MP
001 Aberdeen Proving Ground, MD 21005

504 Chief, CERCOM Aviation Electronics Ofc
ATTN: DRSEL-MME-LAF (2)
001 St. Louis, MO 63166

507 CDR, AVRADCOM
ATTN: DRSAV-E
PO Box 209
001 St. Louis, MO 63166

515 PM, FIREFINDER/REMBASS
ATTN: DRCPM-FER
001 Fort Monmouth, NJ 07703

516 Proj Manager, NAVCON
ATTN: DRCPM-NC-TM
Bldg 2539
001 Fort Monmouth, NJ 07703

517 Commander
US Army Satellite Comm Agcy
ATTN: DRCPM-3C-3
002 Fort Monmouth, NJ 07703

529 CDR, US Army Research Ofc
ATTN: Dr. Horst Wittmann
PO Box 12211
001 Research Triangle Park, NC
27709

531 CDR, US Army Research Ofc
ATTN: DRKRO-IP
PO Box 12211
002 Research Triangle Park, NC
27709

533 Commandant
US Army Inst for Military
Assistance
ATTN: ATSU-CTD-MO
002 Fort Bragg, NC 28307

563 Commander, DARCOM
ATTN: DRCDE
5001 Eisenhower Ave
001 Alexandria, VA 22333

564 CDR, US Army Signals
Warfare Lab
ATTN: DELSW-03
Vint Hill Farms Station
001 Warrenton, VA 22186

567 Commandant
US Army Engineer School
ATTN: ATZA-TDL
002 Fort Belvoir, VA 22060

571 Dir, Applied Technology
Lab, US Army Research &
Technology Labs (AVRADCOM)
ATTN: Technical Library
001 Fort Eustis, VA 23604

572 Commander
US Army Logistics Center
ATTN: ATCL-MC
002 Fort Lee, VA 22801

573 Commander
US Army Logistics Center
ATTN: ATCL-MA
001 Fort Lee, VA 23801

575 Commander
TRADOC
ATTN: ATDOC-TA
001 Fort Monroe, VA 23561

577 Commander
US Army Training & Doctrine Comd
ATTN: ATCD-TM
001 Fort Monroe, VA 23561

602 CDR, Night Vision & Electro-Optics
Laboratory
ERADCOM
ATTN: DELNV-D
001 Fort Belvoir, VA 22060

603 CDR, Atmospheric Sciences Lab
ERADCOM
ATTN: DELAS-SY-S
001 White Sands Missile Range, NM 88002

612 CDR, ERADCOM
ATTN: DRDEL-CT
2800 Powder Mill Road
002 Adelphi, MD 20783

619 CDR, ERADCOM
ATTN: DRDEL-PA
2800 Powder Mill Road
001 Adelphi, MD 20783

622 HQ, Harry Diamond Lab
ATTN: DELHD-TD (Dr. W. W. Carter)
2800 Powder Mill Road
001 Adelphi, MD 20783

680 CDR, ERADCOM Fort Monmouth, NJ
1 DELEW-D 07703
1 DELET-D
1 DELCS-D
*2 DELSD-L-S
1 DELSD-L

681 CDR, CORADCOM, Fort Monmouth
1 DRDCO-COM-D NJ 07703
1 DRDCO-TCS-B

683 HQs
AVRADA, Fort Monmouth, NJ
1 DAVAA-D 07703
25 Originating Office

701 MIT -Lincoln Lab
ATTN: Library (Rm A-082)
PO Box 73
002 Lexington, MA 02173

703 NASA Scientific & Tech
Info Facility
Baltimore/Washington
Intl Airport
001 PO Box 8757, MD 21240

706 Advisory Group on Electron
Devices
ATTN: Secy, Working Grp D
(Lasers)
201 Varick Street
002 New York, NY 10014

707 TACTEC
Battelle Memorial Inst
505 King Avenue
001 Columbus, OH 43201

710 Ketrion, Inc
1400 Wilson Blvd, Arch Bldg
002 Arlington, VA 22209

712 R. C. Hansen, Inc.
PO Box 215
001 Tarsana, CA 91356

713 MITRE Corp
ATTN: Frederick Leuppert
120 Dolly Madison Blvd
001 McLean, VA 22102

714 Dynalectron Corp
GIDEP Engineering &
Support Dept
PO Box 398
001 Norco, CA 91760

*Unclassified reports only